

1. Report No. FHWA/TX-95/1442-1F		2. Government Accession No.		3. Recipient's Catalog No.	
4. Title and Subtitle  SHORT-RADIUS THRIE BEAM TREATMENT FOR INTERSECTING STREETS AND DRIVES				5. Report Date November 1994	
				6. Performing Organization Code	
7. Author(s) Roger P. Bligh, Hayes E. Ross, Jr., and Dean C. Alberson				8. Performing Organization Report No. Research Report 1442-1F	
9. Performing Organization Name and Address Texas Transportation Institute The Texas A&M University System College Station, Texas 77843-3135				10. Work Unit No. (TRAIS)	
				11. Contract or Grant No. Study No. 0-1442	
12. Sponsoring Agency Name and Address Texas Department of Transportation Research and Technology Transfer Office P. O. Box 5080 Austin, Texas 78763-5080				13. Type of Report and Period Covered Final: September 1993 - August 1994	
				14. Sponsoring Agency Code	
15. Supplementary Notes Research performed in cooperation with the Texas Department of Transportation and the U.S. Department of Transportation, Federal Highway Administration. Research Study Title: Treatment at Intersecting Streets and Drives: Bridge Railing End Treatments					
16. Abstract  At sites where a driveway or secondary roadway intersects a primary roadway in close proximity to a bridge end, the available space will not accommodate a standard length of approach guardrail, and alternate treatments are required. In Study 1263, a short-radius nested W-beam treatment was developed for use at these locations. Although the design offered improved impact performance over existing systems, it failed to pass one of the design test conditions. This study was undertaken to develop and test a new short-radius thrie-beam guardrail treatment suitable for use by TxDOT that meets nationally recognized safety standards. The new treatment consists of a single 10-ga. thrie-beam rail mounted at a height of 787 mm (31 in.) and supported on weakened, round wood posts. The system extends approximately 9.75 m (32 ft) from the bridge end along the primary roadway at which point it is curved in a 4.87-m (16-ft) radius and extended down the secondary roadway. A series of five crash tests was used to evaluate the impact performance of this short-radius thrie-beam system. Although it failed to contain a 3/4-ton pickup truck as required by <i>NCHRP Report 350</i> , subsequent testing showed that it successfully meets the guidelines and evaluation criteria set forth in <i>NCHRP Report 230</i> , and is suitable for implementation where site conditions warrant such a treatment. In addition to offering significantly improved impact performance over existing designs, the thrie-beam design should be much easier to install and maintain than the interim nested W-beam design developed under Study 1263.					
17. Key Words  Guardrail, Thrie Beam, Short Radius, Transition, Bridge End, Intersecting Roadway, Crash Test, Safety Treatment, Pickup Truck			18. Distribution Statement No restrictions. This document is available to the public through NTIS: National Technical Information Service 5285 Port Royal Road Springfield, Virginia 22161		
19. Security Classif.(of this report) Unclassified		20. Security Classif.(of this page) Unclassified		21. No. of Pages 144	22. Price

**SHORT-RADIUS THRIE BEAM TREATMENT FOR  
INTERSECTING STREETS AND DRIVES**

by

**Roger P. Bligh  
Assistant Research Engineer  
Texas Transportation Institute**

**Hayes E. Ross, Jr.  
Research Engineer  
Texas Transportation Institute**

and

**Dean C. Alberson  
Assistant Research Engineer  
Texas Transportation Institute**

**Research Report 1442-1F  
Research Study No. 0-1442  
Research Study Title: Treatment at Intersecting Streets and Drives:  
Bridge Railing End Treatments**

**Sponsored by the  
Texas Department of Transportation  
In Cooperation with  
U.S. Department of Transportation  
Federal Highway Administration**

**November 1994**

**TEXAS TRANSPORTATION INSTITUTE  
The Texas A&M University System  
College Station, Texas 77843-3135**

## IMPLEMENTATION STATEMENT

A short-radius thrie-beam guardrail treatment was developed and tested under this study. Although the design failed to contain a 3/4-ton pickup truck as required by *NCHRP Report 350*, it did successfully meet the guidelines and evaluation criteria set forth in *NCHRP Report 230*. Upon development of new design standards, TxDOT can begin immediate implementation of the design where site conditions warrant such a system. Implementation of this treatment will offer significantly improved impact performance over existing designs and it will be much easier to install and maintain than the interim nested W-beam design developed under Study 1263. However, as with all new designs, it is recommended that the short-radius thrie-beam treatment be monitored to provide data regarding its installation, maintenance, and impact performance.

## **DISCLAIMER**

The contents of this report reflect the views of the authors who are responsible for the facts and the accuracy of the data presented herein. The contents do not necessarily reflect the official views or policies of the Federal Highway Administration or the Texas Department of Transportation. This report does not constitute a standard, specification, or regulation, nor is it to be used for construction, bidding, or permit purposes. The engineers in charge of the project were H. E. Ross, Jr., P.E. #26510, and R. P. Bligh, P.E. #78550.

## **ACKNOWLEDGMENTS**

Valuable guidance and input were provided throughout the study by Mr. Robert Cochrane, Project Manager, TxDOT. The authors are also indebted to various other personnel of TxDOT, including Mr. Jeff Cotham, Mr. Mark A. Marek, and Mr. Terry McCoy, and Mr. Bob Musselman of FHWA for providing assistance in selecting and finalizing the design details. The authors are also very grateful to Mr. Jichuan Liu for assistance in conducting various analyses and in preparing drawings. This report was prepared in cooperation with the U.S. Department of Transportation, Federal Highway Administration.

# TABLE OF CONTENTS

	<u>Page</u>
LIST OF FIGURES .....	x
LIST OF TABLES .....	xiv
SUMMARY .....	xv
I. INTRODUCTION AND OBJECTIVES .....	1
II. DEVELOPMENT OF SHORT-RADIUS THRIE-BEAM TREATMENT .....	7
DESIGN CONSIDERATIONS .....	7
DESIGN IMPACT CONDITIONS .....	10
DESIGN PROCESS .....	11
SHORT-RADIUS THRIE-BEAM DESIGN DETAILS .....	12
III. CRASH TEST PROCEDURES .....	17
ELECTRONIC INSTRUMENTATION AND DATA PROCESSING .....	17
PHOTOGRAPHIC INSTRUMENTATION AND DATA PROCESSING .....	18
TEST VEHICLE PROPULSION AND GUIDANCE .....	18
IV. FULL-SCALE CRASH TEST RESULTS .....	21
TEST 1442-1 .....	21
TEST 1442-2 .....	26
TEST 1442-3 .....	33
TEST 1442-4 .....	47
TEST 1442-5 .....	54
V. CONCLUSIONS AND RECOMMENDATIONS .....	67
RECOMMENDATIONS .....	68
REFERENCES .....	69
APPENDIX A - SEQUENTIAL PHOTOGRAPHS .....	71
APPENDIX B - VEHICULAR ACCELERATIONS .....	93
APPENDIX C - VEHICULAR ANGULAR DISPLACEMENTS .....	111
APPENDIX D - CONSTRUCTION DRAWINGS OF SHORT-RADIUS THRIE-BEAM TREATMENT .....	119

## LIST OF FIGURES

<u>Figure</u>		<u>Page</u>
1.	Situation in which runout length is restricted along primary roadway . . . . .	2
2.	FHWA short-radius guardrail treatment . . . . .	3
3.	Short-radius nested W-beam guardrail treatment . . . . .	4
4.	Bumper position of typical 2000P test vehicle . . . . .	9
5.	Short-radius thrie-beam guardrail transition . . . . .	13
6.	Thrie beam to W-beam transition section . . . . .	15
7.	Vehicle before test 414424-1 . . . . .	22
8.	Installation before test 414424-1 . . . . .	23
9.	Vehicle properties for test 414424-1 . . . . .	24
10.	Vehicle/installation geometrics for test 414424-1 . . . . .	25
11.	After impact trajectory, test 414424-1 . . . . .	27
12.	Summary of results for test 414424-1 . . . . .	28
13.	Installation after test 414424-1 . . . . .	29
14.	Vehicle after test 414424-1 . . . . .	30
15.	Installation before test 414424-2 . . . . .	31
16.	Vehicle before test 414424-2 . . . . .	32
17.	Vehicle properties for test 414424-2 . . . . .	34
18.	Vehicle/installation geometrics for test 414424-2 . . . . .	35
19.	Summary of results for test 414424-2 . . . . .	36
20.	Installation after test 414424-2 . . . . .	37
21.	Vehicle after test 414424-2 . . . . .	38

<u>Figure</u>	<u>Page</u>
22. Installation before test 414424-3 .....	40
23. Vehicle before test 414424-3 .....	41
24. Vehicle properties for test 414424-3 .....	42
25. Vehicle/installation geometrics before test 414424-3 .....	43
26. Summary of results for test 414424-3 .....	44
27. Installation after test 414424-3 .....	45
28. Vehicle after test 414424-3 .....	46
29. Installation before test 414424-4 .....	48
30. Vehicle before test 414424-4 .....	49
31. Vehicle properties for test 414424-4 .....	50
32. Vehicle/installation geometrics before test 414424-4 .....	51
33. After impact trajectory, test 414424-4 .....	52
34. Installation after test 414424-4 .....	53
35. Vehicle after test 414424-4 .....	55
36. Summary of results for test 414424-4 .....	56
37. Installation before test 414424-5 .....	57
38. Vehicle before test 414424-5 .....	58
39. Vehicle properties for test 414424-5 .....	59
40. Vehicle/installation geometrics before test 414424-5 .....	60
41. After impact trajectory, test 414424-5 .....	62
42. Summary of results for test 414424-5 .....	63
43. Installation after test 414424-5 .....	64
44. Vehicle after test 414424-5 .....	65



<u>Figure</u>	<u>Page</u>
A-1. Sequential photographs for test 414424-1 (overhead and frontal views) .....	73
A-2 Sequential photographs for test 414424-1 (perpendicular and behind the rail views) .....	75
A-3 Sequential photographs for test 414424-2 (overhead and frontal views) .....	77
A-4 Sequential photographs for test 414424-2 (behind the rail and oblique views) .....	79
A-5 Sequential photographs for test 414424-3 (overhead and frontal views) .....	81
A-6 Sequential photographs for test 414424-3 (behind the rail and oblique views) .....	83
A-7 Sequential photographs for test 414424-4 (overhead and frontal views) .....	85
A-8 Sequential photographs for test 414424-4 (perpendicular and behind the rail views) .....	87
A-9 Sequential photographs for test 414424-5 (overhead and frontal views) .....	89
A-10 Sequential photographs for test 414424-5 (perpendicular and behind the rail views) .....	91
B-1 Vehicle longitudinal accelerometer trace for test 414424-1 .....	95
B-2 Vehicle lateral accelerometer trace for test 414424-1 .....	96
B-3 Vehicle vertical accelerometer trace for test 414424-1 .....	97
B-4 Vehicle longitudinal accelerometer trace for test 414424-2 .....	98
B-5 Vehicle lateral accelerometer trace for test 414424-2 .....	99
B-6 Vehicle vertical accelerometer trace for test 414424-2 .....	100
B-7 Vehicle longitudinal accelerometer trace for test 414424-3 .....	101
B-8 Vehicle lateral accelerometer trace for test 414424-3 .....	102

<u>Figure</u>	<u>Page</u>
B-9 Vehicle vertical accelerometer trace for test 414424-3 .....	103
B-10 Vehicle longitudinal accelerometer trace for test 414424-4 .....	104
B-11 Vehicle lateral accelerometer trace for test 414424-4 .....	105
B-12 Vehicle vertical accelerometer trace for test 414424-4 .....	106
B-13 Vehicle longitudinal accelerometer trace for test 414424-5 .....	107
B-14 Vehicle lateral accelerometer trace for test 414424-5 .....	108
B-15 Vehicle vertical accelerometer trace for test 414424-5 .....	109
C-1 Vehicle angular displacements during test 414424-1 .....	113
C-2 Vehicle angular displacements during test 414424-2 .....	114
C-3 Vehicle angular displacements during test 414424-3 .....	115
C-4 Vehicle angular displacements during test 414424-4 .....	116
C-5 Vehicle angular displacements during test 414424-5 .....	117
D-1 Construction drawing for short-radius thrie-beam guardrail treatment .....	121

**LIST OF TABLES**

<u>Table</u>		<u>Page</u>
1	Comparison of Design Test Vehicles .....	8

## SUMMARY

At sites where a driveway or secondary roadway intersects a primary roadway in close proximity to a bridge end, the available space will not accommodate a standard length of approach guardrail, and alternate treatments are required. In Study 1263, a short-radius nested W-beam treatment was developed for use at these locations. Although the design offered improved impact performance over existing systems, it failed to pass one of the design test conditions. This study was undertaken to develop and test a new short-radius thrie-beam guardrail treatment suitable for use by TxDOT that meets nationally recognized safety standards.

The new treatment consists of a single 10-ga. thrie-beam rail mounted at a height of 787 mm (31 in.) and supported on weakened, round wood posts. The system extends approximately 9.75 m (32 ft) from the bridge end along the primary roadway at which point it is curved in a 4.87-m (16-ft) radius and extended down the secondary roadway. A thrie beam-to-W-beam transition section is used to reduce the height of the rail at the bridge end and permit connection of treatment to both 813 mm (32-in) and 686 mm (27-in.) tall bridge parapets. A similar transition section is used to transition to a W-beam turndown anchor along the secondary roadway.

A series of five crash tests was used to evaluate the impact performance of this short-radius thrie-beam system. When tested in accordance with the requirements of *NCHRP Report 350*, the short-radius system was unable to contain a 3/4-ton pickup truck impacting the curved section of rail at a nominal speed of 100 km/h (62.2 mph). It was concluded that the observed vaulting failure was due to a combination of vehicle geometrics and the low torsional stiffness of the open thrie-beam section. When tested in accordance with *NCHRP Report 230*, the short-radius treatment successfully contained both a small and large passenger car impacting into the curved section of rail at 96.6 km/h (60 mph). Since there are currently no existing designs which meet the new requirements of *NCHRP Report 350*, and the new short-radius thrie-beam system meets the guidelines and evaluation criteria set forth in *NCHRP Report 230*, it is considered suitable for implementation where site conditions warrant such a treatment.

In addition to providing significantly improved impact performance over existing TxDOT practices, it is believed that the thrie-beam system will be easier to install and maintain than the previously tested nested W-beam system. Furthermore, the material costs of the new thrie-beam system are expected to be equal to or less than the nested W-beam alternative.

## I. INTRODUCTION AND OBJECTIVES

Rigid barriers or railings are typically erected on either side of a bridge to prevent errant vehicles from leaving the roadway. Since the end of this railing can present a severe hazard to motorists, an approach barrier is typically used to shield the exposed end and to prevent vehicles from encountering the hazard the bridge is spanning.

Although the length of the approach guardrail varies with roadway type and traffic volume, it is usually at least 30.5 m (100 ft) in length. However, in some cases, such as when a side road or driveway intersects the main roadway in close proximity to the bridge end, the available space will not accommodate the standard length of approach guardrail. Under these conditions, the bridge end is usually shielded by a short length of guardrail that is either terminated at the secondary road or curved on a tight radius and terminated along the secondary road, as shown in Figure 1.

In a previous study conducted by Southwest Research Institute, a short-radius guardrail treatment was developed for the Federal Highway Administration (FHWA) and the Washington Department of Transportation (1). As shown in Figure 2, the system consisted of a steel W-beam guardrail curved at a radius of 2.6 m (8 ft-6 in.), with a modified breakaway cable terminal (BCT) anchoring the system. Weakened rectangular wood posts were spaced at 1.9 m (6 ft-3 in.) along the curved portion of the rail, and the portion of the system adjacent to the main roadway was angled towards the road at a 10-to-1 slope. While the FHWA system was reported to have performed acceptably during full-scale crash testing, it was concluded that development of another system which more specifically addresses the needs and requirements of the Texas Department of Transportation (TxDOT) was warranted. This includes the use of standard Texas hardware and end anchorages and the development of a suitable transition from the approach guardrail to the rigid bridge rail.

This problem was addressed by the Texas Transportation Institute in a two-year study sponsored cooperatively by TxDOT and FHWA (2). The work accomplished under Study 1263 consisted of (a) a survey of typical sites to identify the precise nature of the problem, (b) the design of new preliminary short-radius guardrail treatments, (c) a benefit/cost analysis of available systems and the proposed new designs, (d) the development and crash testing of a selected short-

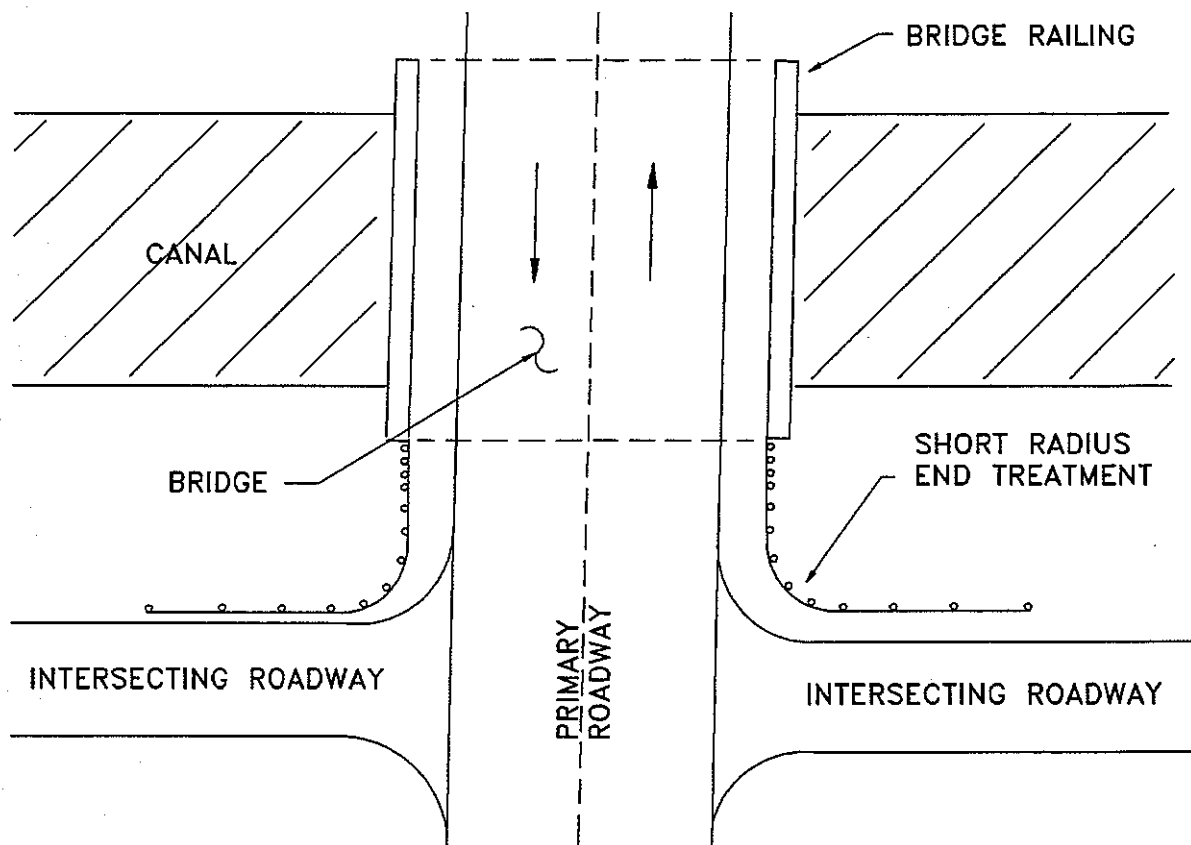


Figure 1. Situation in which runout length is restricted along primary roadway (2).

radius treatment, and (e) the identification of recommended alternatives to the problem for various types of roadways and traffic volumes.

The system that was tested under this study is shown in Figure 3. The curved section of rail consists of nested 12-ga. W-beam installed on a radius of 4.9 m (16 ft). Weakened 177.8 mm (7-in.) diameter wood posts were used in the curved region to facilitate fracture during impact. The system extends 18.5 m (60 ft-8 in.) along the intersecting road at which point it is terminated with a standard TxDOT turndown. The transition region near the bridge end was strengthened through the use of a 3.8 m (12 ft-6 in.) section of tubular W-beam supported by standard TxDOT posts spaced at 457.2 mm (1 ft-6 3/4 in.). In addition, a BCT (breakaway cable terminal) anchor was used at the upstream end of the transition to facilitate redirection of vehicles impacting in the transition section.

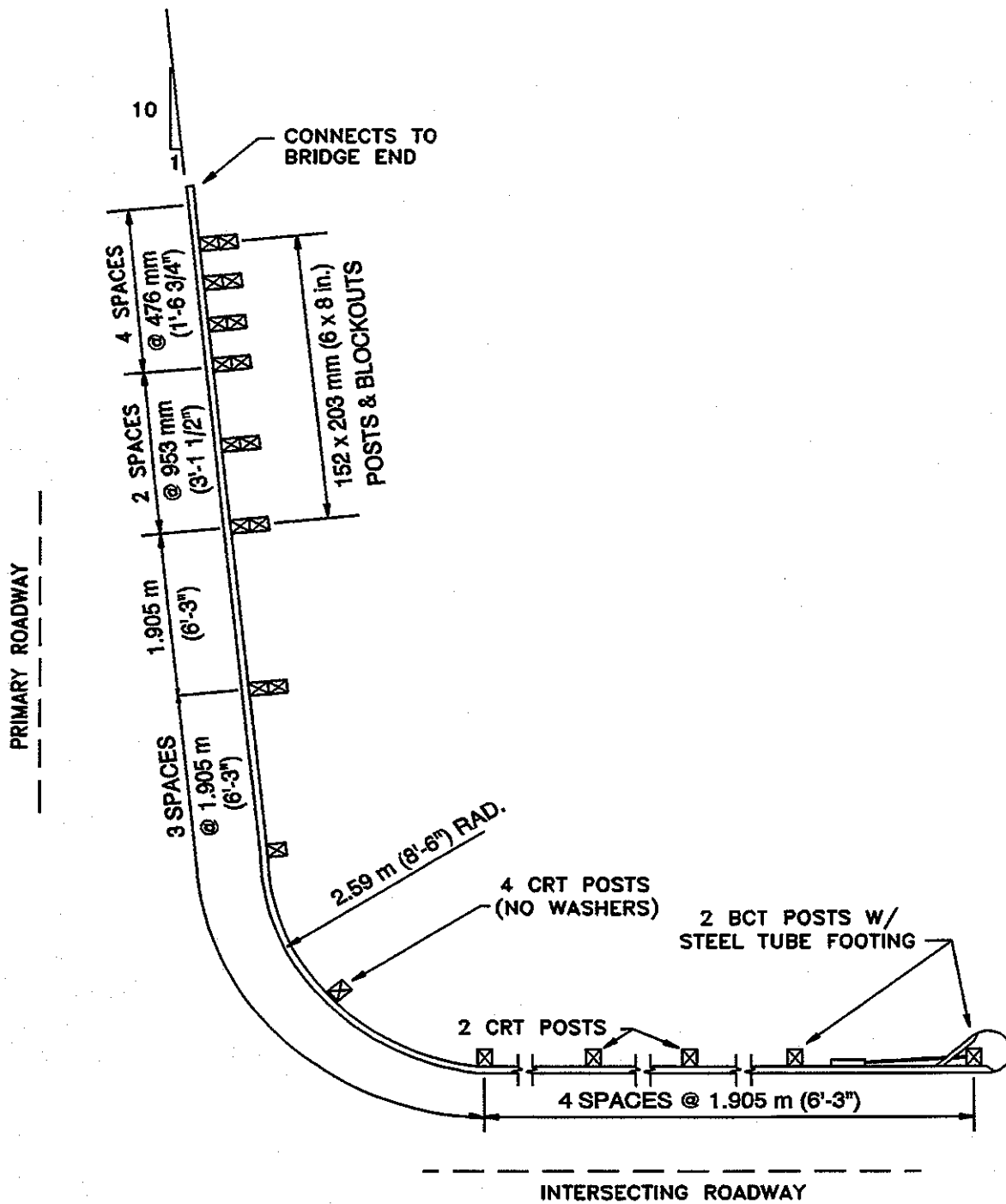


FIGURE 2. FHWA short-radius guardrail treatment (1).

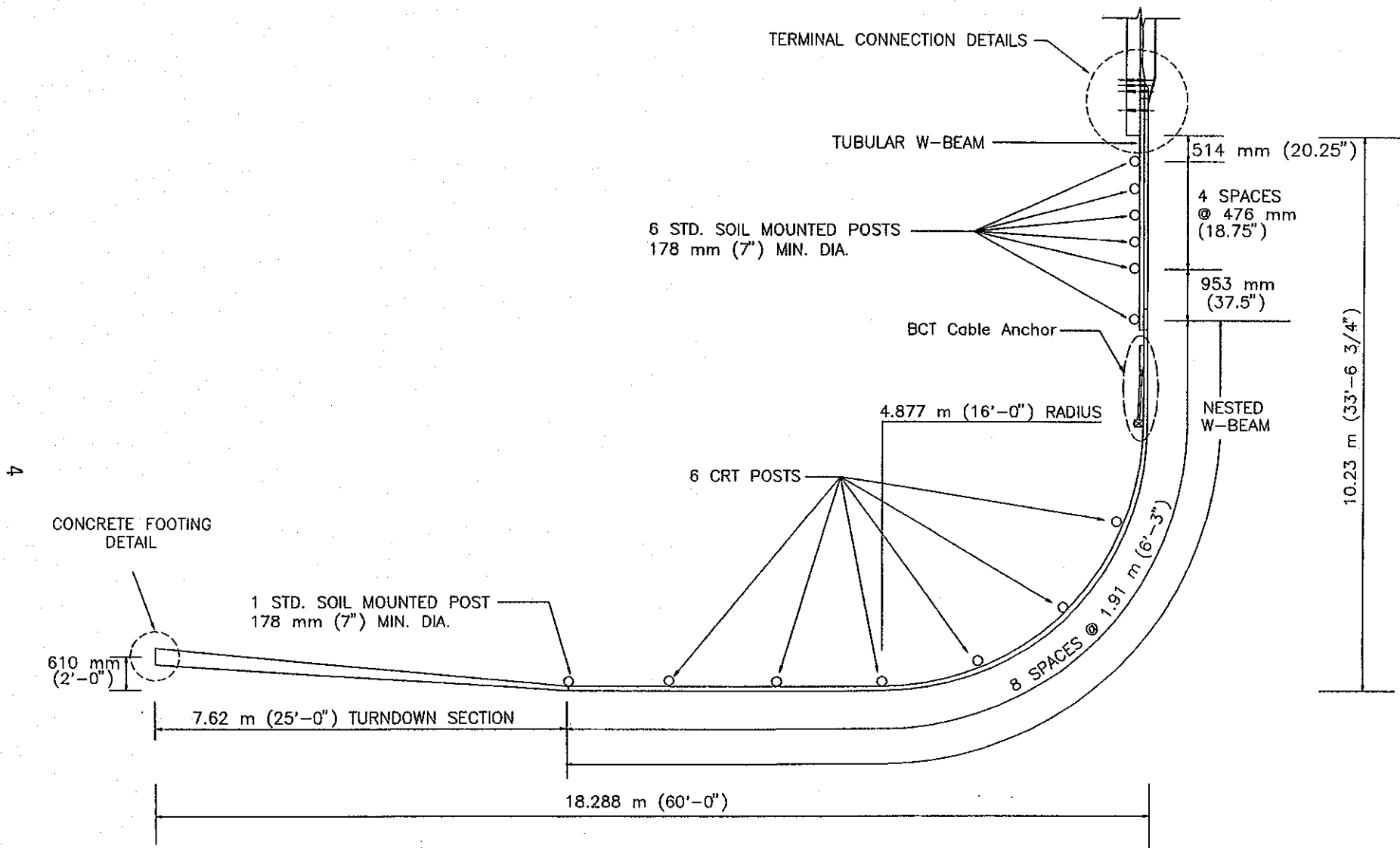


Figure 3. Short-radius nested W-beam guardrail treatment (2).



With one exception, this short-radius nested W-beam system passed each of the four crash tests selected as critical design impact conditions. The one failure involved a 2,043 kg (4,500 lb) vehicle impacting at the center of the curved segment of rail at a nominal speed and angle of 96.6 km/h (60 mph) and 25 deg. In this test the vehicle went under the guardrail after the system dissipated approximately 90 percent of the initial vehicular kinetic energy. Considering the extreme nature of the test conditions, it was concluded that the system could be expected to perform as intended for most real world impacts and would serve at least as an interim solution where site conditions warrant.

However, in light of the test failure, it was recommended that consideration be given to the development and use of a short-radius thrie beam alternative. It was believed that a suitably designed thrie-beam system would satisfy all design impact conditions, would be easier to install, and would cost less than the nested W-beam system. Thus, the objective of this study was to develop a new short-radius thrie-beam guardrail treatment suitable for use by TxDOT that meets nationally recognized safety standards.

## II. DEVELOPMENT OF SHORT-RADIUS THRIE-BEAM TREATMENT

The development of the short-radius thrie-beam guardrail treatment was divided into two distinct areas of effort. The first was to select and finalize details of the thrie beam design, including appropriate transitions to both the bridge rail and the terminal end anchorage on the secondary roadway. The second major task involved testing and evaluating the selected design in accordance with nationally recognized safety standards. A more detailed description of these efforts is described in the sections which follow.

### DESIGN CONSIDERATIONS

As discussed in Study 1263 (2), it was believed that the performance of the short-radius treatment could be improved to the point of meeting *NCHRP Report 230* (3) evaluation criteria by replacing the nested W-beam rails with a single 10-ga. thrie-beam rail. In terms of strength, a 10-ga. thrie beam has approximately the same section properties (area, section modulus, and moment of inertia) as two nested 12-ga. W-beam rails. The thrie beam has a depth (vertical dimension) of 508.0 mm (20 in.) and is typically installed with a ground clearance of 304.8 mm (12 in.), whereas a W-beam has a depth of 311.1 mm (12.25 in.) and a ground clearance of 304.8 mm (12 in.). The combined effect of increased height and lower ground clearance of the thrie beam was considered sufficient to prevent the underriding observed with the nested W-beam design.

After selection of the rail type, the next most important design consideration was the mounting height. The standard mounting height of a thrie-beam guardrail is 787.4 mm (31 in.), compared to a nominal height of 685.8 mm (27 in.) for a W-beam. Although the standard mounting height was believed to be adequate for purposes of containing large cars impacting in the curved portion of rail, it was initially considered desirable to lower the height of the thrie-beam rail to match that of the W-beam. This would further minimize the potential for vehicular underride, permit direct connection of the thrie beam to a greater number of TxDOT bridge rails (most of which are 685.8 mm [27 in.] high), and maintain existing sight distance for vehicles entering the primary roadway.

However, during the course of approving this follow-up study, a comprehensive update of the procedures for the safety performance evaluation of highway features was published as

*NCHRP Report 350 (4)*. The test conditions used for evaluation under the basic test level, test level (TL) 3, in *Report 350* are fundamentally the same as those used in *Report 230* with small differences in impact speed attributed to a hard conversion to SI units of measurement. However, there was a significant departure in the design test vehicle specified by the two documents. *Report 350* specifies the use of a 3/4-ton pickup truck, designated 2000P, as the new design vehicle for evaluating the structural adequacy of a barrier. This vehicle replaces the 2,043 kg (4,500 lb) passenger sedan (4500S) used in the previous study under *Report 230*.

There are some major differences between the 2000P and 4500S which can have a profound effect on the impact performance of these vehicles with certain roadside features. Table 1 presents a comparison of several significant vehicular characteristics which were

Table 1. Comparison of Design Test Vehicles

Vehicle Property		2000P	4500S
C.G. Location, mm (in.)	above ground	711 (28)	559 (22)
	aft of front axle	1549 (61)	1295 (51)
Bumper Height, mm (in.)	top	711 (28)	533 (21)
	bottom	470 (18.5)	318 (12.5)
Front Overhang, mm (in.)		787 (31)	1092 (43)

considered particularly relevant to the design of the short-radius thrie-beam treatment. The dimensions shown for the 4500S are average values obtained from vehicles used in full-scale crash tests conducted in accordance with *Report 230* requirements. The properties shown for the 2000P are average values for 3/4-ton pickup trucks obtained from crash tests, parking lot surveys, and the literature. As shown in this table, the bumper height of the 2,043-kg (4,500-lb) passenger sedan typically ranges from 317.5 mm (12.5 in.) at the bottom to 533.4 mm (21 in.) at the top. In comparison, the bumper height of a typical 2000-kg pickup truck ranges from an average of 469.9 mm (18.5 in.) at the bottom to 711.2 mm (28 in.) at the top. As illustrated in Figure 4,

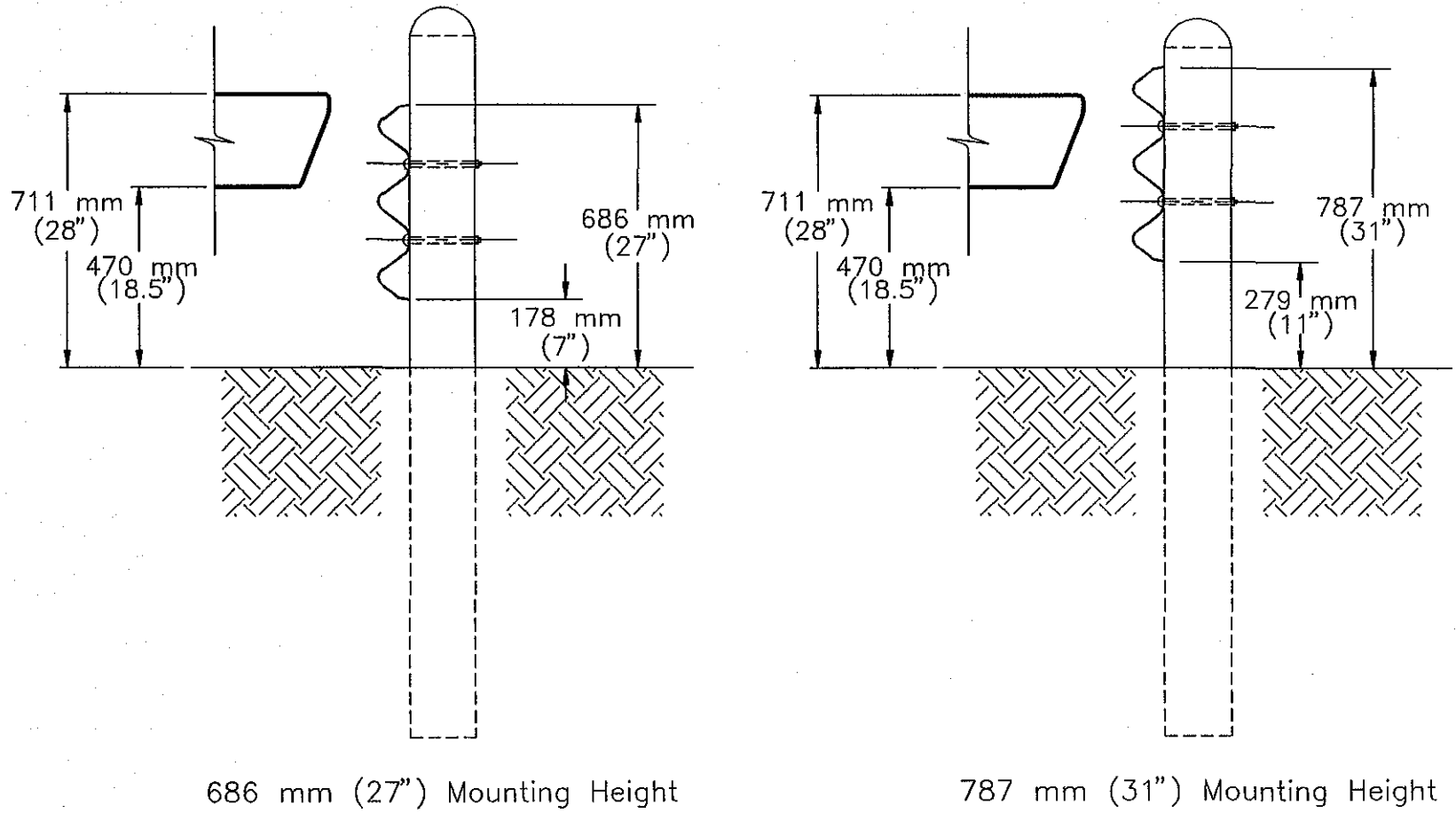


Figure 4. Bumper position of typical 2000P test vehicle.

this places the top of the bumper of the 2000P above the mounting height of 685.8 mm (27 in.) which is currently used for the standard metal beam guardfence and which was considered desirable for the new three-beam treatment. This fact, combined with a greater center-of-gravity (c.g.) height, significantly increases the potential for the 2000P test vehicle to override the rail element. It was therefore considered essential that the 787.4 mm (31-in.) standard mounting height of the three beam be maintained in order to increase the likelihood of containing the 3/4-ton pickup truck impacting into the curved portion of rail.

Another important design consideration, and an integral part of any short-radius guardrail treatment, is the transition from the guardrail to the rigid bridge rail. The transition must be strong enough to redirect a vehicle while preventing excessive pocketing or snagging of the vehicle with the transition or bridge rail end. This becomes even more critical when one considers that the average front overhang of a 3/4-ton pickup is 304.8 mm (12 in.) less than a typical 2,043-kg (4500-lb) passenger sedan (see Table 1). The shorter front overhang of the pickups increases the degree of interaction between the front tire of the vehicle and the barrier components. This additional wheel and frame interaction can result in more severe wheel snagging, greater vehicular decelerations, and increased deformation of the occupant compartment.

In addition to addressing the structural concerns mentioned above, it was desirable that the transition be capable of connecting with 685.8-mm (27-in.) tall bridge rails. This would increase the versatility and application of the short-radius system since many of TxDOT's standard bridge rails conform to this height restriction.

## **DESIGN IMPACT CONDITIONS**

Neither *NCHRP Report 350* (4), nor its predecessor *NCHRP Report 230* (3), provide definitive guidelines for short-radius curved guardrail treatments. In the absence of such guidelines, an attempt was made in Study 1263 (2) to define "worst case" impact conditions for short-radius treatments that were within general guidelines given in *Report 230* for design vehicles, impact speeds, and impact angles for more conventional barrier systems. These design impact conditions included (a) angled impacts into the curved portion of rail, (b) an angled impact in the transition region, and (c) an impact in the curved portion of rail with the vehicle approaching parallel to the normal direction of traffic on the primary roadway.

With one exception, these same tests were selected for use in evaluating the short-radius thrie-beam treatment. The test that was eliminated was impact condition (c). In this test, the centerline of the vehicle was aligned with the centerline of that portion of the rail parallel to the primary road. The purpose of this design impact was to insure that the vehicle did not spear or penetrate into the rigid tubular W-beam section that was used to transition to the bridge rail in the short-radius nested W-beam treatment. Since this previous test was very successful, and the short-radius thrie-beam design does not have a similar hardpoint, this test was considered unnecessary.

Generally speaking, the other test conditions remained unchanged with regard to vehicle weight, impact speed, impact angle, and impact location. However, since the tests were conducted under the general guidelines set forth in *NCHRP Report 350 (4)*, the 2,043-kg (4,500-lb) passenger sedan was replaced by a 2,000 kg (4,404 lb), 3/4-ton pickup truck. The final test matrix included (a) angled impacts into the curved section of rail with both a 820 kg (1,806 lb) passenger car and a 2,000 kg (4,404 lb) pickup truck at 100 km/h (62.1 mph) and at an angle of 20 and 25 degrees, respectively, and (b) an angled impact in the transition region with the 2000 kg (4,404 lb) pickup at 100 km/h (62.1 mph) and 25 degrees. For impact conditions (a), the centerlines of the test vehicles were aligned with the midpoint of the curved section of rail with the impact angle being defined as the angle between the normal direction of traffic on the primary road and the approach path of the impacting vehicle. For impact condition (c), the vehicle impact speed was 96.6 km/h (60 mph) and the impact angle was 25 deg.

## DESIGN PROCESS

Design of the short-radius thrie-beam treatment consisted of an iterative process. Initially, several design options were selected based on previous research and the collective judgement of the researchers. These designs were then evaluated by the Barrier VII computer simulation program (5) for the design impact conditions described in the previous section.

Barrier VII is a two-dimensional finite element simulation code that models vehicular impacts with deformable barriers. The program employs a sophisticated barrier model that is idealized as an assemblage of discrete structural members possessing geometric and material nonlinearities. The vehicle is idealized as a plain rigid body surrounded by a series of discrete inelastic springs. Because of its two-dimensional nature, the program is unable to predict

overriding or vaulting-type behavior. This represented a major limitation in its ability to predict the behavior of the 3/4-ton pickup during angled impacts into the curved region of rail. Nonetheless, Barrier VII was considered useful in making relative comparisons of occupant risk parameters and maximum dynamic deflection for the various design alternatives that were considered. The program was also used as a tool in the design of the transition section to predict dynamic deflections and the extent of snagging on the bridge end.

Modifications were then made as deemed necessary and the modified designs were again evaluated by Barrier VII for the design impact conditions. When applicable, critical design details identified in Study 1263 (2), such as radius of curvature, runout distance along the secondary roadway, and the use of weakened breakaway posts in the curved region, were incorporated directly into the new thrie beam design to minimize the development effort.

After the preliminary design options had been developed, the researchers worked closely with TxDOT personnel in selecting the final design details to help ensure the applicability and implementation of the system. Primary emphasis was to be placed on factors such as the types of bridge rails and anchorages typically used by TxDOT, the use of standard hardware items to help reduce cost and inventory, and other factors such as ease of installation and maintenance.

### **SHORT-RADIUS THRIE-BEAM DESIGN DETAILS**

The final short-radius thrie-beam guardrail treatment selected for full-scale crash testing is illustrated in Figure 5. It consists of two straight segments of guardrail connected by a curved section having a radius of 4.9 m (16 ft). The system extends approximately 9.8 m (32 ft) from the bridge end along the primary roadway, and approximately 18.3 m (60 ft) along the intersecting road. With the exception of the turndown and transition sections, the system is composed of single 10-ga. thrie beam rail mounted at a height of 787.4 mm (31 in.). The curved segments of thrie beam, as well as the straight segment of thrie beam along the secondary roadway, are supported at 1.9 m (6 ft-3 in.) intervals by weakened 177.8 mm (7-in.) diameter wood posts. The purpose of the weakened posts is to facilitate fracture during head-on impacts, thus reducing the potential for vehicle ramping. The posts are embedded 1.1 m (44 in.) and are weakened by drilling holes at the ground line and 406.4 mm (16 in.) below the ground line. This type of weakened post is commonly referred to as a CRT post.

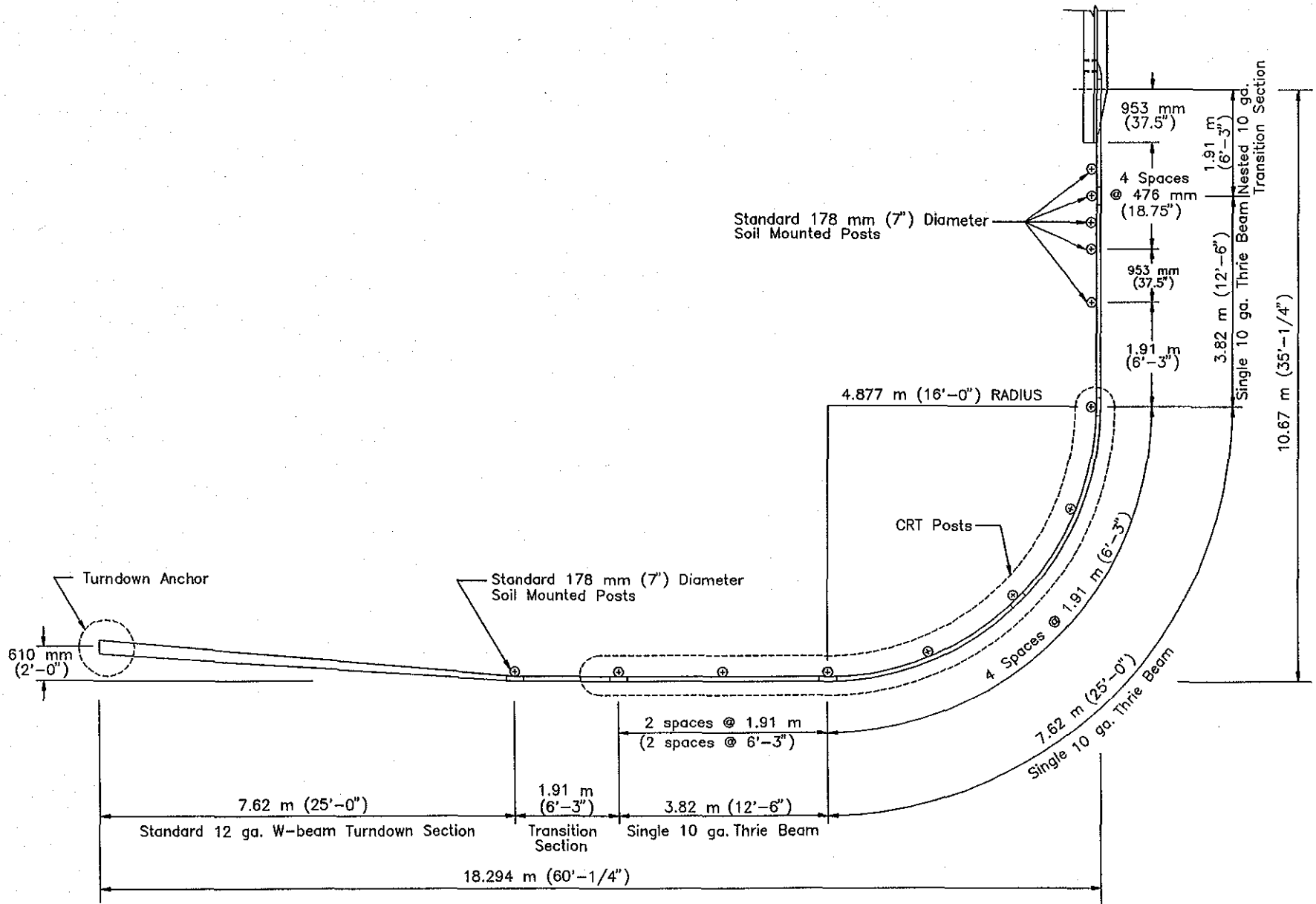


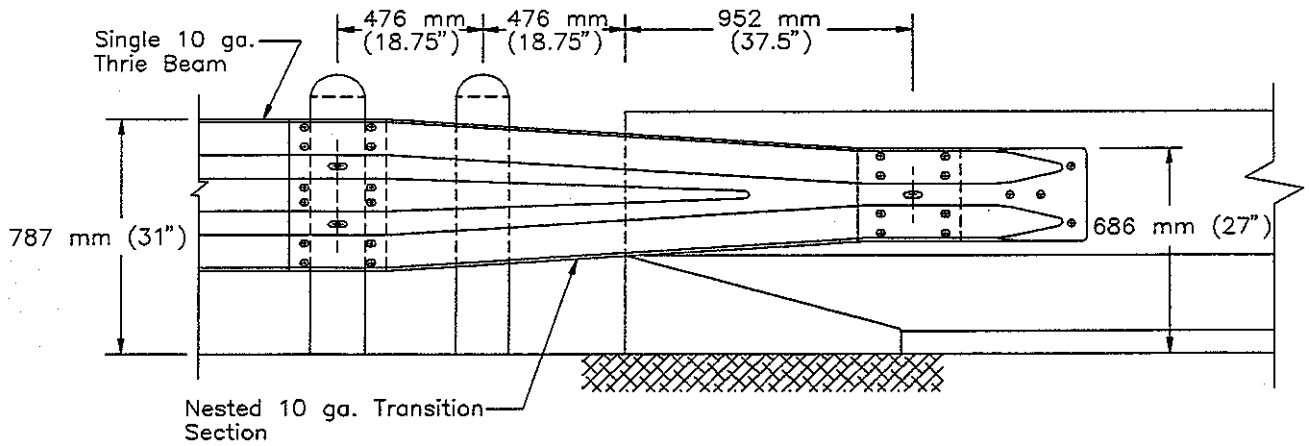
Figure 5. Short-radius thrie-beam guardrail transition.



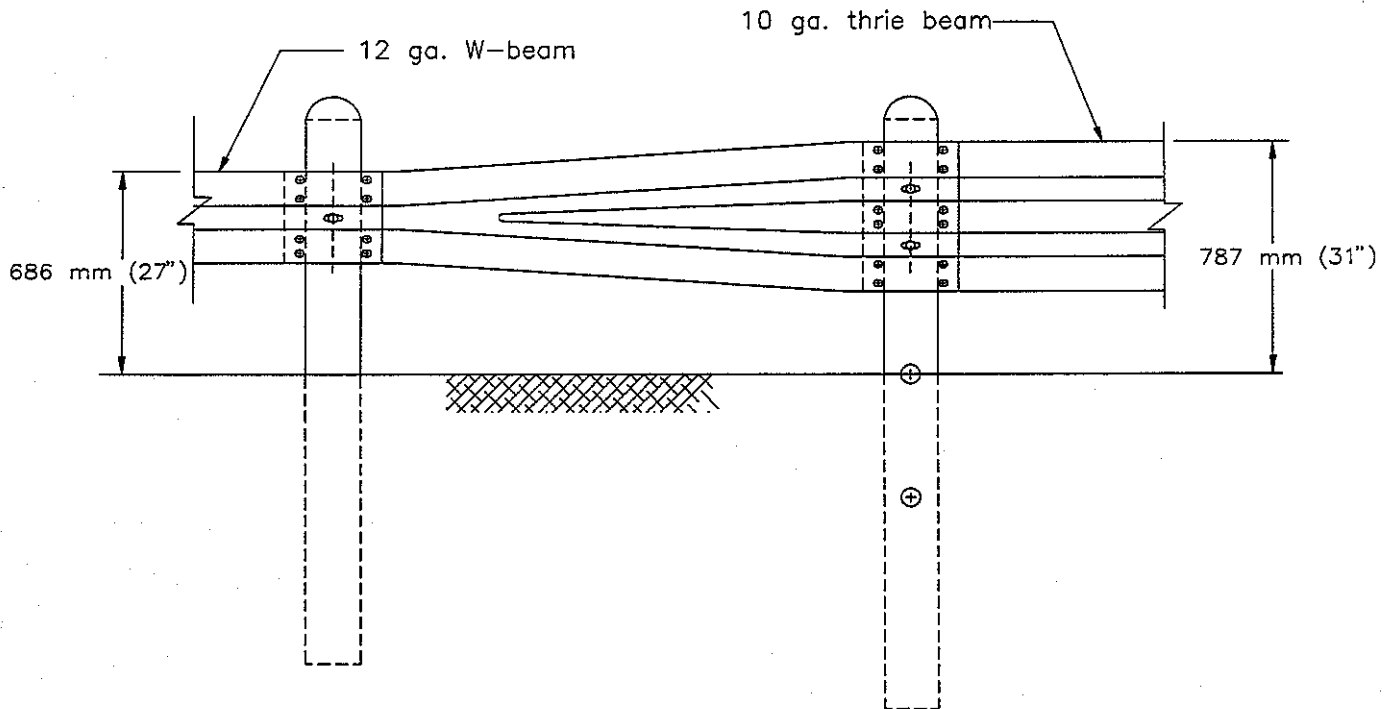
The design uses a standard 1.9 m (6 ft-3 in.) thrie beam-to-W-beam transition section to reduce the height of the rail from 787.4 mm (31 in.) to 685.8 mm (27 in.) at the bridge end connection. Use of this transition section permits connection of the short-radius treatment to 685.8 mm (27-in.) bridge parapets using a standard W-beam terminal connector. In order to increase shielding of the bridge end, the transition section is carried 952.5 mm (37.5 in.) onto the bridge parapet. This is the maximum distance that can be achieved without interfering with the sloped toe of the concrete safety-shaped barrier. To strengthen the transition region for angled impacts, the thrie beam-to-W-beam transition section is nested and the post spacing is reduced to 476.2 mm (18.75 in.) near the bridge end. Details of this transition region are shown in Figure 6(a).

The thrie beam on the intersecting roadway is transitioned to a W-beam using a transition section similar to that used at the bridge end. The treatment is then terminated with a 7.6 m (25 ft) W-beam turndown. Details of the transition on the secondary roadway are shown in Figure 6(b).

In addition to satisfying all of the design impact conditions, it was believed that the thrie beam system would be easier to install than the nested W-beam system. Installation of the curved, nested W-beam rail proved to be very difficult. Since the splice holes did not readily align, forced alignment (by use of driven alignment pins) was required to install the splice bolts. Splicing a single curved thrie beam is considerably less difficult. Furthermore, the material costs of the thrie beam system are equal to or less than the nested W-beam system due to the elimination of the intermediate BCT anchorage and the welded tubular W-beam section.



(a) transition to concrete bridge parapet



(b) transition to W-beam turndown section along secondary roadway

Figure 6. Thrie beam to W-beam transition section.

### III. CRASH TEST PROCEDURES

#### ELECTRONIC INSTRUMENTATION AND DATA PROCESSING

Each test vehicle was instrumented with three solid-state angular rate transducers to measure roll, pitch and yaw rates; a triaxial accelerometer at the vehicle center-of-gravity to measure longitudinal, lateral, and vertical acceleration levels; and a back-up biaxial accelerometer in the rear of the vehicle to measure longitudinal and lateral acceleration levels. The accelerometers were strain gauge type with a linear millivolt output proportional to acceleration.

The electronic signals from the accelerometers and transducers were transmitted to a base station by means of constant bandwidth FM/FM telemetry link for recording on magnetic tape and for display on a real-time strip chart. Provision was made for the transmission of calibration signals before and after the test, and an accurate time reference signal was simultaneously recorded with the data. Pressure-sensitive contact switches on the bumper were actuated just prior to impact by wooden dowels to indicate the elapsed time over a known distance to provide a measurement of impact velocity. The initial contact also produced an "event" mark on the data record to establish the exact instant of contact with the luminaire support.

The multiplex of data channels, transmitted on one radio frequency, was received at a data acquisition station, and demultiplexed into separate tracks of Intermediate Range Instrumentation Group (I.R.I.G.) tape recorders. After the test, the data were played back from the tape machines, filtered with a SAE J211 Class 180 filter, and were digitized using a microcomputer for analysis and evaluation of impact performance. The digitized data were then processed using two computer programs: DIGITIZE and PLOTANGLE. Brief descriptions on the functions of these two computer programs are given below.

The DIGITIZE program uses digitized data from vehicle-mounted linear accelerometers to compute occupant/compartiment impact velocities, time of occupant/compartiment impact after vehicle impact, and the highest 10-msec average ridedown acceleration. The DIGITIZE program also calculates a vehicle impact velocity and the change in vehicle velocity at the end of a given impulse period. In addition, maximum average accelerations over 50-msec intervals in each of the three directions are computed. Acceleration versus time curves for the longitudinal, lateral,

and vertical directions are then plotted from the digitized data of the vehicle-mounted linear accelerometers using a commercially available software package.

The PLOTANGLE program uses the digitized data from the yaw, pitch, and roll rate charts to compute angular displacement in deg at 0.00067-second intervals and then instructs a plotter to draw a reproducible plot of yaw, pitch, and roll versus time. It should be noted that these angular displacements are sequence dependent with the sequence being yaw-pitch-roll for the data presented herein. These displacements are in reference to the vehicle-fixed coordinate system with the initial position and orientation of the vehicle-fixed coordinate system being those which existed at initial impact.

## **PHOTOGRAPHIC INSTRUMENTATION AND DATA PROCESSING**

Photographic coverage of each test included three high-speed cameras: one overhead with a field of view perpendicular to the ground and directly over the impact point; one placed to have a field of view parallel to and aligned with the tangent of the guardrail treatment; and a third placed behind the short-radius treatment at an angle. A flash bulb activated by pressure-sensitive tapeswitches was positioned on the impacting vehicle to indicate the instant of contact with the support structure and was visible from each camera. The films from these high-speed cameras were analyzed on a computer-linked Motion Analyzer to observe phenomena occurring during the collision and to obtain time-event, displacement, and angular data. A professional video camera and a Betacam videotape recorder along with still cameras were used for documentary purposes and to record conditions of the test vehicle and test installation before and after the test.

## **TEST VEHICLE PROPULSION AND GUIDANCE**

The test vehicles were towed into the support structure using a steel cable guidance and reverse tow system. A steel cable for guiding the test vehicles was tensioned along the impact path, anchored at each end, and threaded through a guide plate attachment anchored to the front wheel of the test vehicle. Another steel cable was connected to the test vehicles, passed around a pulley near the impact point, through a pulley on the tow vehicle, and then anchored to the ground such that the tow vehicle moved away from the test site. A 2-to-1 speed ratio between the test and tow vehicle existed with this system. Just prior to impact with the guardrail system, the test vehicle was released to be free-wheeling and unrestrained. The vehicle remained free-

wheeling, i.e., no steering or braking inputs, until the vehicle cleared the immediate area of the test site, at which time brakes on the vehicle were activated to bring the vehicle to a safe and controlled stop.

## IV. FULL-SCALE CRASH TEST RESULTS

A total of five crash tests were conducted on the short-radius three-beam system. The initial objective of the test program was to develop a system which meets the requirements of *NCHRP Report 350*. However, when attempts to contain the 3/4-ton pickup truck during angled impacts into the curved section of rail were unsuccessful, the remaining project resources were devoted toward obtaining a system which meets *NCHRP Report 230* criteria. Following is a summary of each test and modifications made to the design and test matrix during the course of the test program. Sequential photographs of the tests are shown in Appendix A. Vehicular acceleration traces are presented in Appendix B, and vehicular angular displacements are given in Appendix C.

### TEST 1442-1

This test was conducted to ascertain the redirective capability of the transition from the short-radius guardrail treatment's transition to a concrete safety-shaped barrier (CSSB). The geometry of the CSSB was considered to be critical in terms of the potential for vehicular snagging on the end of the parapet. The test conditions followed the recommendations of *NCHRP Report 350 (4)* for transition impacts. The impact location for this test was 1.7 m (5.5 ft) upstream from the end of the safety shape which was determined to be the critical impact point along the transition. The critical impact location is defined as the location which maximizes the potential for vehicle contact on the end of the bridge parapet.

The test vehicle for this test was a 1986 2500 Series Chevrolet pickup shown in Figure 7. A plan view of the test installation is given in Figure 5. Photos of the completed test installation are shown in Figure 8. Test inertia mass of the vehicle was 2000 kg (4409 lb), and its gross static mass was also 2000 kg (4409 lb). The bumper height of the pickup varied from 450 mm (17.7 in.) at its lower edge to 678 mm (26.7 in.) at its upper edge. Additional dimensions and information pertaining to the test vehicle are given in Figure 9. Figure 10 presents the profile of the pickup in relation to the barrier. The vehicle impacted the transition at a speed of 98.1 km/h (60.9 mph) at an angle of 26.0 degrees relative to the tangent section of rail along the primary roadway.



Figure 7. Vehicle before test 414424-1.

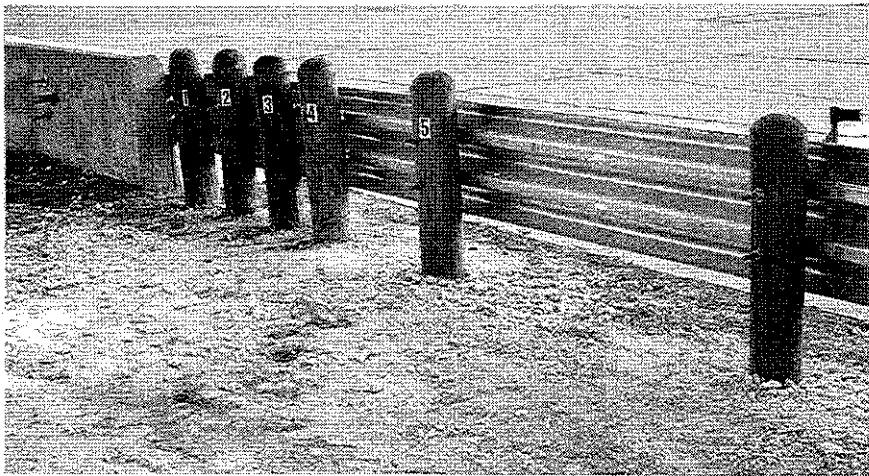
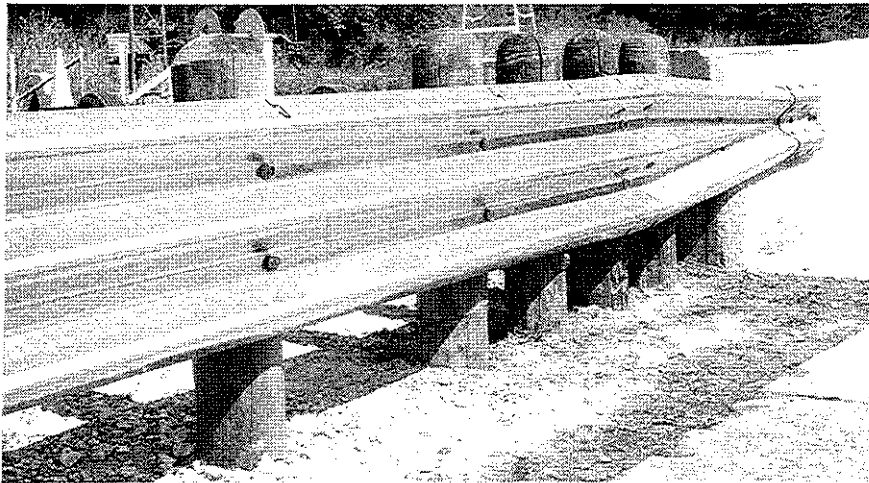
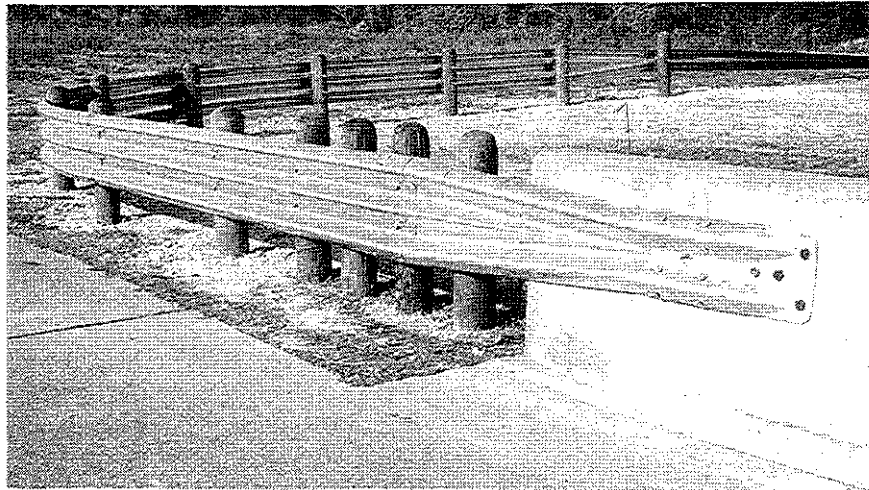


Figure 8 . Installation before test 414424-1.

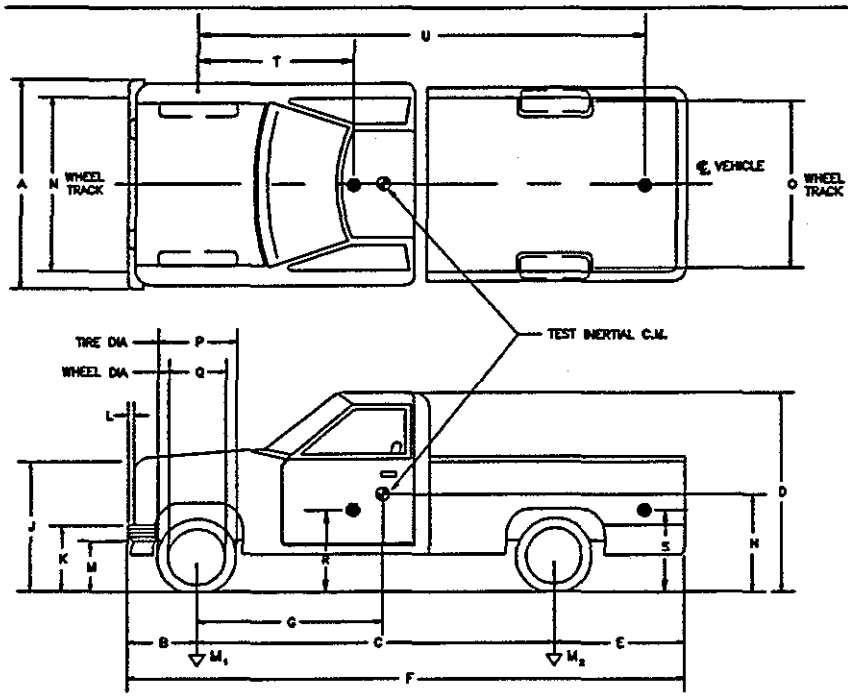


DATE: 7-27-94 TEST NO.: 414424-1 VIN NO.: 1GCGC24M5GS129784 MAKE: Chevy  
 MODEL: 2500 YEAR: 1986 ODOMETER: 85334 GVW: 3900  
 TIRE SIZE: LT235 85/R16 TIRE INFLATION PRESSURE: \_\_\_\_\_ TREAD TYPE: \_\_\_\_\_

MASS DISTRIBUTION (kg) LF 532 RF 554 LR 473 RR 441

DESCRIBE ANY DAMAGE TO VEHICLE PRIOR TO TEST:

Windshield cracked marked



● Denotes accelerometer location.  
 NOTES: \_\_\_\_\_  
 \_\_\_\_\_  
 \_\_\_\_\_

ENGINE TYPE: 8 cyl Gasoline  
 ENGINE CID: 5.7 L

TRANSMISSION TYPE:  
 AUTO  
 MANUAL

OPTIONAL EQUIPMENT:  
 \_\_\_\_\_  
 \_\_\_\_\_  
 \_\_\_\_\_

DUMMY DATA:  
 TYPE: \_\_\_\_\_  
 MASS: \_\_\_\_\_  
 SEAT POSITION: \_\_\_\_\_

GEOMETRY - (mm)

A	1940	E	1330	J	1145	N	1670	R	645
B	820	F	5490	K	678	O	1670	S	991
C	3340	G	1526.4	L	70	P	775	T	1540
D	1830	H		M	450	Q	450	U	4175

<u>MASS - (kg)</u>	<u>CURB</u>	<u>TEST INERTIAL</u>	<u>GROSS STATIC</u>
M <sub>1</sub>	<u>1145</u>	<u>1086</u>	_____
M <sub>2</sub>	<u>891</u>	<u>914</u>	_____
M <sub>T</sub>	<u>2036</u>	<u>2000</u>	_____

Figure 9. Vehicle properties for test 414424-1.

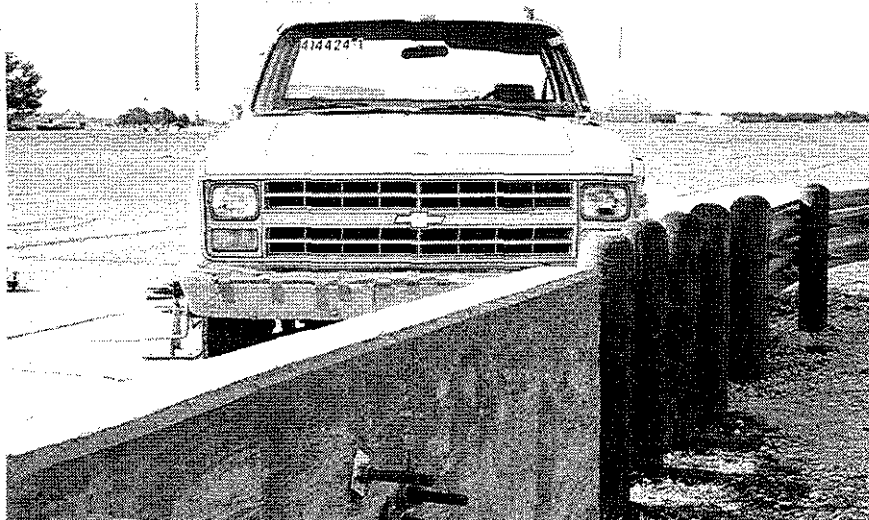
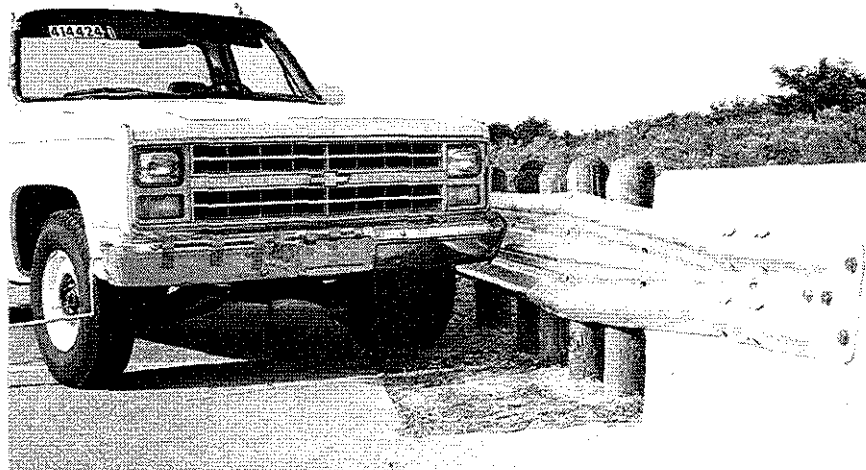


Figure 10. Vehicle/installation geometrics for test 414424-1.

Shortly after impact, the front wheels were pulled hard to the left, apparently as a result of contact with the concrete parapet. As the vehicle continued to be redirected, the front end became airborne. After being in contact with the barrier for a distance of 4.78 m (15.7 ft), the vehicle safely exited the test installation traveling at a speed of 66.8 km/h (41.5 mph) and an exit angle of 2.5 degrees. The vehicle came to rest 41.1 m (135 ft) downstream from the point of impact adjacent to the concrete barrier as shown in Figure 11. A summary of the test data is presented in Figure 12.

Damage to the test installation is shown in Figure 13. The first three posts adjacent to the bridge end were fractured at ground level, and post 4 was deflected laterally approximately 57 mm (2.25 in.). Although the end of the safety-shaped barrier was cracked, there was no visible evidence of wheel contact on the end of the barrier. The maximum residual deformation was measured to be 127 mm (5.0 in.). The maximum dynamic deflection was not obtained.

Figure 14 shows the damage sustained by the test vehicle. The maximum crush was measured to be 580 mm (22.8 in.) at the left front corner of the vehicle at bumper height. The driver side door was deformed outward 160 mm (6.3 in.), and the floorpan was pushed inward toward the occupant compartment 95 mm (3.75 in.). The wheelbase was measured to be 2980 mm (117.3 in.) and 3320 mm (130.7 in.) on the driver and passenger sides, respectively.

In summary, this test was judged to be a success. First and foremost, the installation successfully contained and redirected the test vehicle. Although not required in the evaluation of a strength test, the occupant risk indices were all well within the recommended limits of *NCHRP Report 350*. In addition, the vehicle remained upright and stable both during the impact event and after exiting from the installation. Although the deformation to the floorpan of the occupant compartment was significant, it was not considered to be life threatening.

## **TEST 1442-2**

The installation for this test was identical to the one evaluated in Test 1442-1. Photos of the completed test installation are shown in Figure 15. The purpose of this test was to determine if the short-radius thrie-beam system could safely contain a 3/4-ton pickup truck without allowing vehicular override or penetration through the barrier.

The test vehicle for this test was a 1985 2500 Series Chevrolet pickup shown in Figure 16. The height to the lower edge of the bumper was 445 mm (17.5 in.), and the height to the

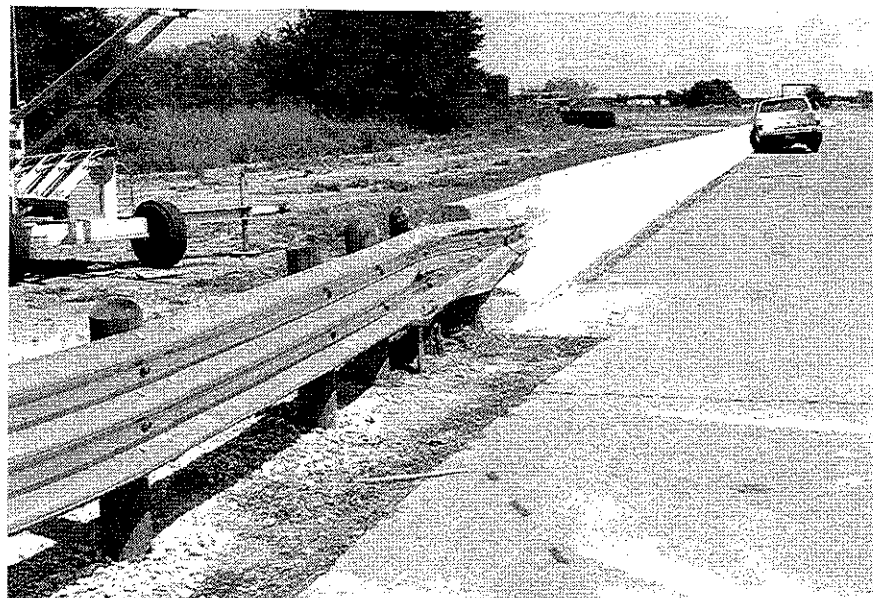
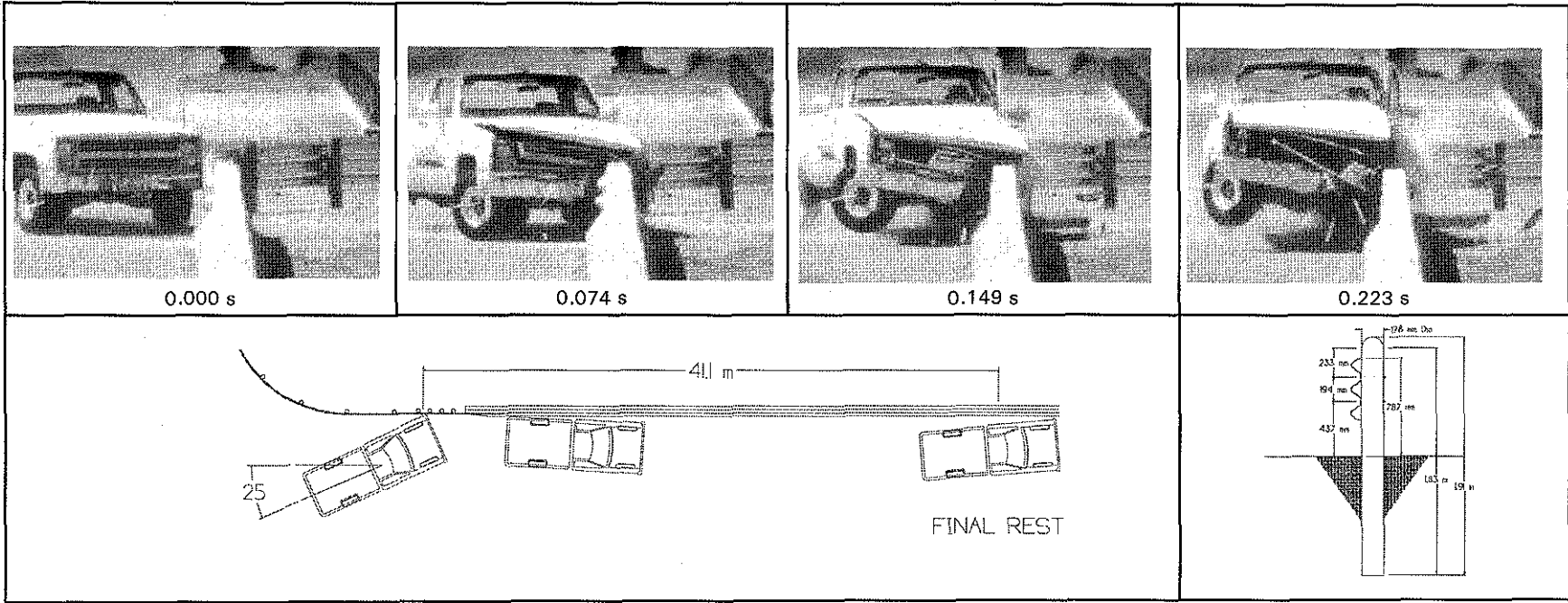


Figure 11. After impact trajectory, test 414424-1.



<b>General Information</b>		<b>Impact Conditions</b>		<b>Test Article Deflections (m)</b>	
Test Agency	Texas Transportation Institute	Speed (km/h)	98.1 (60.9 mi/h)	Dynamic	Unavailable
Test No.	414424-1	Angle (deg)	26.0	Permanent	0.09 (0.29 ft)
Date	07/27/94	<b>Exit Conditions</b>		<b>Vehicle Damage</b>	
<b>Test Article</b>		Speed (km/h)	66.8 (41.5 mi/h)	<b>Exterior</b>	
Type	Short Radius Guardrail	Angle (deg)	2.5	VDS	FL-6
Name or Manufacturer	TxDOT	<b>Occupant Risk Values</b>		CDC	11FLEW5
Installation Length (m)	4.8 m (16.0 ft) Radius	Impact Velocity (m/s)		<b>Interior</b>	
Size and/or dimension and material of key elements	Thriebeam Guardrail	x-direction	7.3 (24.1 ft/s)	OCDI	LF0115100
Soil Type and Condition	17.8 cm (7.0 in) Round Posts	y-direction	8.0 (26.2 ft/s)	<b>Maximum Exterior</b>	
Test Vehicle	Strong soil, Dry	THIV (optional)		Vehicle Crush (mm)	705 (27.8 in)
Type	Production	Ridedown Accelerations (g's)		Max. Occ. Compart. Deformation (mm)	95 (3.78 in)
Designation	2000P	x-direction	-7.1	<b>Post-Impact Behavior</b>	
Model	1986 Chevrolet Pickup	y-direction	11.7	Max. Roll Angle (deg)	-18.8
Mass (kg) Curb	2036 (4488 lb)	PHD (optional)		Max. Pitch Angle (deg)	5.8
Test Inertial Dummy	2000 (4409 lb)	ASI (optional)		Max. Yaw Angle (deg)	21.3
Gross Static	2000 (4409 lb)	Max. 0.050-sec Average (g's)			
		x-direction	10.0		
		y-direction	10.6		
		z-direction	-12.5 (Floor Pan Bent)		

Figure 12. Summary of results for test 414424-1.

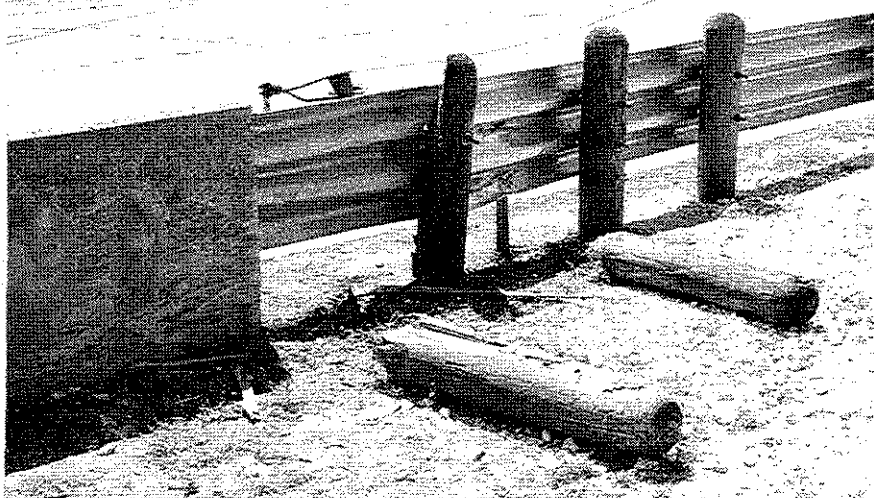
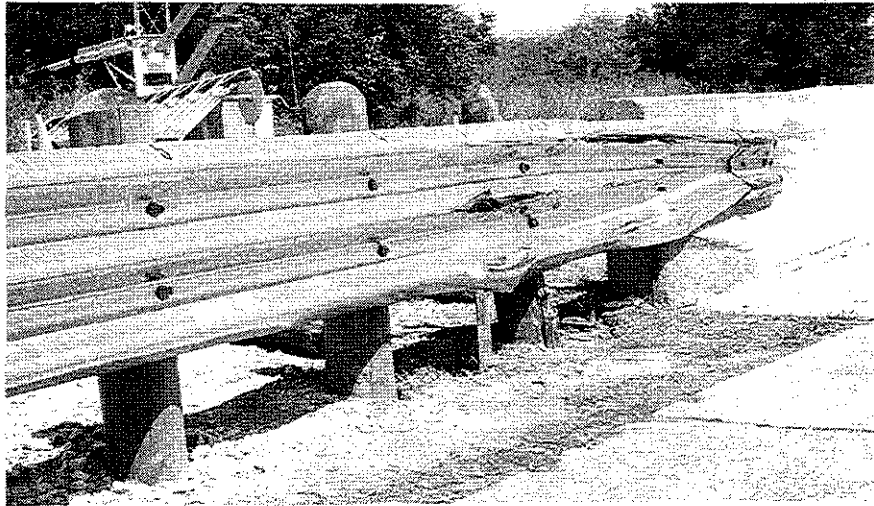
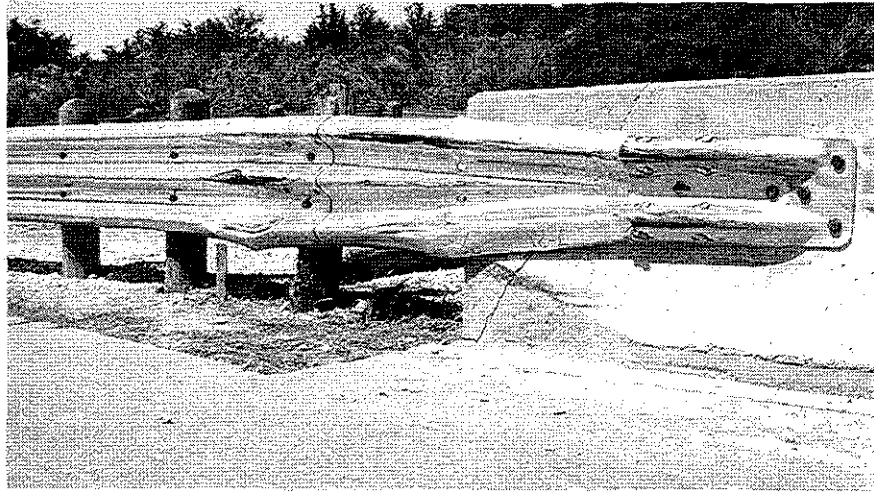


Figure 13. Installation after test 414424-1.



Figure 14. Vehicle after test 414424-1.

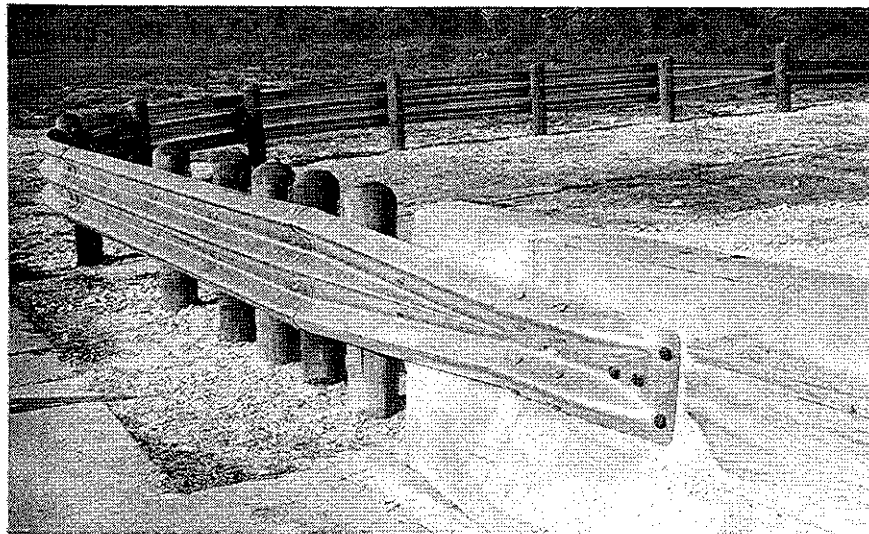
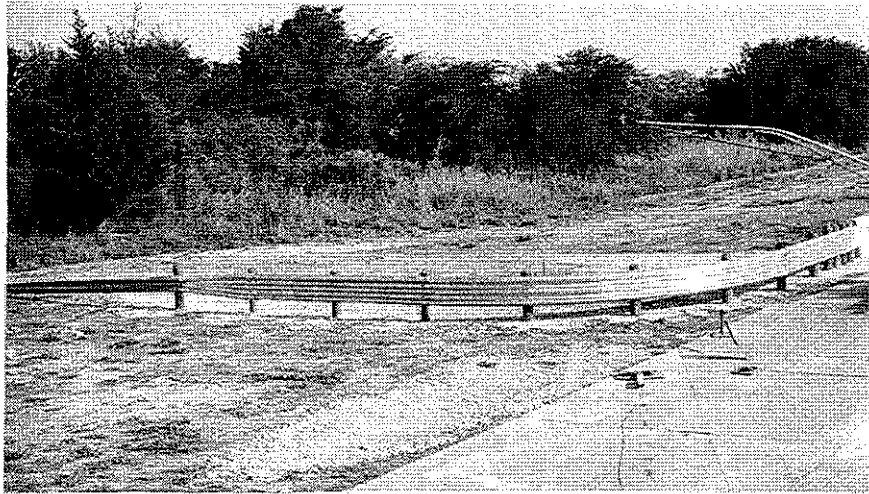


Figure 15. Installation before test 414424-2.





Figure 16. Vehicle before test 414424-2.

upper edge of the bumper was 680 mm (26.8 in.). Additional dimensions and information pertaining to the test vehicle are given in Figure 17. The vehicle and barrier geometrics are shown in Figure 18. The vehicle impacted the midpoint of the curved section of rail traveling at a speed of 101.4 km/h (63.0 mph) at an angle of 25.6 degrees relative to the tangent section of rail along the primary roadway.

Shortly after impact, the three-beam rail began to twist, with the top edge rotating downward and away from the impacting vehicle. As the vehicle proceeded forward, the bumper of the vehicle overrode the barrier allowing the front tires to climb the dropping three beam rail. The vehicle subsequently became airborne and vaulted the barrier. At the time of separation, the vehicle was traveling at a speed of 75.9 km/h (47.2 mph) and an angle of 23.5 degrees. The vehicle came to rest 57.6 m (189.0 ft) downstream and 14.6 m (48.0 ft) behind the point of impact. A summary of the test data is presented in Figure 19.

Damage to the test installation is shown in Figure 20. Posts 7, 8, 9, 10 in the curved section of rail all broke at ground level. Maximum dynamic deflection was 3.05 m (10.0 ft), and the maximum residual deformation was 2.84 m (9.3 ft) at post 8. As shown in Figure 21, damage sustained by the vehicle was relatively minor. The maximum crush was recorded to be 280 mm (11.0 in.) at the left front corner at bumper height.

This test was judged to be a failure since it failed to contain the test vehicle. Analysis of the high-speed film appeared to indicate that the posts in the impact region were at least partially responsible for the observed twisting and dropping behavior of the rail. It was theorized that the posts were rotating in the soil and initiating the rotation of the three beam before they had sufficient time to release from the rail and/or fracture at the ground line. The short-radius treatment was subsequently modified in an attempt to minimize this behavior. The modification consisted of removing the post bolts from posts 7, 8, and 9 in the curved section of rail. A 3/8-in diameter lag screw was used to provide vertical support to the rail at these locations. The modified system was then retested as described below.

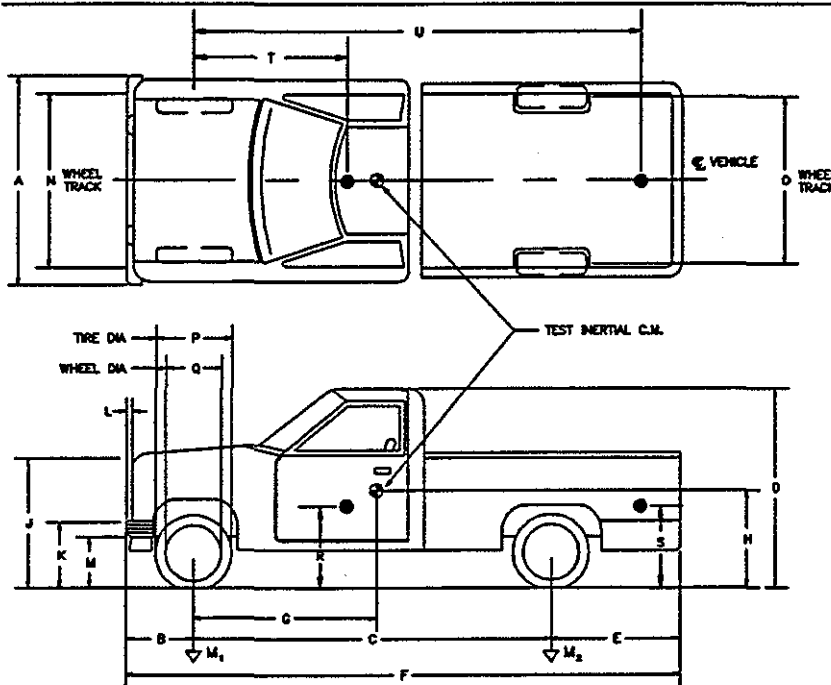
### **TEST 1442-3**

In an effort to decrease the rotation of the three-beam rail observed in the previous test, the post bolts were removed from several posts in the curved section of rail. The pickup-truck

DATE: 7-29-94 TEST NO.: 414424-2 VIN NO.: 1GCGC24H7FS121653 MAKE: Chevy  
 MODEL: Custom Deluxe YEAR: 1985 ODOMETER: 27457 GVW: 3900 KG  
 TIRE SIZE: 7.50 16 TIRE INFLATION PRESSURE: \_\_\_\_\_ TREAD TYPE: Hwy

MASS DISTRIBUTION (kg) LF 565 RF 537 LR 444 RR 454

DESCRIBE ANY DAMAGE TO VEHICLE PRIOR TO TEST:



● Denotes accelerometer location.

NOTES: \_\_\_\_\_

ENGINE TYPE: 8 cyl Gasoline

ENGINE CID: 5.7 L

TRANSMISSION TYPE:

AUTO  
 MANUAL

OPTIONAL EQUIPMENT:

DUMMY DATA:

TYPE: \_\_\_\_\_

MASS: \_\_\_\_\_

SEAT POSITION: \_\_\_\_\_

GEOMETRY - (mm)

A	1960	E	1320	J	1140	N	1680	R	650
B	830	F	5480	K	680	O	1670	S	980
C	3330	G	1495.2	L	76	P	820	T	154.5
D	1860	H		M	445	Q	447	U	4105

<u>MASS - (kg)</u>	<u>CURB</u>	<u>TEST INERTIAL</u>	<u>GROSS STATIC</u>
M <sub>1</sub>	1179	1102	_____
M <sub>2</sub>	915	898	_____
M <sub>T</sub>	2094	2000	_____

Figure 17. Vehicle properties for test 414424-2.

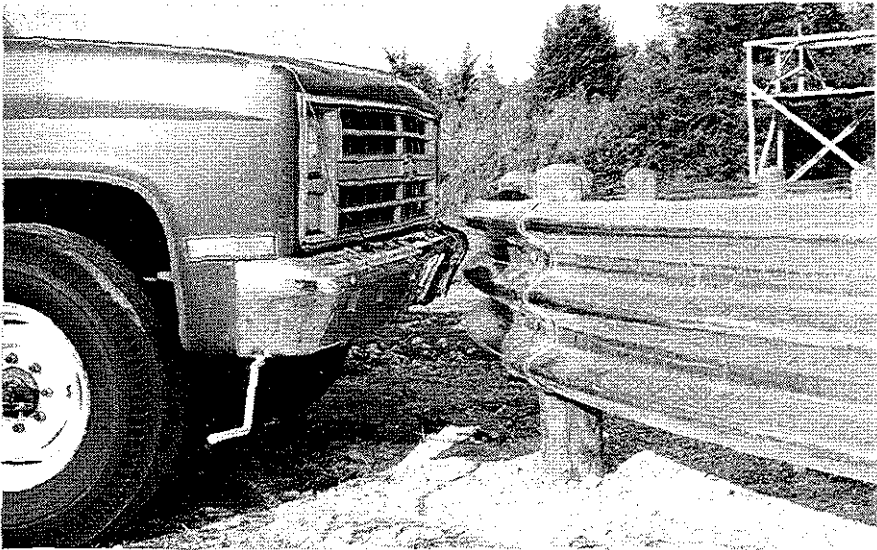
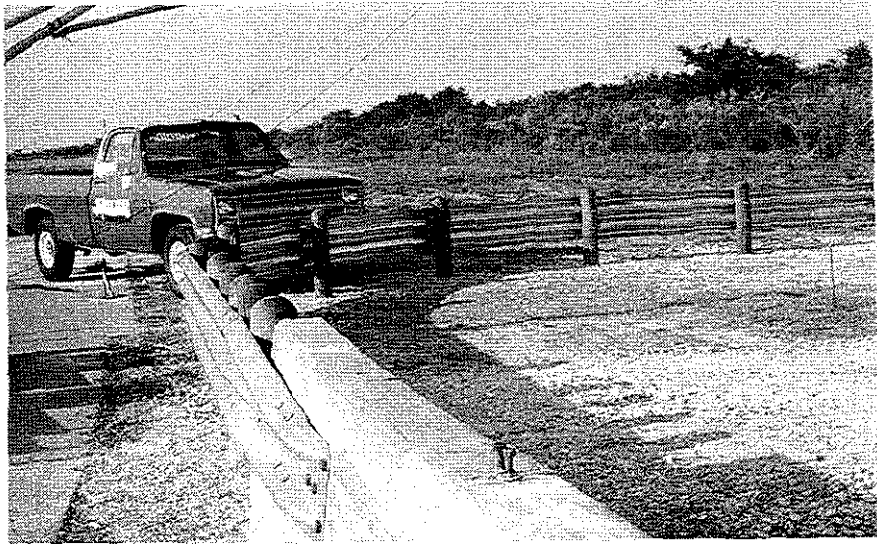
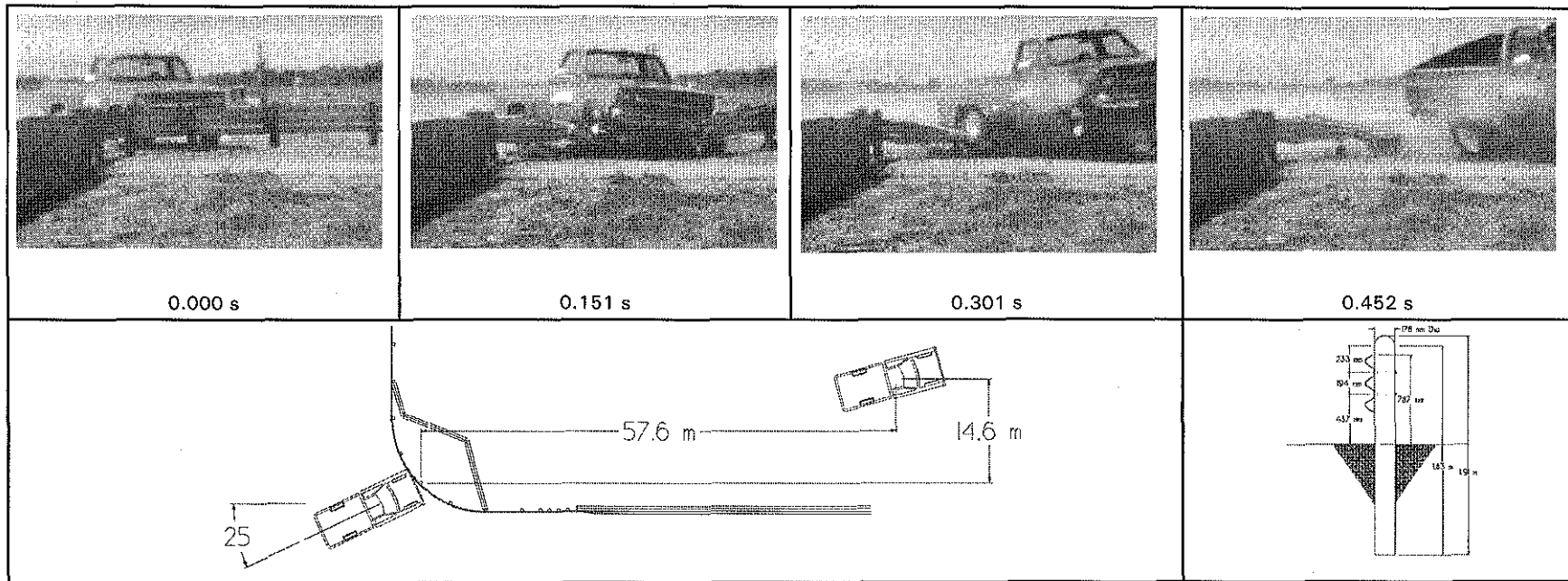


Figure 18. Vehicle/installation geometrics for test 414424-2.



<b>General Information</b>		<b>Impact Conditions</b>		<b>Test Article Deflections (m)</b>	
Test Agency	Texas Transportation Institute	Speed (km/h)	101.4 (63.0 mi/h)	Dynamic	3.05 (10.0 ft)
Test No.	414424-2	Angle (deg)	25.6	Permanent	2.84 (9.3 ft)
Date	07/29/94	<b>Exit Conditions</b>		<b>Vehicle Damage</b>	
<b>Test Article</b>		Speed (km/h)	75.9 (47.2 mi/h)	<b>Exterior</b>	
Type	Short Radius Guardrail	Angle (deg)	23.5	VDS	FD-2
Name or Manufacturer	TxDOT	<b>Occupant Risk Values</b>		CDC	12FDEW1
Installation Length (m)	4.8 m (16.0 ft) Radius	Impact Velocity (m/s)		<b>Interior</b>	
Size and/or dimension and material of key elements	Thriebeam Guardrail 17.8 cm (7.0 in) Round Posts	x-direction	5.2 (17.2 ft/s)	OCDI	AS0000000
Soil Type and Condition	Strong soil, Dry	y-direction	0.8 (2.6 ft/s)	<b>Maximum Exterior</b>	
<b>Test Vehicle</b>		THIV (optional)		Vehicle Crush (mm)	280 (11.0in)
Type	Production	Ridedown Accelerations (g's)		<b>Max. Occ. Compart.</b>	
Designation	2000P	x-direction	-10.4	Deformation (mm)	0
Model	1985 Chevrolet Pickup	y-direction	5.6	<b>Post-Impact Behavior</b>	
Mass (kg) Curb	2094 (4616 lb)	PHD (optional)		Max. Roll Angle (deg)	29.1
Test Inertial Dummy	2000 (4409 lb)	ASI (optional)		Max. Pitch Angle (deg)	7.3
Gross Static	2000 (4409 lb)	Max. 0.050-sec Average (g's)		Max. Yaw Angle (deg)	-12.6
		x-direction	-6.0		
		y-direction	-3.9		
		z-direction	-4.3		

Figure 19. Summary of results for test 414424-2.

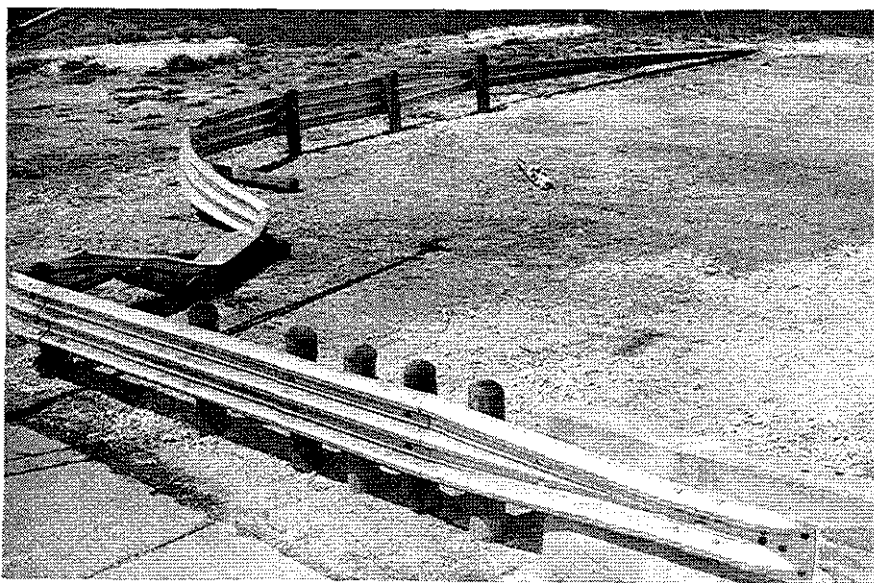
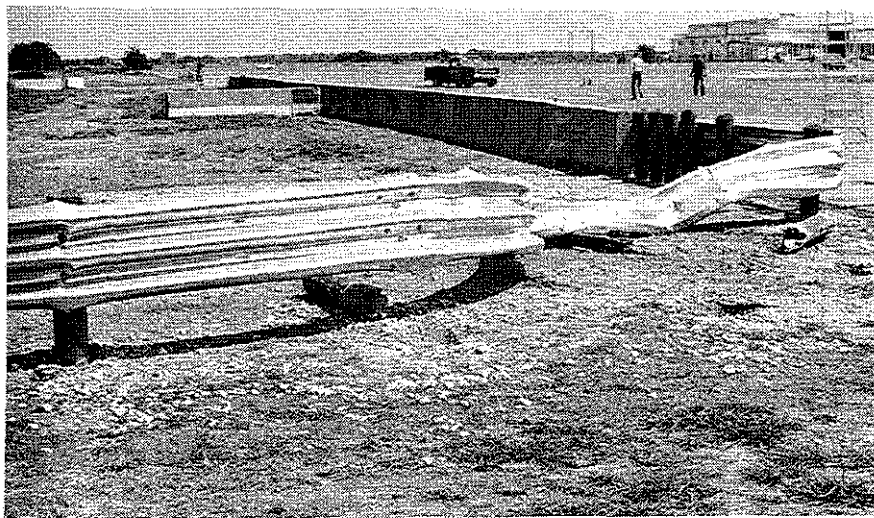


Figure 20. Installation after test 414424-2.

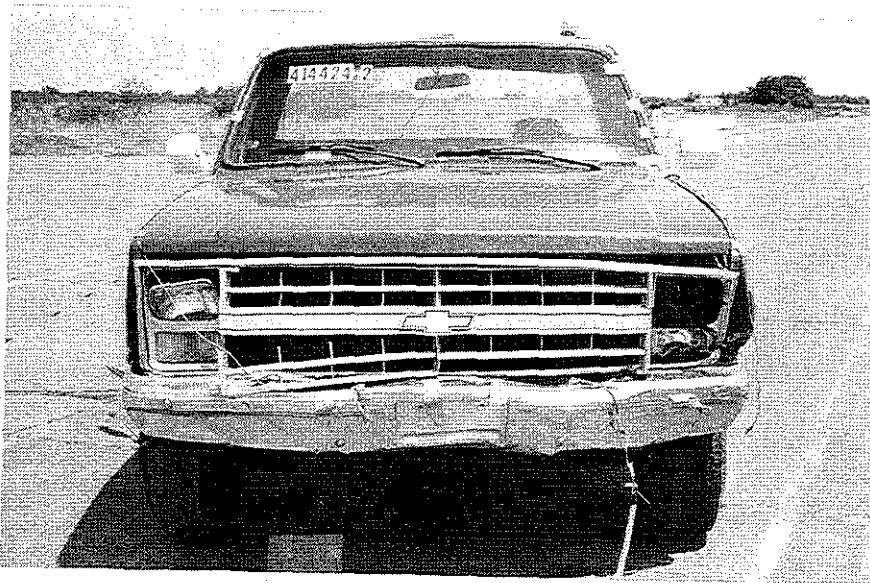


Figure 21. Vehicle after test 414424-2.

test was then repeated using the same impact conditions as Test 1442-2. Photographs of the modified system are shown in Figure 22.

A 1988 F250 Series Ford pickup, shown in Figure 23, was used for this retest. The bumper height of the pickup ranged from 470 mm (18.5 in.) to 710 mm (28.0 in.) Additional dimensions and information pertaining to the test vehicle are given in Figure 24. The vehicle profile in relation to the test installation is shown in Figure 25. The vehicle impacted the midpoint of the curved section of rail (post 8) at a speed of 101.4 km/h (63.0 mph) at an angle of 24.6 degrees.

The observed impact behavior of this test was virtually identical to that of the previous test. Immediately after impact, the thrie-beam rail began to twist and drop, allowing the test vehicle to climb over the barrier and penetrate behind the installation. At time of separation, the vehicle was traveling at a speed of 79.3 km/h (49.3 mph) at an angle of 22.9 degrees relative to the tangent section of rail along the primary roadway. As it traveled behind the test installation, the vehicle impacted a tree and eventually came to rest 31.7 m (104 ft) downstream and 18.3 m (60 ft) behind the point of impact. A summary of the test results is presented in Figure 26.

Damage to the test installation is shown in Figure 27. As in the previous test, posts 7, 8, 9, 10 in the curved section of rail all broke at ground level. Maximum dynamic deflection was 3.27 m (10.7 ft), and the maximum residual deformation was 2.90 m (9.5 ft) at post 8. Damage to the test vehicle is shown in Figure 28. Most of the damage was sustained in the secondary impact with a tree after the vehicle vaulted the test installation.

As with the previous test, the test installation failed to contain the 3/4-ton pickup truck and, therefore, the test was judged to be a failure. After close examination of the test results, it was concluded that the rotation of the rail was attributable to a combination of the low torsional stiffness of the open thrie-beam section and the eccentric loading applied by the bumper of the vehicle on the upper portion of the rail. Based on this analysis, it became evident that any potential solutions to this problem would require substantial modifications to the short-radius system along with some level of developmental testing. After consultation with TxDOT personnel, it was mutually decided that the best use of the remaining project resources would be to certify the short-radius thrie-beam design under *NCHRP Report 230 (3)*. This approach would provide TxDOT with a crashworthy short-radius treatment that could be implemented until such time that a treatment meeting the requirements of *NCHRP Report 350* can be developed. Since



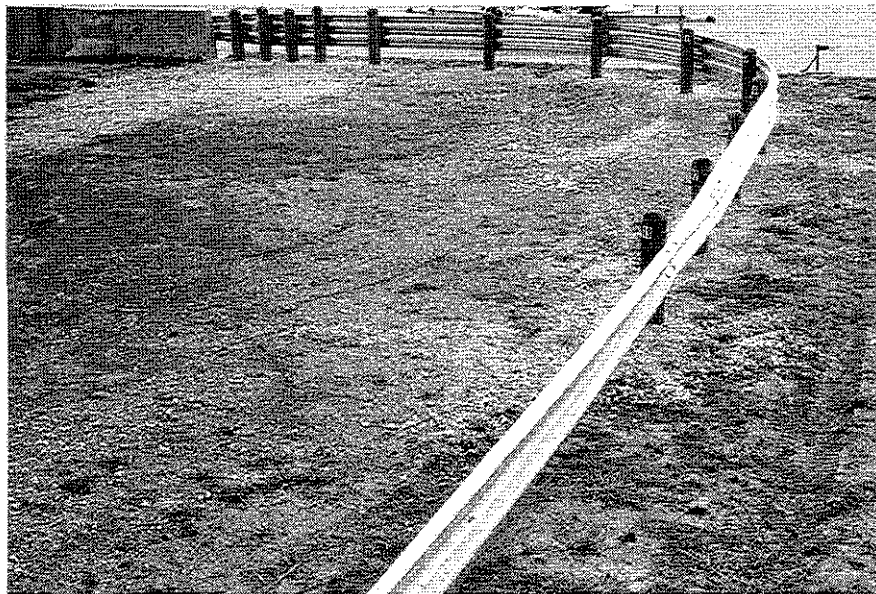
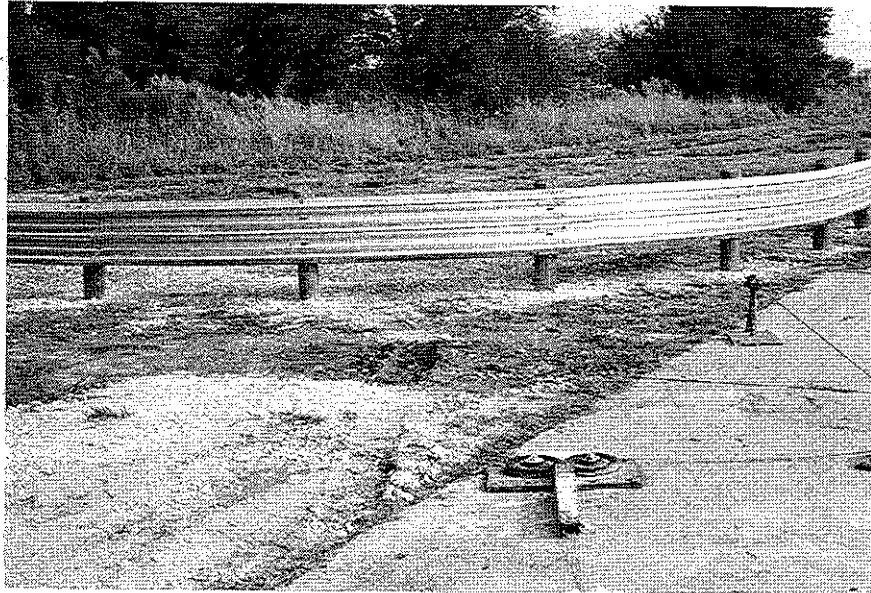


Figure 22. Installation before test 414424-3.



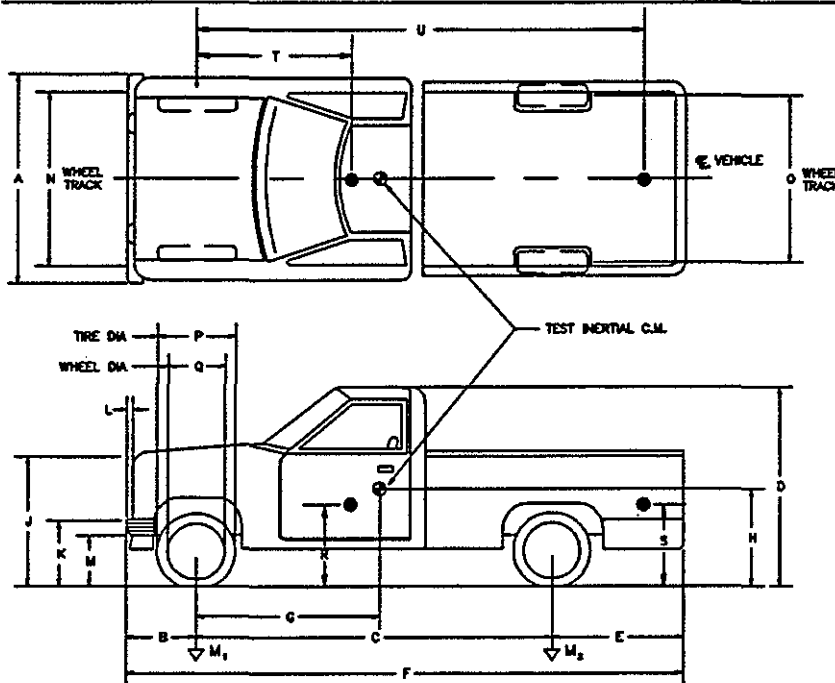
Figure 23. Vehicle before test 414424-3.

DATE: 8-16-94 TEST NO.: 414424-3 VIN NO.: 1FTHF25H7JNB716 MAKE: Ford  
 MODEL: F250 YEAR: 1988 ODOMETER: 36504 GW: 3900 kg  
 TIRE SIZE: LT235/85R16 TIRE INFLATION PRESSURE: \_\_\_\_\_ TREAD TYPE: Hwy

MASS DISTRIBUTION (kg) LF 548 RF 570 LR 441 RR 441

DESCRIBE ANY DAMAGE TO VEHICLE PRIOR TO TEST:

Windshield cracked (marked)



● Denotes accelerometer location.

NOTES: \_\_\_\_\_

ENGINE TYPE: 8 cyl EFI

ENGINE CID: \_\_\_\_\_

TRANSMISSION TYPE:

AUTO  
 MANUAL

OPTIONAL EQUIPMENT:

DUMMY DATA:

TYPE: \_\_\_\_\_

MASS: \_\_\_\_\_

SEAT POSITION: \_\_\_\_\_

GEOMETRY - (mm)

A	1910	E	1290	J	1220	N	1665	R	750
B	760	F	5430	K	710	O	1640	S	1130
C	3380	G	1490.6	L	85	P	790	T	1420
D	1860	H		M	470	Q	450	U	4120

<u>MASS - (kg)</u>	<u>CURB</u>	<u>TEST INERTIAL</u>	<u>GROSS STATIC</u>
M <sub>1</sub>	1156	1118	
M <sub>2</sub>	903	882	
M <sub>T</sub>	2059	2000	

Figure 24. Vehicle properties for test 414424-3.

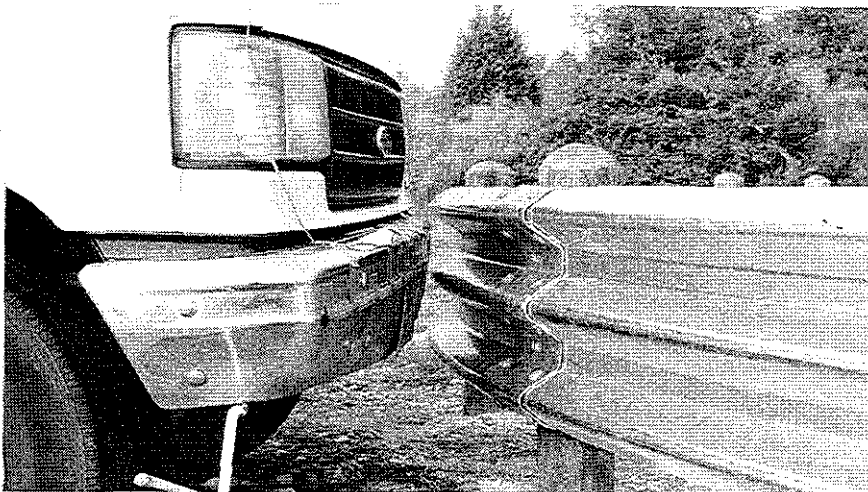
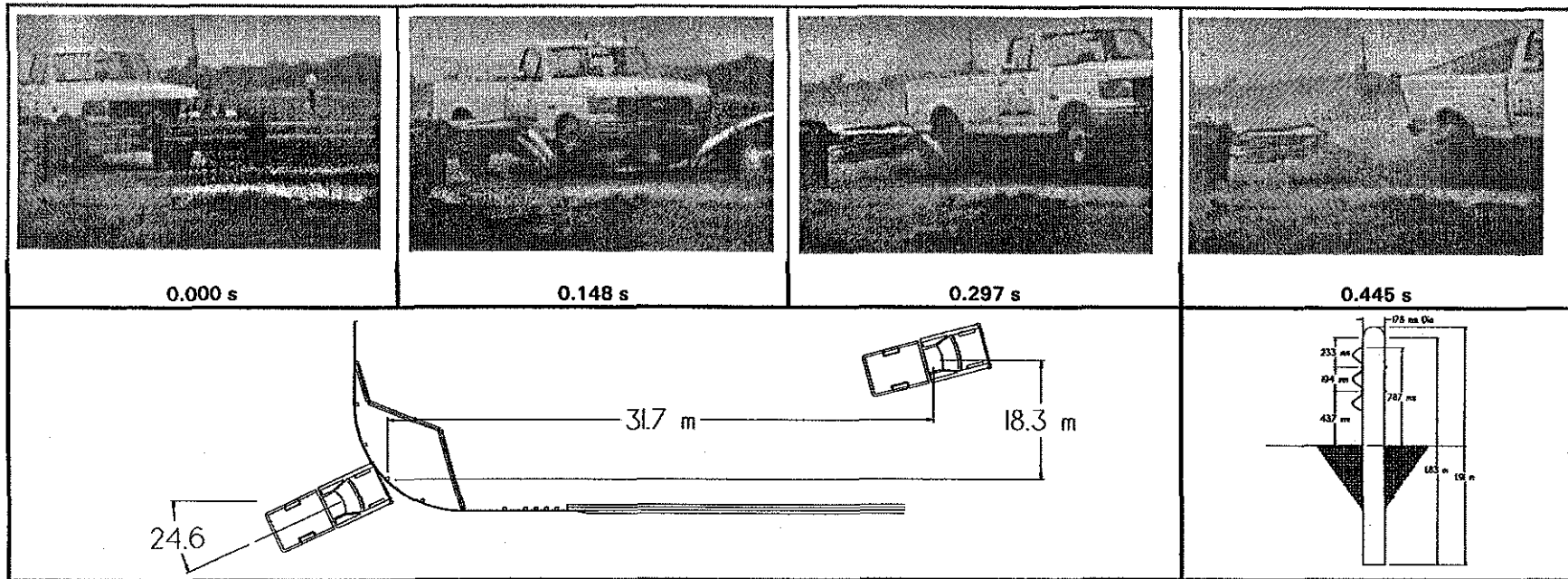


Figure 25. Vehicle/installation geometrics before test 414424-3.



44

<b>General Information</b>		<b>Impact Conditions</b>		<b>Test Article Deflections (m)</b>	
Test Agency	Texas Transportation Institute	Speed (km/h)	101.4 (63.0 mi/h)	Dynamic	3.27 (10.7 ft)
Test No.	414424-3	Angle (deg)	24.6	Permanent	2.90 (9.5 ft)
Date	08/16/94	<b>Exit Conditions</b>		<b>Vehicle Damage</b>	
<b>Test Article</b>		Speed (km/h)	79.3 (49.3 mi/h)	<b>Exterior</b>	
Type	Short Radius Guardrail	Angle (deg)	22.9	VDS	FD-2 (EST.)
Name or Manufacturer	TxDOT	<b>Occupant Risk Values</b>		CDC	12FDEW1
Installation Length (m)	4.8 m (16.0 ft) Radius	Impact Velocity (m/s)		<b>Interior</b>	
Size and/or dimension and material of key elements	Thriebeam Guardrail 17.8 cm (7.0 in) Round Posts	x-direction	5.0 (16.5 ft/s)	OCDI	AS0000000
Soil Type and Condition	Strong soil, Dry	y-direction	1.0 (3.3 ft/s)	<b>Maximum Exterior</b>	
<b>Test Vehicle</b>		THIV (optional)		Vehicle Crush (mm)	Unavailable
Type	Production	Ridedown Accelerations (g's)		Max. Occ. Compart.	(Tree impact)
Designation	2000P	x-direction	-6.17	Deformation (mm)	0 (estimated)
Model	1988 Ford F250 Pickup	y-direction	-9.58	<b>Post-Impact Behavior</b>	
Mass (kg) Curb	2059 (4539 lb)	PHD (optional)		Max. Roll Angle (deg)	15.7
Test Inertial Dummy	2000 (4409 lb)	ASI (optional)		Max. Pitch Angle (deg)	-9.8
Gross Static	2000 (4409 lb)	Max. 0.050-sec Average (g's)		Max. Yaw Angle (deg)	-4.3
		x-direction	-5.7		
		y-direction	-4.3		
		z-direction	-2.9		

Figure 26. Summary of results for test 414424-3.

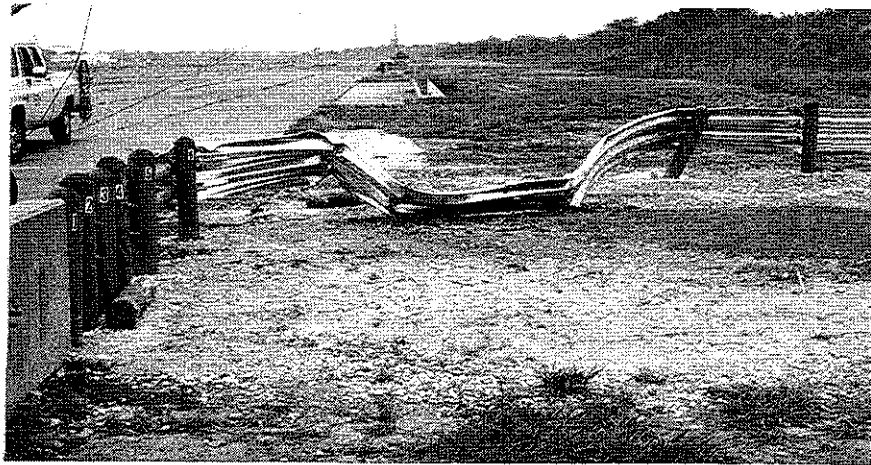
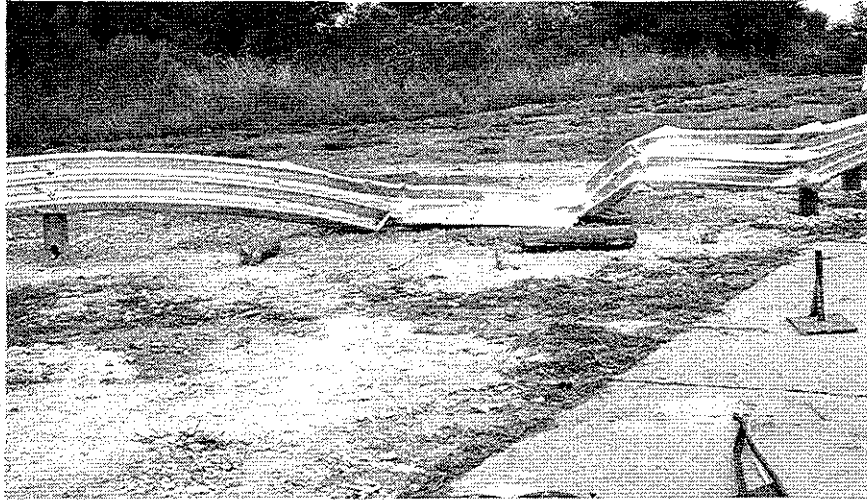


Figure 27. Installation after test 414424-3.

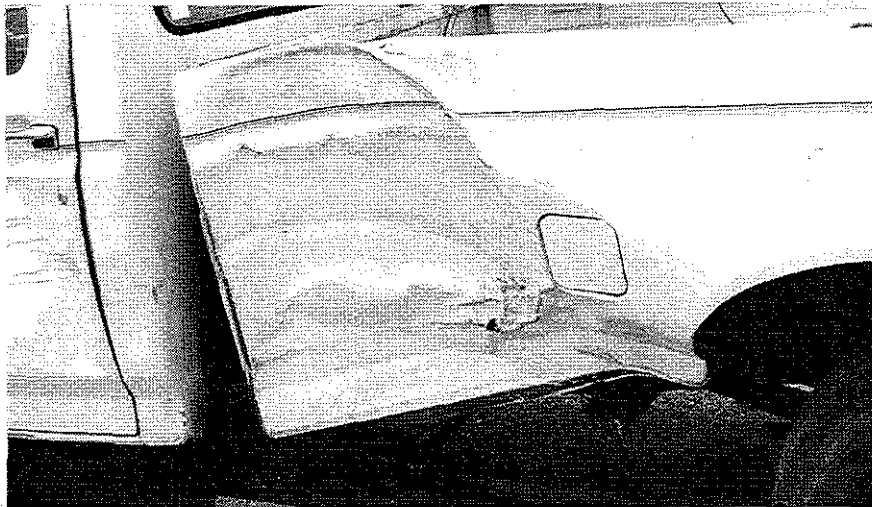
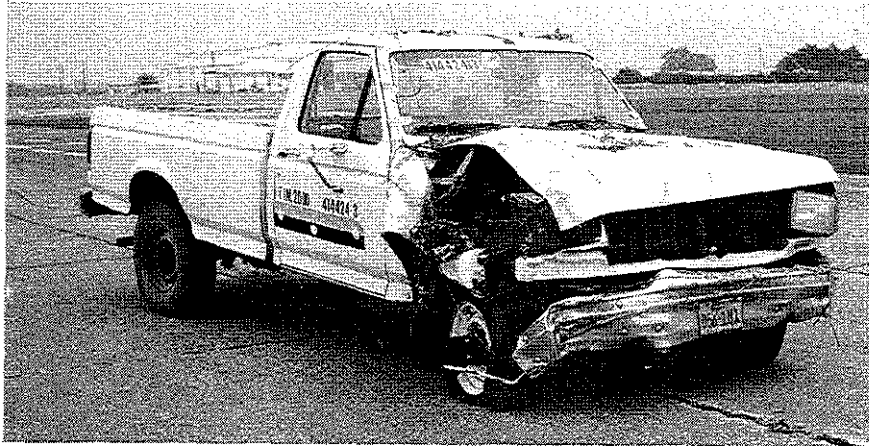


Figure 28. Vehicle after test 414424-3.

the transition test with the pickup truck (Test 1442-1) was considered more critical than an equivalent impact with a passenger sedan, only two additional compliance tests were required. These were the angled impacts into the curved region of rail with both the large and small passenger cars.

#### **TEST 1442-4**

The purpose of this test was to evaluate the performance of the short-radius thrie-beam guardrail treatment for small car impacts into the curved section of barrier. Nominal impact conditions for test under *NCHRP Report 230* guidelines involve a 817.2 kg (1,800 lb) vehicle impacting at 96.6 km/h (60 mph) and 20 degrees. Of primary concern for this test is the evaluation of occupant risk criteria. Details of the test installation were identical to those used in Test 1442-3. Photographs of the completed short-radius treatment are shown in Figure 29.

The test vehicle for this test was a 1988 Chevrolet Sprint shown in Figure 30. Test inertia mass of the vehicle was 820 kg (1808 lb), and its gross static mass was 897 kg (1978 lb). The height to the lower edge of the bumper was 410 mm (16.1 in) and the height to the top of the bumper was 520 mm (20.5 in.). Additional dimensions and information pertaining to the test vehicle are given in Figure 31. Figure 32 shows the relationship between vehicle and barrier geometrics. The vehicle impacted the midpoint of the curved section of rail at a speed of 96.7 km/h (60.1 mph) at an angle of 19.1 degrees relative to the tangent section of rail along the primary roadway.

Upon impact, the weakened wood posts fractured as designed and the thrie beam began to deform around the front of the vehicle. However, as the vehicle continued forward into the installation, the top of the rail started rotating toward the vehicle and the thrie beam began to override the hood. At a point when most of the vehicular kinetic energy had been dissipated, the thrie beam contacted the A-pillar. The vehicle finally came to rest 4.0 m (13.1 ft) downstream and 2.1 m (7.0 ft) behind the point of impact as shown in Figure 33.

Damage received by the guardrail is shown in Figure 34. Posts 7, 8, and 9 fractured at or below the ground line as designed. Posts 6, 10, 11, 12, and 13 were disturbed. Maximum dynamic rail deflection was 3.22 m (10.6 ft), and the maximum residual deformation was 2.90 m (9.5 ft) at post 8.



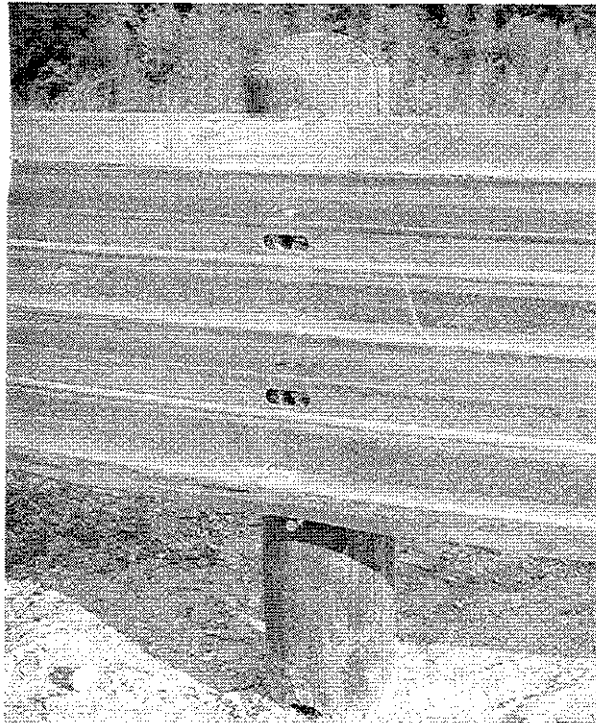
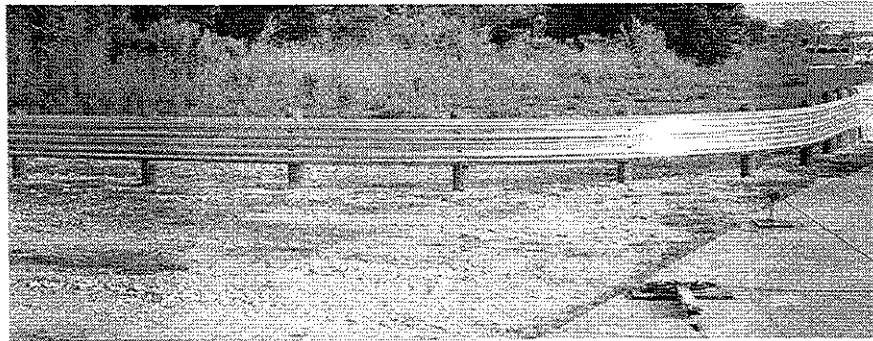


Figure 29. Installation before test 414424-4.

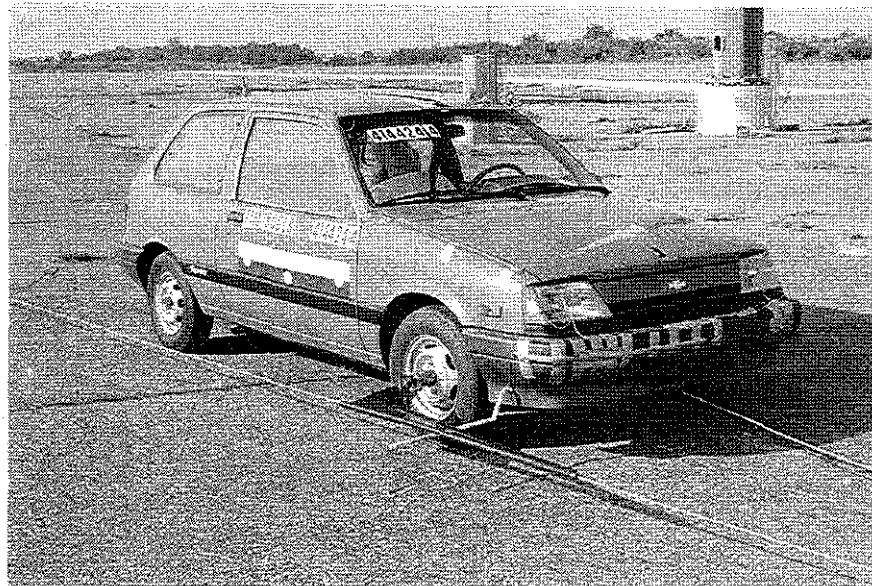
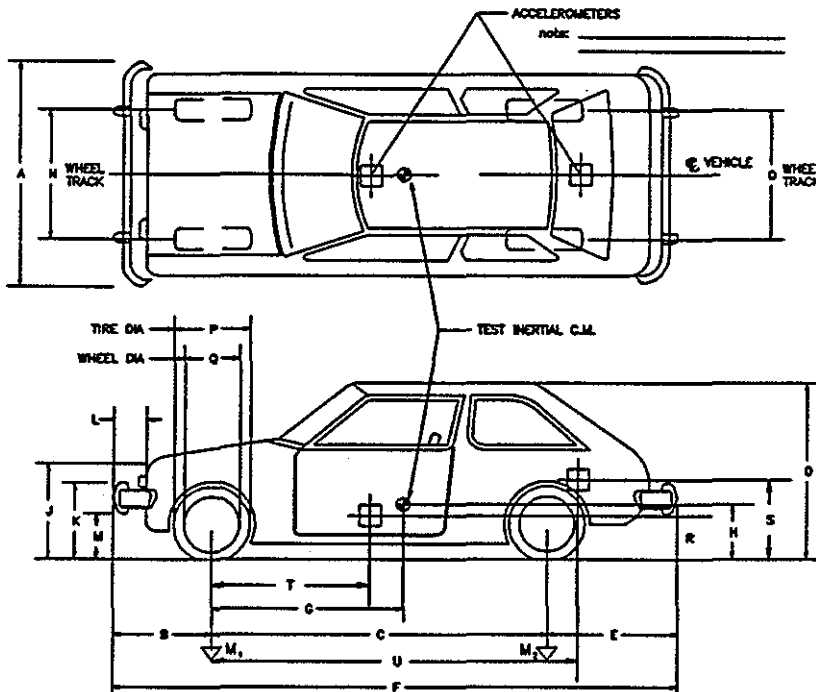


Figure 30. Vehicle before test 414424-4.

DATE: 8-26-94 TEST NO.: 414424-4 VIN NO.: JG1MR2152JK757431 MAKE: Chevy  
 MODEL: Sprint YEAR: 1988 ODOMETER: 12198 TIRE SIZE: 145 80R12  
 TIRE INFLATION PRESSURE: \_\_\_\_\_

MASS DISTRIBUTION (kg) LF 251 RF 253 LR 166 RR 150

DESCRIBE ANY DAMAGE TO VEHICLE PRIOR TO TEST:  
 \_\_\_\_\_  
 \_\_\_\_\_



ENGINE TYPE: 3 cyl  
 ENGINE CID: 1.0 Liter  
 TRANSMISSION TYPE:  
 AUTO  
 MANUAL  
 OPTIONAL EQUIPMENT:  
 \_\_\_\_\_  
 \_\_\_\_\_  
 \_\_\_\_\_  
 DUMMY DATA:  
 TYPE: \_\_\_\_\_  
 MASS: \_\_\_\_\_  
 SEAT POSITION: \_\_\_\_\_

GEOMETRY - (mm)

A	<u>1430</u>	E	<u>620</u>	J	<u>740</u>	N	<u>1330</u>	R	<u>400</u>
B	<u>690</u>	F	<u>3555</u>	K	<u>520</u>	O	<u>1300</u>	S	<u>740</u>
C	<u>2245</u>	G	<u>865.1</u>	L	<u>175</u>	P	<u>540</u>	T	<u>930</u>
D	<u>1340</u>	H	_____	M	<u>410</u>	Q	<u>335</u>	U	<u>2555</u>

<u>MASS - (kg)</u>	<u>CURB</u>	<u>TEST INERTIAL</u>	<u>GROSS STATIC</u>
$M_1$	<u>473</u>	<u>504</u>	<u>540</u>
$M_2$	<u>247</u>	<u>316</u>	<u>357</u>
$M_T$	<u>720</u>	<u>820</u>	<u>897</u>

Figure 31. Vehicle properties for test 414424-4.

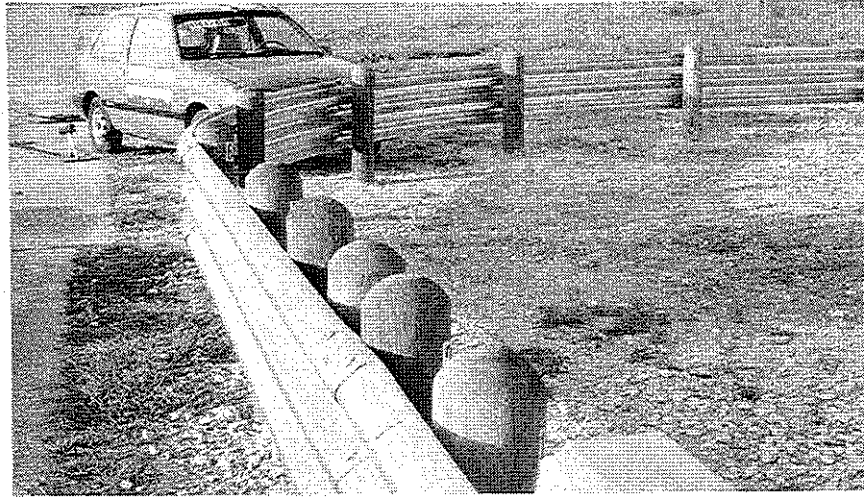


Figure 32. Vehicle/installation geometrics before test 414424-4.



Figure 33. After impact trajectory, test 414424-4.

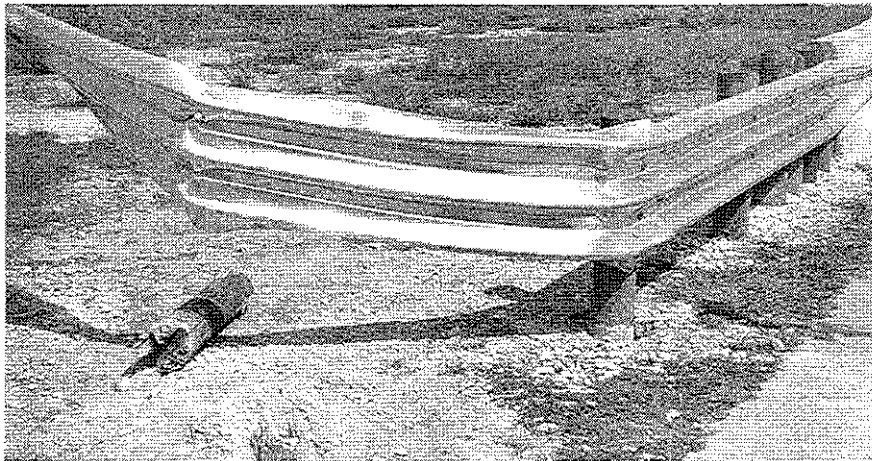
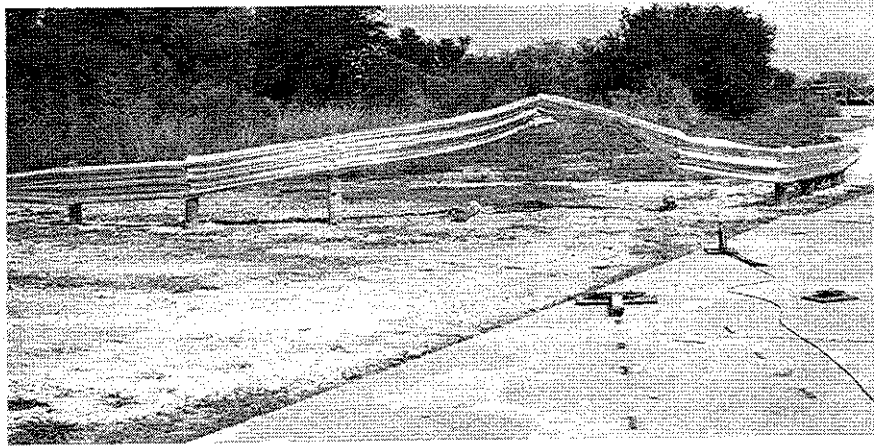


Figure 34. Installation after test 414424-4.

Damage sustained by the vehicle is shown in Figure 35. Although the windshield and passenger side window were shattered, there was no intrusion of vehicular or barrier components into the passenger compartment. The maximum crush was measured to be 570 mm (22.4 in.) at the left front corner of the vehicle at bumper height.

Data from the accelerometer located at the center of gravity (c.g.) were digitized for evaluation and computation of occupant risk factors. In the longitudinal direction, the occupant impact velocity was 10.6 m/s (34.7 ft/s), the highest 0.010-second average ridedown acceleration was -8.6 g, and the maximum 0.050-second average acceleration was -14.0 g. In the lateral direction, the occupant impact velocity was 2.4 m/s (7.8 ft/s), the highest 0.010-second average ridedown acceleration was -3.0 g, and the maximum 0.050-second average acceleration was -2.2 g. These data and other pertinent information from the test are summarized in Figure 36.

In summary, this test was judged to be a success. The short-radius thrie-beam system contained and decelerated the test vehicle within the acceptable limits set forth in *NCHRP Report 230*. The vehicle remained upright and stable throughout the impact event, and there was no intrusion of the occupant compartment.

#### **TEST 1442-5**

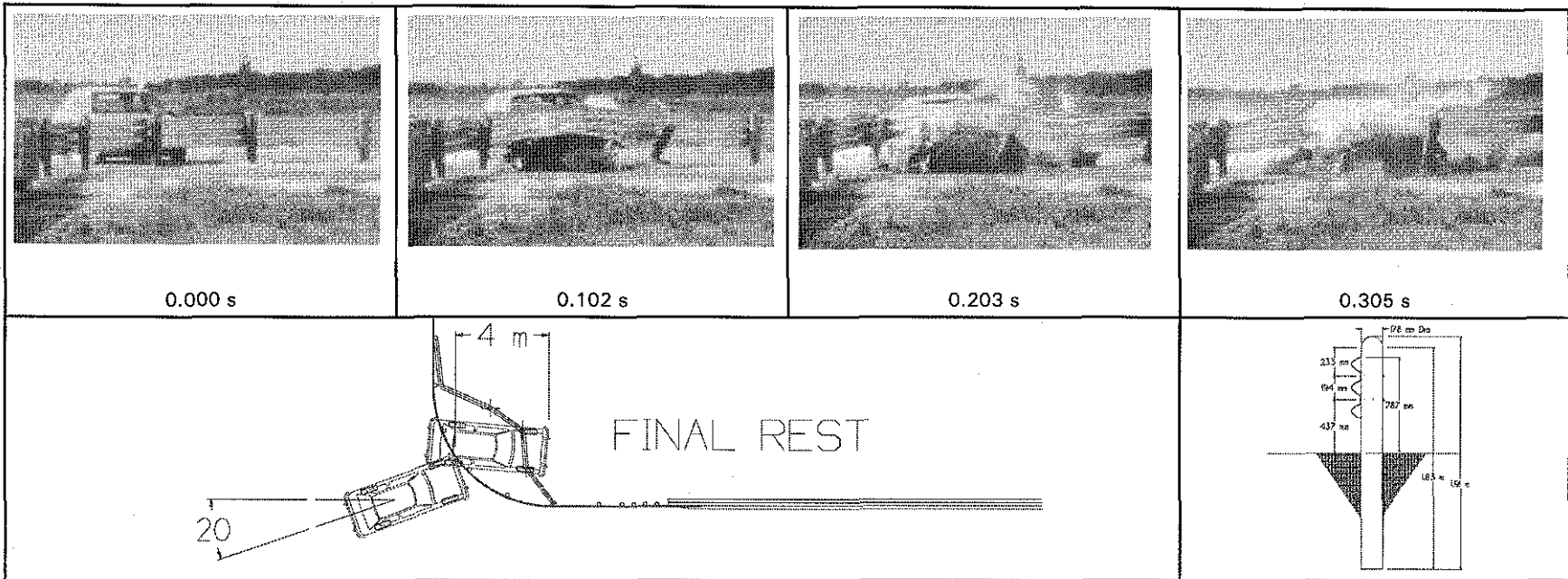
The installation for this test was identical in design to the one of test 1442-4. Photographs of the completed test installation are shown in Figure 37. The test conditions followed the general guidelines of *NCHRP Report 230* and consisted of a 2,043 kg (4,500-lb) passenger sedan impacting the midpoint of the curved portion at 96.6 km/h (60 mph) and 25 degrees. The purpose of this test was to determine if the short-radius thrie-beam system could safely contain a large vehicle without allowing excessive deflections or vehicular penetration.

A 1984 Lincoln Town Car, shown in Figure 38, was used for the final crash test. The bumper height of this passenger car ranged from 322 mm (12.7 in.) at the lower edge, to 530 mm (20.9 in.) at the upper edge. Additional dimensions and information pertaining to the test vehicle are given in Figure 39. Figure 40 shows the relationship between vehicle and barrier geometrics. The vehicle impacted the midpoint of the curved section of rail at a speed of 97.2 km/h (60.4 mph) at an angle of 24.5 degrees relative to the tangent section of rail along the primary roadway.



Figure 35. Vehicle after test 414424-4.





56

General Information		Impact Conditions		Test Article Deflections (m)	
Test Agency	Texas Transportation Institute	Speed (km/h)	96.7 (60.1 mi/h)	Dynamic	3.22 (10.6 ft)
Test No.	414424-4	Angle (deg)	19.1	Permanent	2.90 (9.5 ft)
Date	08/26/94	Exit Conditions		Vehicle Damage	
Test Article	Short Radius Guardrail	Speed (km/h)	Vehicle Contained	Exterior	
Type	Short Radius Guardrail	Angle (deg)	N/A	VDS	FD-3
Name or Manufacturer	TxDOT	Occupant Risk Values		CDC	11FDEW4
Installation Length (m)	4.8 m (16.0 ft) Radius	Impact Velocity (m/s)		Interior	
Size and/or dimension and material of key elements	Thriebeam Guardrail 17.8 cm (7.0 in) Round Posts	x-direction	10.6 (34.7 ft/s)	OCDI	AS1011000
Soil Type and Condition	Strong soil, Dry	y-direction	2.4 (7.8 ft/s)	Maximum Exterior	
Test Vehicle		THIV (optional)		Vehicle Crush (mm)	570 (22.4 in)
Type	Production	Ridedown Accelerations (g's)		Max. Occ. Compart.	
Designation	820C	x-direction	-8.59	Deformation (mm)	86 (3.4 in)
Model	1988 Chevrolet Sprint	y-direction	-3.02	Post-Impact Behavior	
Mass (kg) Curb	720 (1587 lb)	PHD (optional)		Max. Roll Angle (deg)	4.5
Test Inertial	820 (1808 lb)	ASI (optional)		Max. Pitch Angle (deg)	-4.6
Dummy	77 (170 lb)	Max. 0.050-sec Average (g's)		Max. Yaw Angle (deg)	-7.2
Gross Static	897 (1978 lb)	x-direction	-14.0		
		y-direction	-2.2		
		z-direction	-4.3		

Figure 36. Summary of results for test 414424-4.

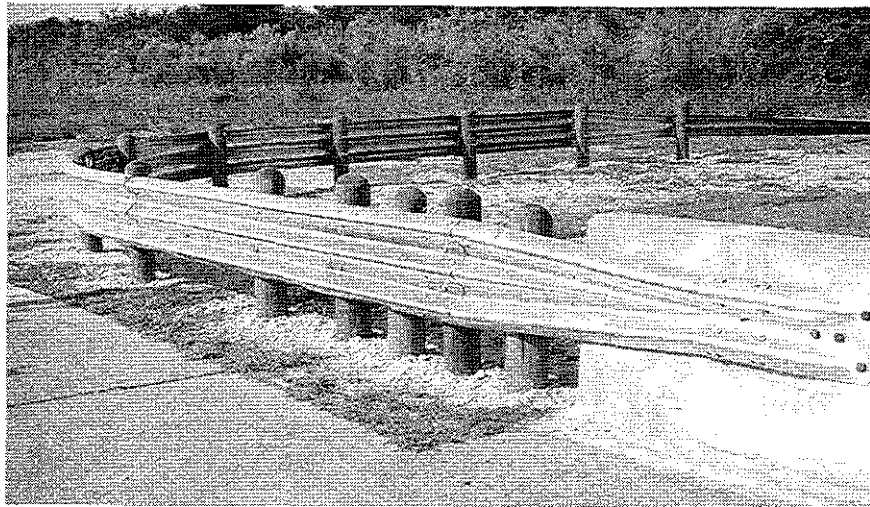
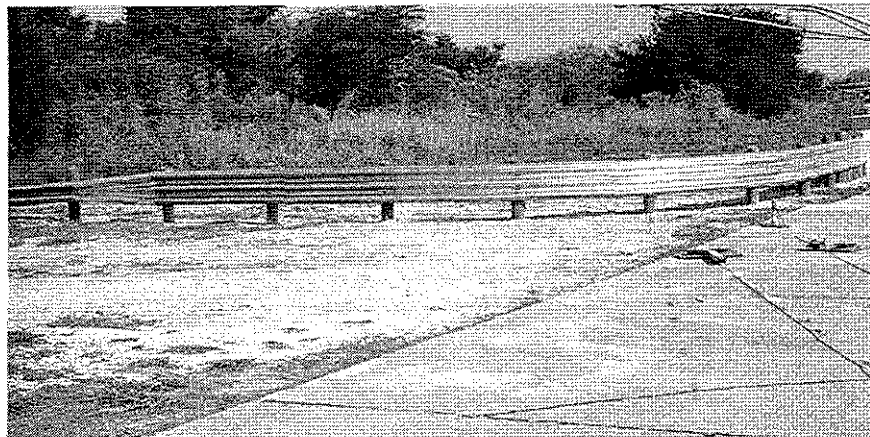
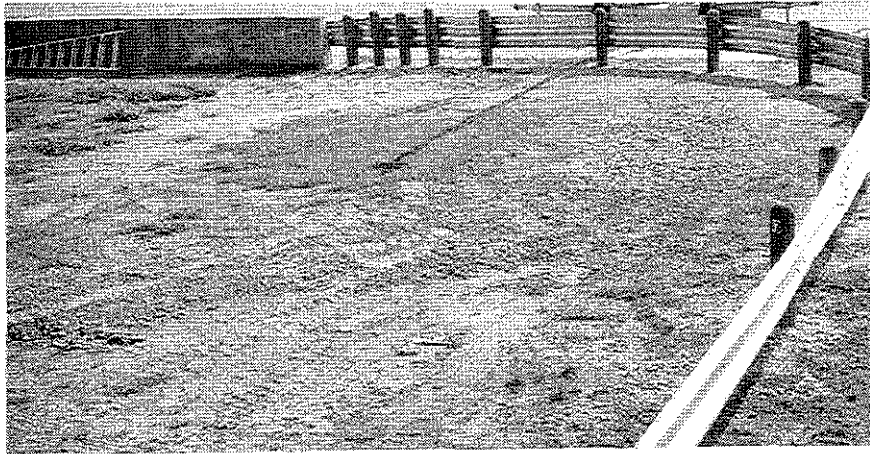


Figure 37. Installation before test 414424-5.

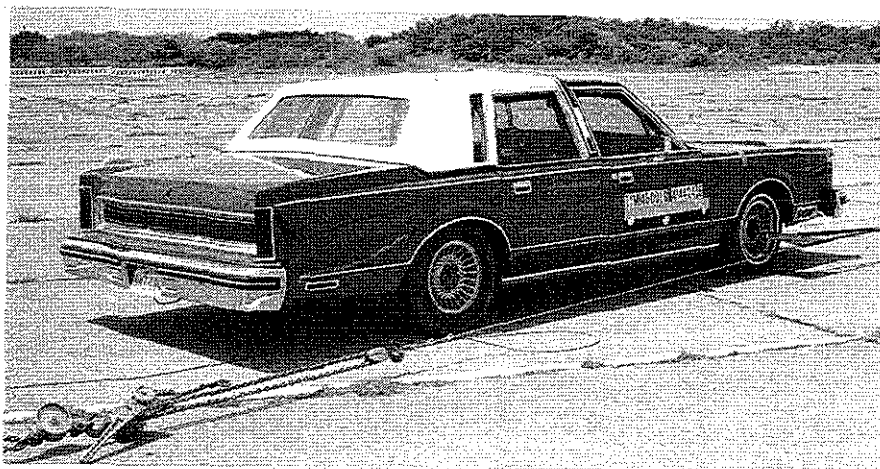
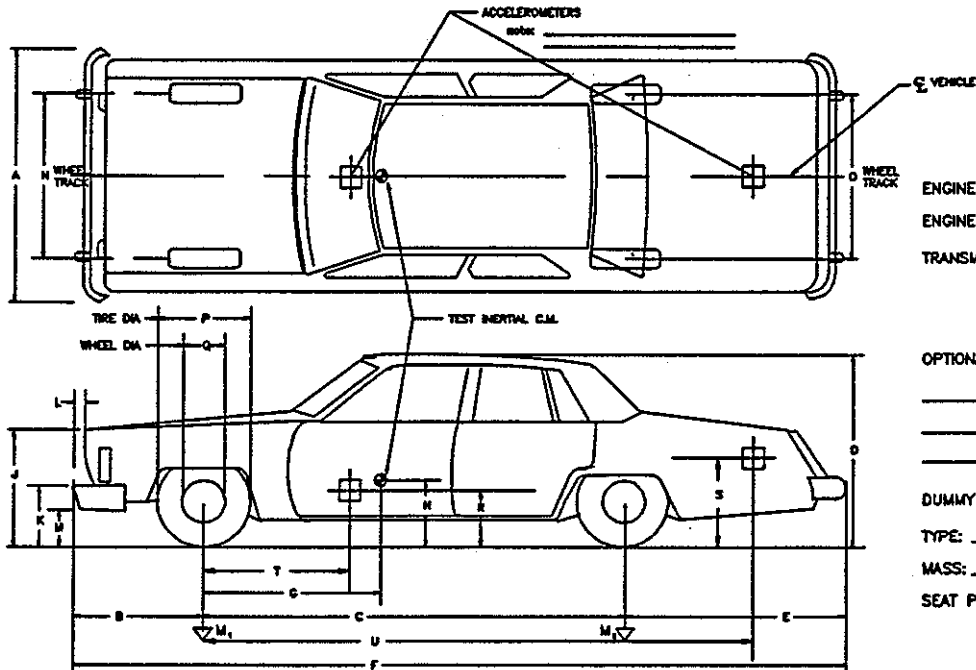


Figure 38. Vehicle before test 414424-5.

DATE: 8-29-94 TEST NO.: 414424-5 VIN NO.: 1LNBP96F8EY710739 MAKE: Ford  
 MODEL: Lincoln TC YEAR: 1984 ODOMETER: 82854 TIRE SIZE: P215 70R15  
 TIRE INFLATION PRESSURE: \_\_\_\_\_

MASS DISTRIBUTION (kg) LF 565 RF 554 LR 461 RR 461

DESCRIBE ANY DAMAGE TO VEHICLE PRIOR TO TEST:  
 \_\_\_\_\_  
 \_\_\_\_\_



ENGINE TYPE: V-8  
 ENGINE CID: 351

TRANSMISSION TYPE:  
 AUTO  
 MANUAL

OPTIONAL EQUIPMENT:  
 \_\_\_\_\_  
 \_\_\_\_\_

DUMMY DATA:  
 TYPE: \_\_\_\_\_  
 MASS: \_\_\_\_\_  
 SEAT POSITION: \_\_\_\_\_

GEOMETRY - (mm)

A	1920	E	1445	J	910	N	1590	R	430
B	1100	F	5530	K	530	O	1590	S	740
C	2985	G	1348.4	L	115	P	665	T	1280
D	1445	H		M	322	Q	415	U	3970

<u>MASS - (kg)</u>	<u>CURB</u>	<u>TEST INERTIAL</u>	<u>GROSS STATIC</u>
M <sub>1</sub>	1053	1119	_____
M <sub>2</sub>	767	922	_____
M <sub>T</sub>	1820	2041	_____

Figure 39. Vehicle properties for test 414424-5.

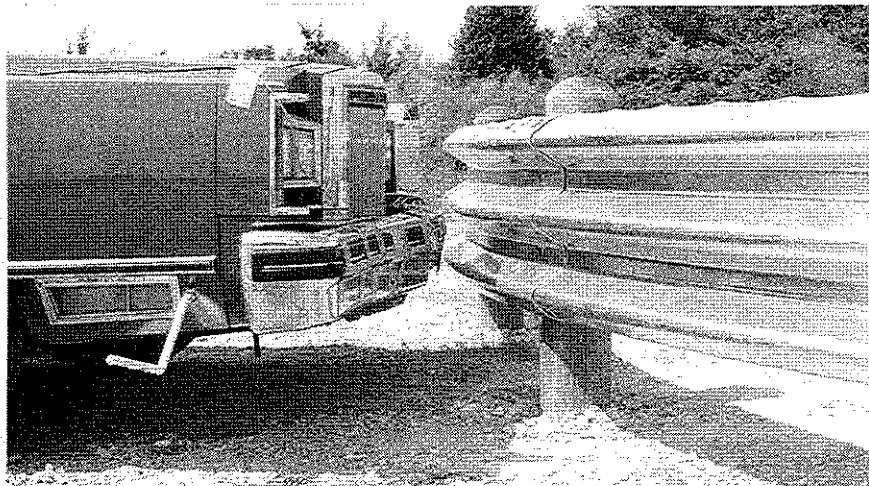
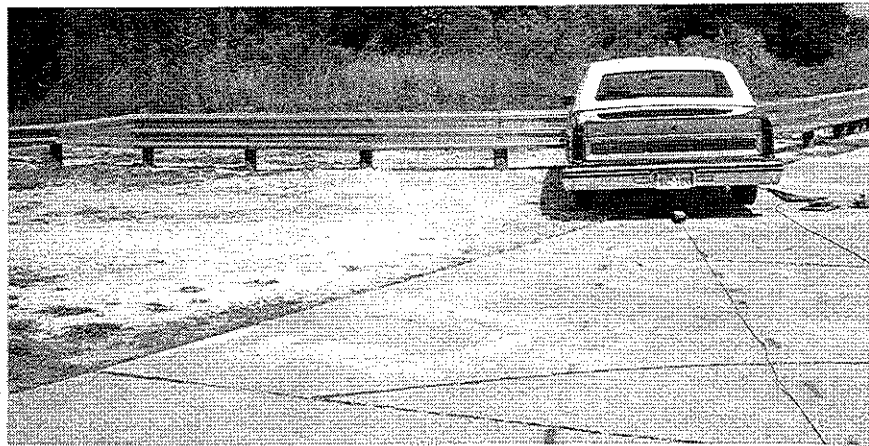
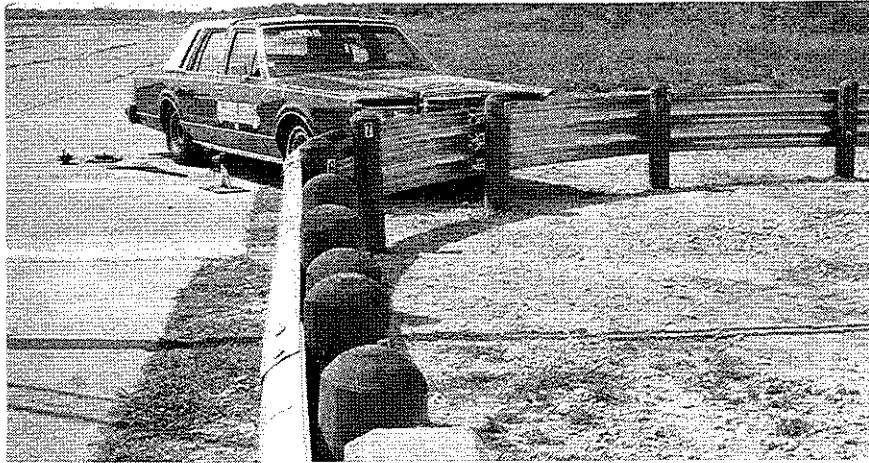


Figure 40. Vehicle/installation geometrics before test 414424-5.

Upon impact, the posts in the impact area fractured as intended and the rail deformed around the front end of the test vehicle. The forward velocity of the vehicle was nearly stopped when the four bolts connecting the W-beam terminal connector to the turndown anchor failed in shear, permitting the rail to swing out in front of the vehicle. As shown in Figure 41, the vehicle rolled to a stop 12.5 m (41.0 ft) downstream and 6.5 m (21.3 ft) behind the point of impact without the brakes being applied. A summary of the test information is presented in Figure 42.

Damage to the test installation is shown in Figure 43. All of the weakened CRT posts (posts 6-12) fractured at or below ground level as intended. Post 5 was pulled from the ground, and post 13 was knocked over in the soil. Maximum dynamic rail deflection was 13.2 m (43.2 ft), and the maximum residual deformation was 11.3 m (37.2 ft). Investigation of the turndown anchorage failure revealed that 5/8-in. diameter bolts were incorrectly substituted for the standard 7/8-in. diameter bolts typically used with the end-shoe type turndown anchor. Analysis shows that a 7/8-in. diameter bolt has approximately twice the shear capacity of a 5/8-in. diameter bolt of similar grade. Since the test vehicle was almost stopped prior to the shear failure of the four 5/8-in. diameter bolts, it is the opinion of the researchers that, had the correct size bolts been installed, this failure would not have occurred. Analysis of the high-speed film indicated that the vehicle traveled approximately 2.4 m (8 ft) after the failure of the turndown anchorage connection. It is, therefore, reasonable to assume that, in the absence of the connection failure, the maximum dynamic rail deflection would be approximately 10.1 m (33 ft) for the given impact conditions.

As shown in Figure 44, damage sustained by the test vehicle was minor for a test of this severity. The maximum crush was measured to be 460 mm (18.1 in.) at the left front corner of the vehicle at bumper height. Damaged areas included the bumper, grill, hood, front fenders, and doors.

In summary, this test was judged to be a success. Although the turndown anchorage connection failed prior to the test vehicle coming to a complete stop, the failure was a result of using incorrect bolt sizes. When properly installed, the system can be expected to bring the vehicle to a smooth, controlled stop over a distance of approximately 9.5 m (31 ft). Furthermore, although not required in the evaluation of a strength test, the occupant risk indices were all well within the recommended limits of *NCHRP Report 230*. In addition, the vehicle remained upright

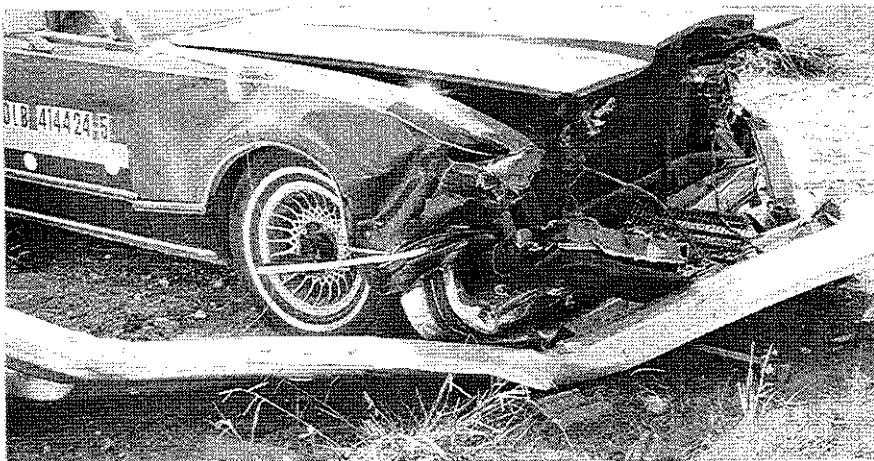
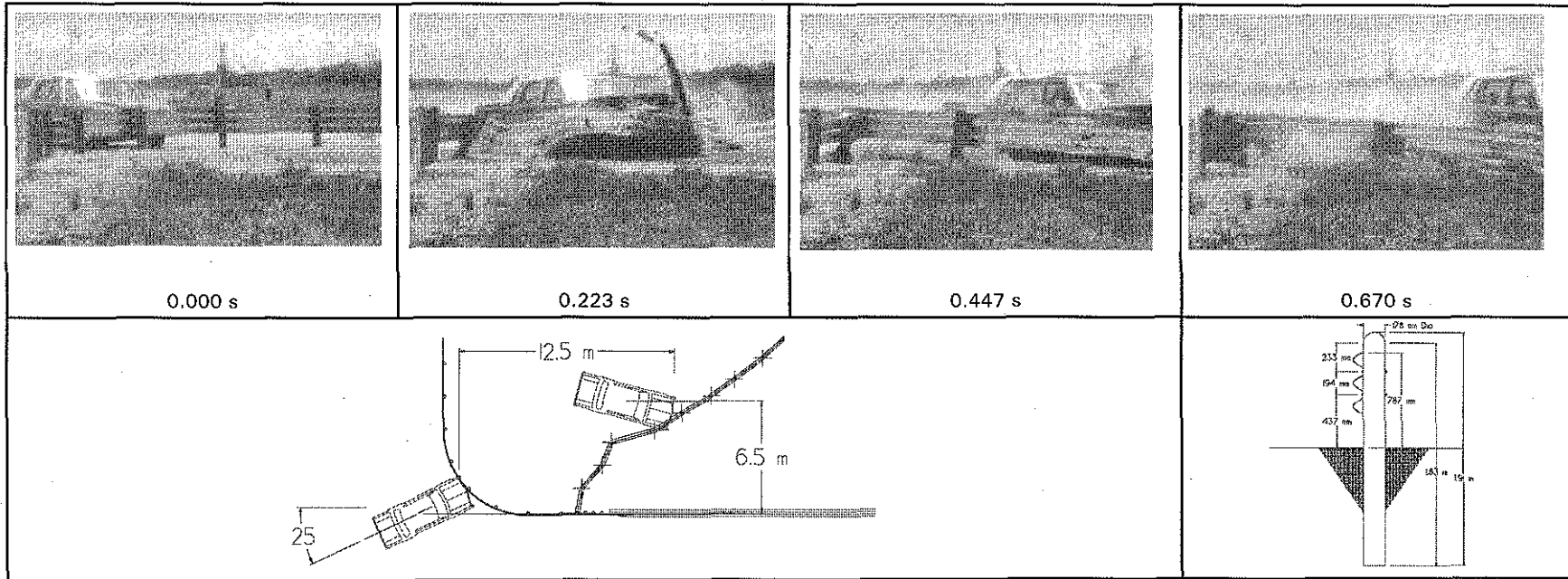


Figure 41. After impact trajectory, test 414424-5.



63

General Information		Impact Conditions		Test Article Deflections (m)	
Test Agency	Texas Transportation Institute	Speed (km/h)	97.2 (60.4 mi/h)	Dynamic	At Post 8 13.2 (43.2 ft)
Test No.	414424-5	Angle (deg)	24.5	Permanent	11.3 (37.2 ft)
Date	08/29/94	Exit Conditions		Vehicle Damage	
Test Article	Short Radius Guardrail	Speed (km/h)	Vehicle Contained	Exterior	
Type	TxDOT	Angle (deg)	N/A	VDS	
Name or Manufacturer	4.8 m (16.0 ft) Radius	Occupant Risk Values		CDC	
Installation Length (m)	Thriebeam Guardrail	Impact Velocity (m/s)		Interior	
Size and/or dimension and material of key elements	17.8 cm (7.0 in) Round Posts	x-direction	6.1 (20.0 ft/s)	OCDI	
Soil Type and Condition	Strong soil, Dry	y-direction	2.5 (8.0 ft/s)	Maximum Exterior	
Test Vehicle	Production	THIV (optional)		Vehicle Crush (mm)	
Type	Full Size Automobile	Ridedown Accelerations (g's)		Max. Occ. Compart.	
Designation	1984 Lincoln Town Car	x-direction	-5.24	Deformation (mm)	
Model	1820 (4012 lb)	y-direction	-2.75	0	
Mass (kg) Curb	2041 (4500 lb)	PHD (optional)		Post-Impact Behavior	
Test Inertial Dummy	2041 (4500 lb)	ASI (optional)		Max. Roll Angle (deg)	
Gross Static	2041 (4500 lb)	Max. 0.050-sec Average (g's)		Max. Pitch Angle (deg)	
		x-direction	-7.2	Max. Yaw Angle (deg)	
		y-direction	-2.5		
		z-direction	-2.3		

Figure 42. Summary of results for test 414424-5.



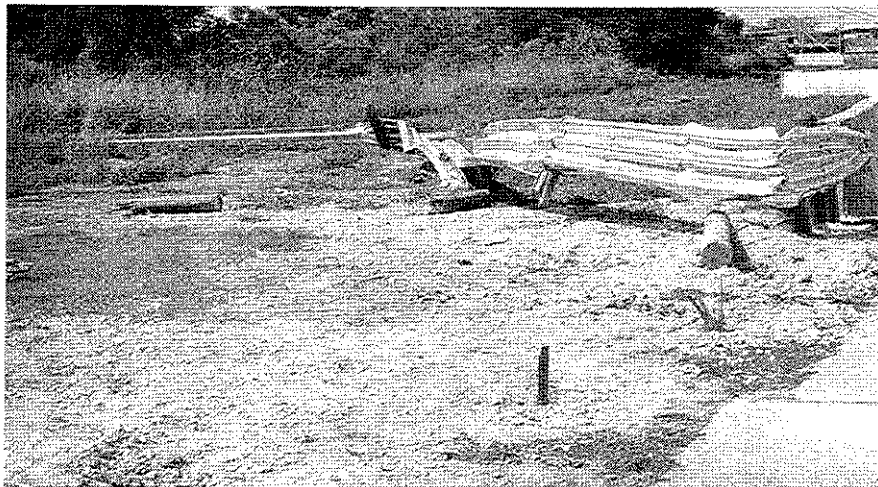


Figure 43. Installation after test 414424-5.

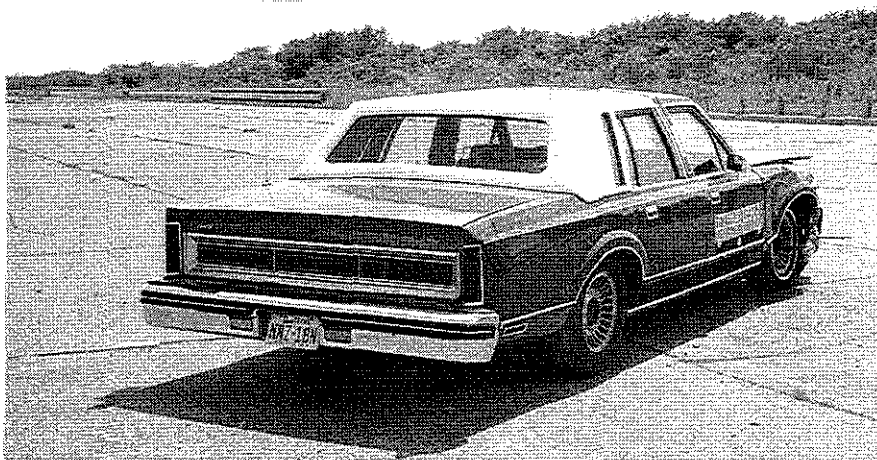
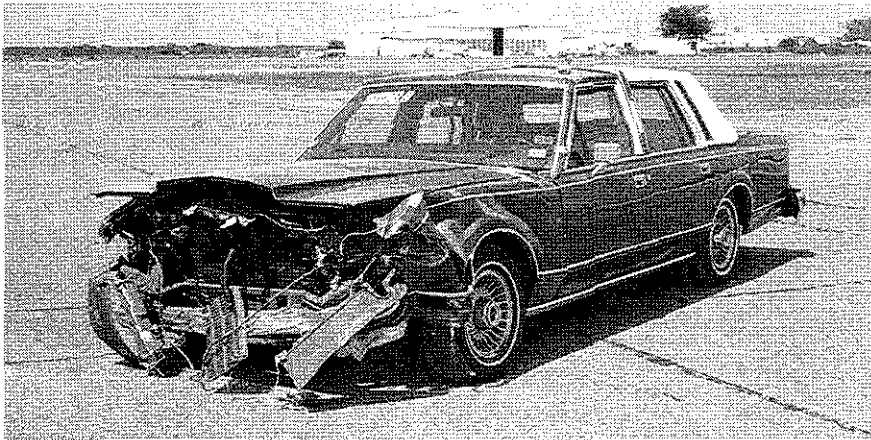
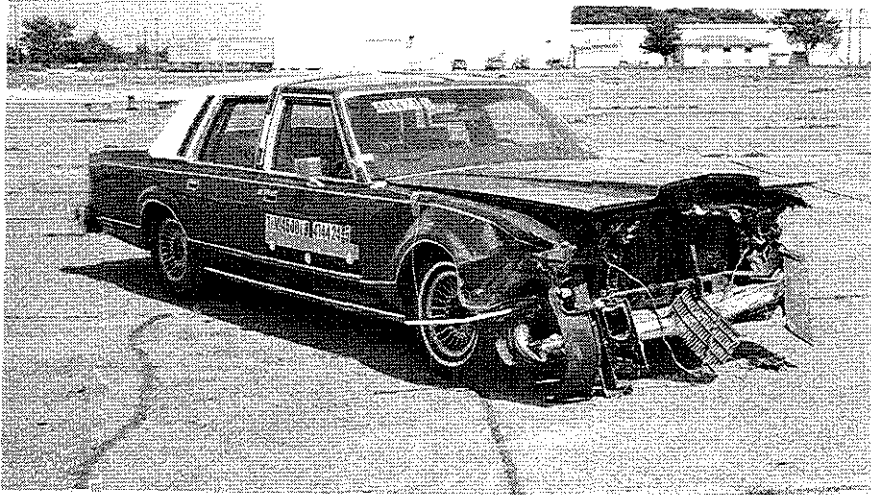


Figure 44. Vehicle after test 414424-5.

and stable during the impact event, and there was no deformation or intrusion into the occupant compartment.

## V. CONCLUSIONS AND RECOMMENDATIONS

This study was undertaken to develop and test a new short-radius thrie-beam guardrail treatment suitable for implementation at sites where a secondary roadway intersects a primary roadway in close proximity to a bridge end. The system consists of two straight segments of guardrail connected by a curved section having a radius of 4.9 m (16 ft) and supported by weakened timber posts. With the exception of the turndown and transition sections, the system is composed of single 10-ga. thrie-beam rail mounted at a height of 9.5 m (31 in.). The design uses a standard 1.9 m (6 ft-3 in.) thrie beam-to-W-beam transition section to reduce the height of the rail at the bridge end and permit connection of treatment to 685.8 mm (27-in.) tall bridge parapets. A similar transition section is used to transition to a W-beam turndown anchor along the secondary roadway. A complete set of construction drawings for the final short-radius thrie-beam design is presented in Appendix D.

When tested in accordance with the requirements of *NCHRP Report 350*, the short-radius system was unable to contain a 3/4-ton pickup truck impacting the midpoint of the curved section at a nominal speed and angle of 100 km/h (62.2 mph) and 25 degrees, respectively. It was concluded that the observed vaulting failure was due to a combination of vehicle geometrics and a low torsional stiffness of the open thrie-beam section. After further analysis, it became evident that any potential solutions to this problem would require substantial modifications to the short-radius system along with additional funding for further developmental testing. It was therefore decided to use the remaining project resources to certify the short-radius thrie-beam design under *NCHRP Report 230*.

When tested in accordance with *NCHRP Report 230*, the short-radius treatment successfully contained both a small and large passenger car impacting into the curved section of rail at 96.6 km/h (60 mph). In addition to satisfying the requirements of *NCHRP Report 230*, it is believed that the newly developed thrie-beam system will be easier to install than the previously tested nested W-beam system. Installation of the curved, nested W-beam rail has proven to be very difficult. Since the splice holes do not readily align, forced alignment (by use of driven alignment pins) is required to install the splice bolts. Splicing a single curved thrie beam is considerably less difficult. Furthermore, the material costs of the new thrie-beam system

are expected to be equal to or less than the nested W-beam alternative due to the elimination of details such as the intermediate BCT anchorage and the welded tubular W-beam section.

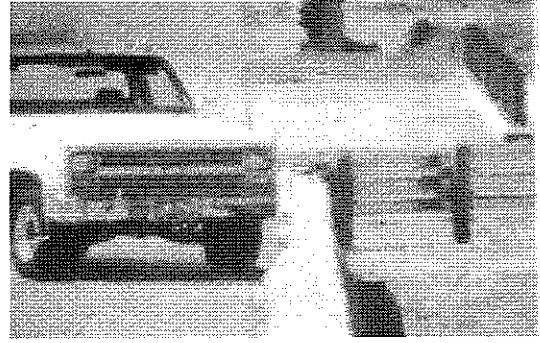
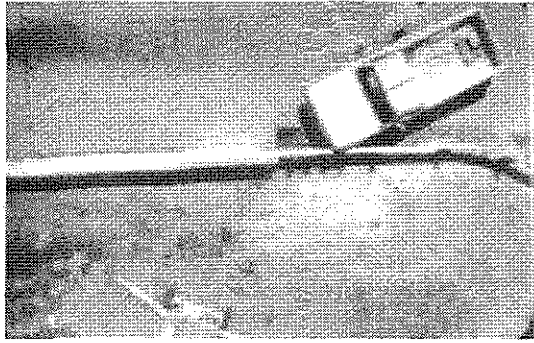
## **RECOMMENDATIONS**

Containment of the 2000P design test vehicle of *NCHRP Report 350* is proving to be very challenging for many of our safety appurtenances. Currently, there are no short-radius guardrail treatments which have been successfully tested with the 3/4-ton pickup truck. Until such time that a treatment meeting the requirements of *NCHRP Report 350* can be developed, it is recommended that a crashworthy treatment meeting the guidelines of *NCHRP Report 230* be adopted and implemented. The short-radius thrie-beam treatment developed under this study satisfies this requirement. Implementation of this treatment will offer significantly improved impact performance over existing designs and it will be much easier to install and maintain than the interim nested W-beam design developed under Study 1263.

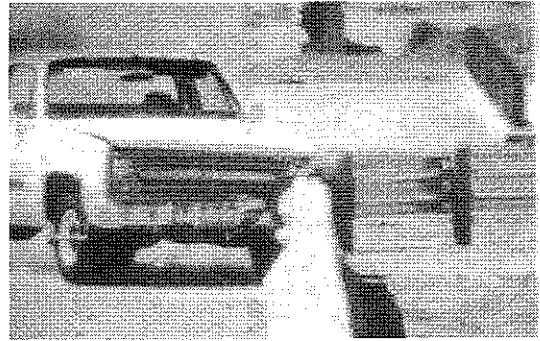
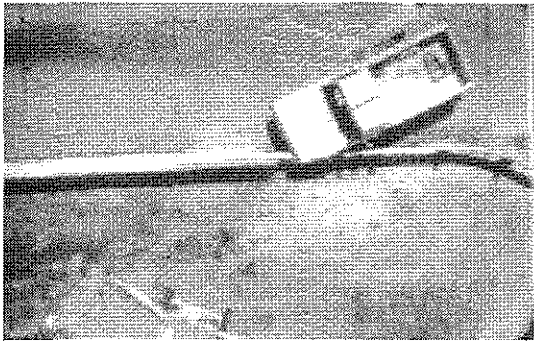
## REFERENCES

1. Bronstad, M. E., Calcote, L. R., Ray, M. H., and Mayer, J. B., "Guardrail - Bridge Rail Transition Designs," Report No. FHWA/RD-86/178, San Antonio, Texas, 1989.
2. Ross, H. E., Jr., Bligh, R. B., and Parnell, C. B., "Bridge Railing End Treatments at Intersecting Streets and Drives," Research Report 1263-1F, Texas Transportation Institute, College Station, Texas, November 1992.
3. Michie, J. D., "Recommended Procedures for the Safety Performance Evaluation of Highway Appurtenances." NCHRP Report 230, National Research Council, Washington, D. C., 1981.
4. Ross, H. E., Jr., Sicking, D. L., Zimmer, R. A., and Michie, J. D., "Recommended Procedures for the Safety Performance Evaluation of Highway Features," NCHRP Report 350, National Research Council, Washington, D. C., 1993.
5. Powell, G. H., "Barrier VII: A Computer Program for Evaluation of Automobile Barrier Systems," Report No. FHWA-RD-73-51, Federal Highway Administration, Washington, D.C., 1973.

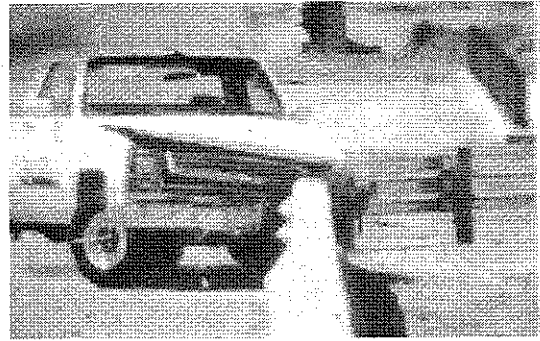
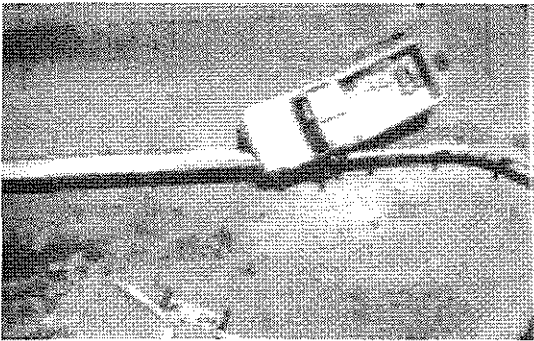
**APPENDIX A**  
**SEQUENTIAL PHOTOGRAPHS**



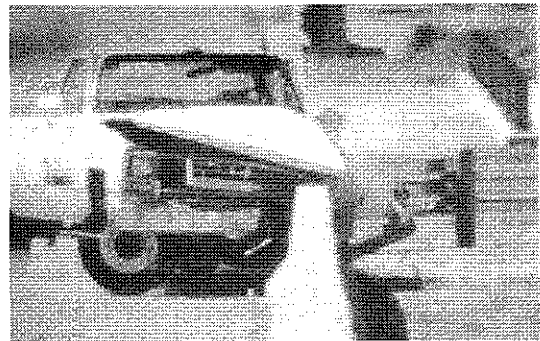
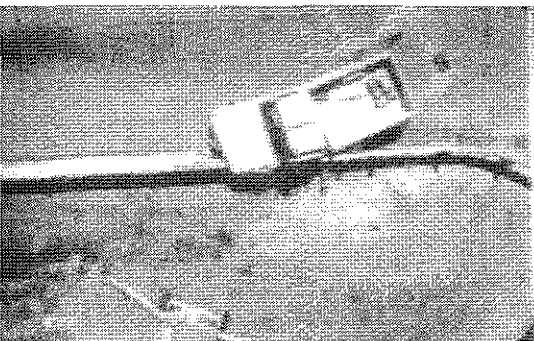
0.000 s



0.037 s



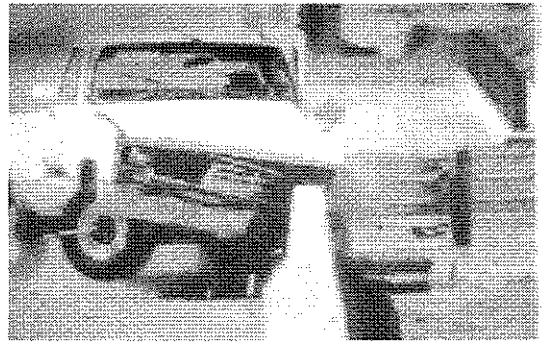
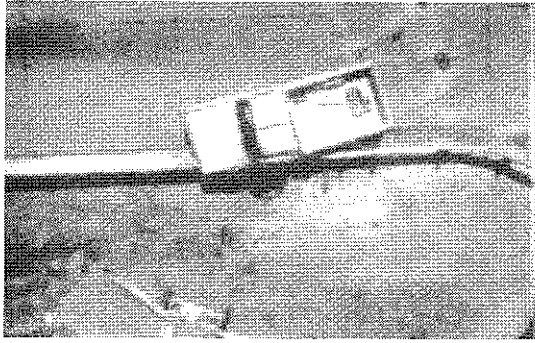
0.074 s



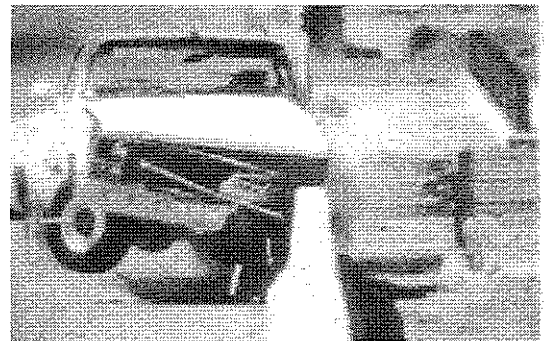
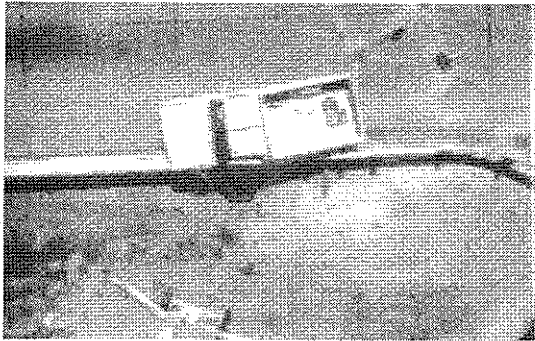
0.112 s

Figure A-1. Sequential photographs for test 414424-1.  
(overhead and frontal views)

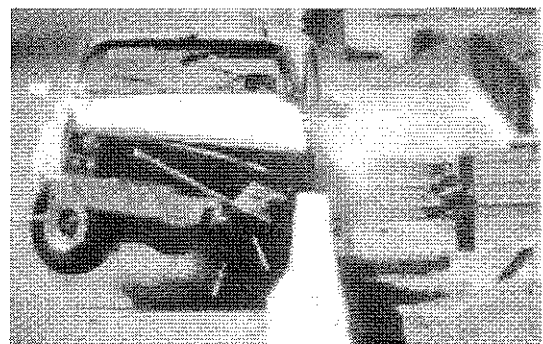
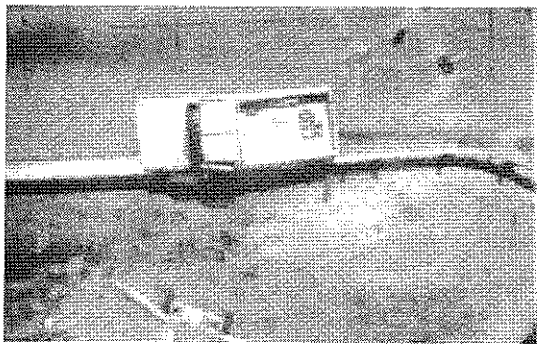




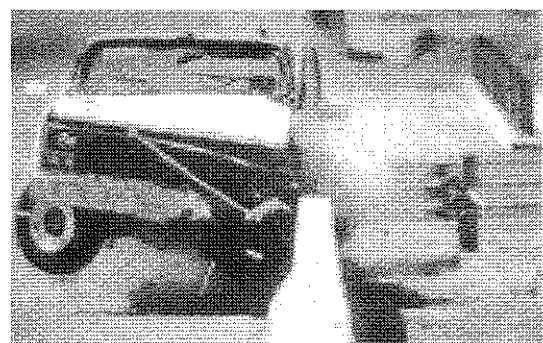
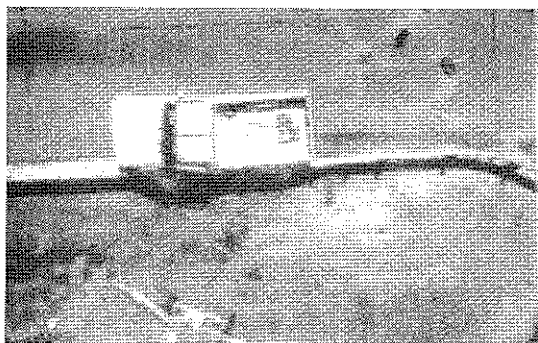
0.149 s



0.186 s

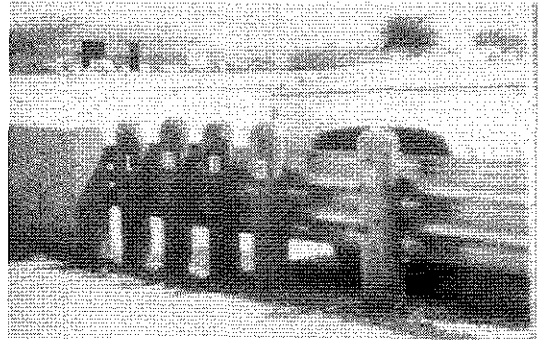


0.223 s

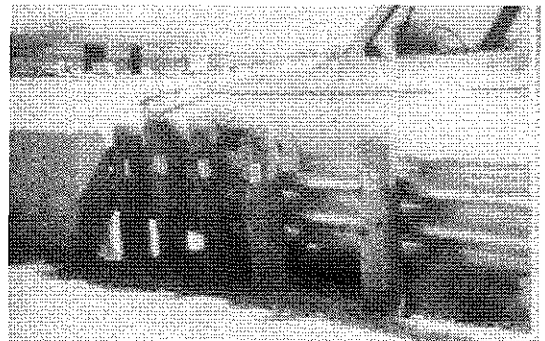


0.260 s

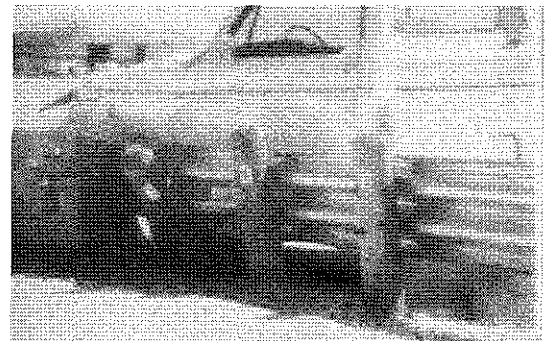
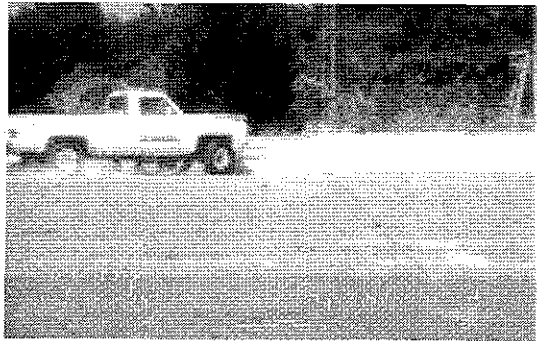
Figure A-1. Sequential photographs for test 414424-1 (continued).  
(overhead and frontal views)



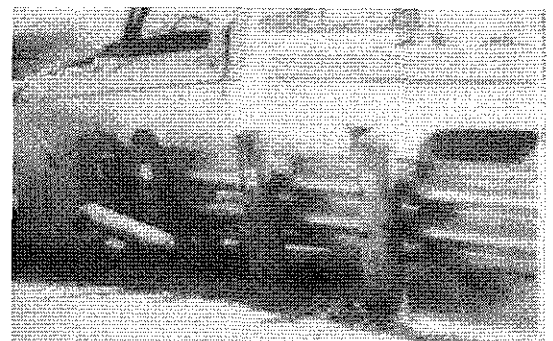
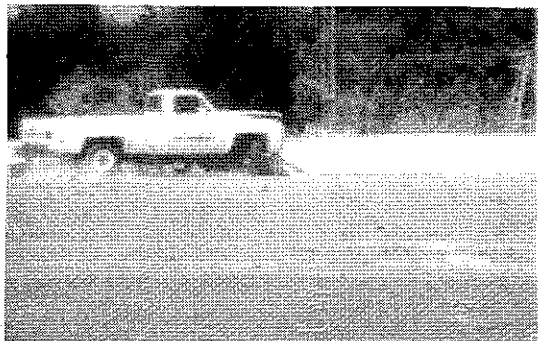
0.000 s



0.037 s

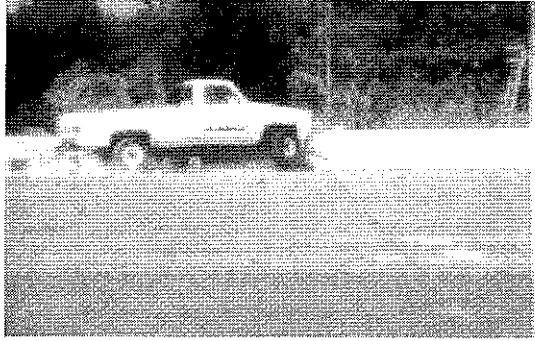


0.074 s

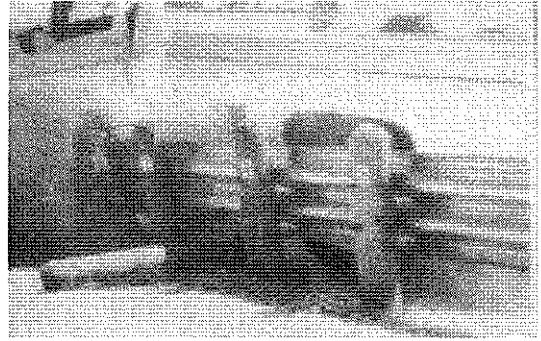


0.112 s

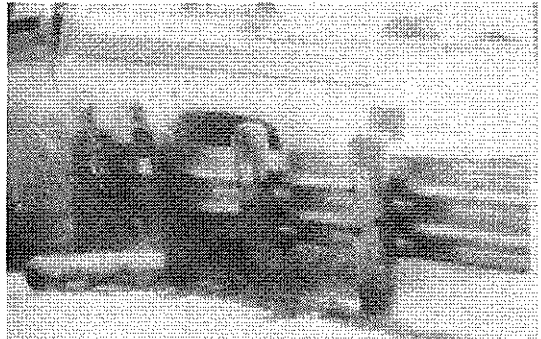
Figure A-2. Sequential photographs for test 414424-1.  
(perpendicular and behind the rail views)



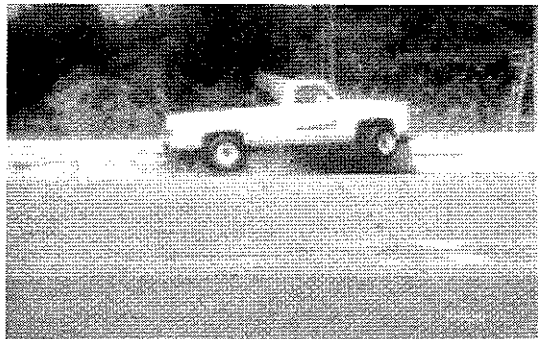
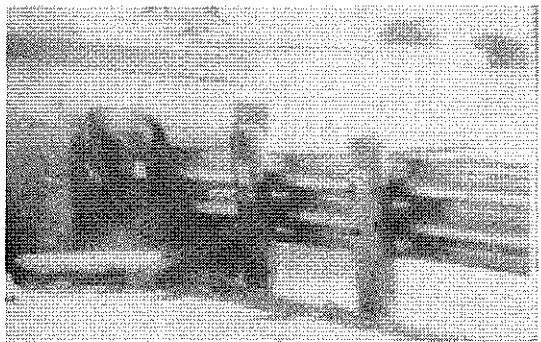
0.149 s



0.186 s



0.223 s



0.260 s

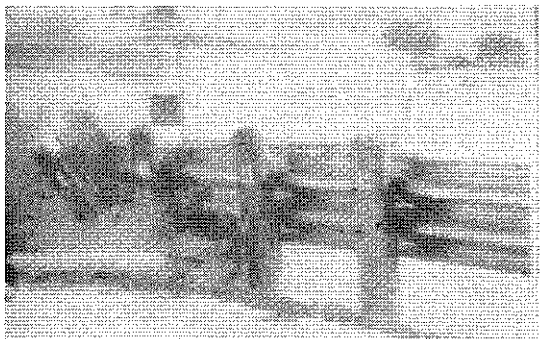
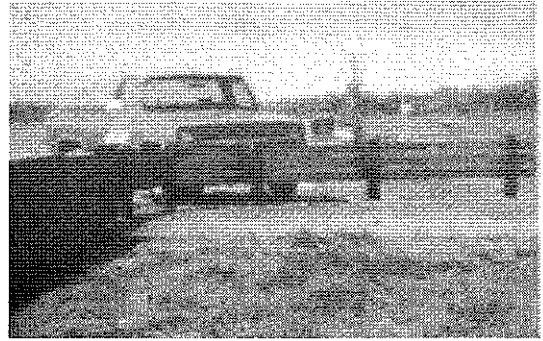
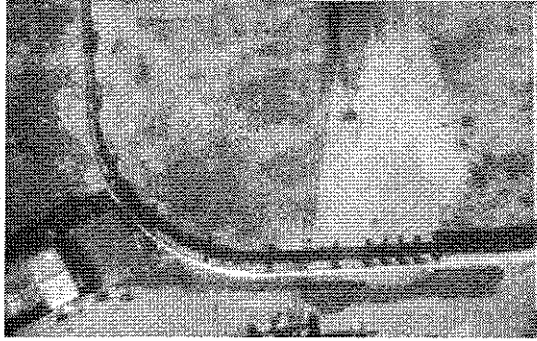
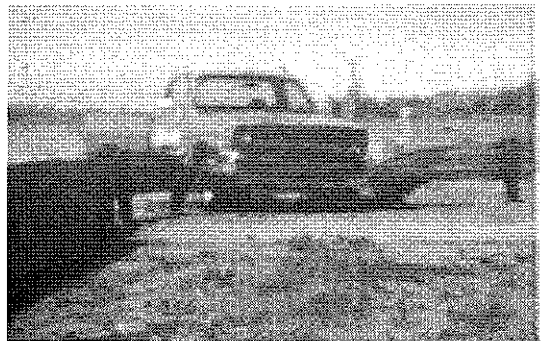
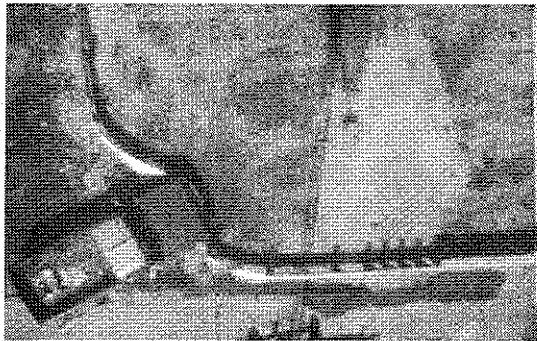


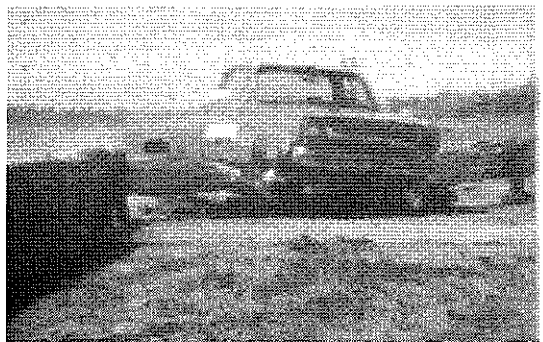
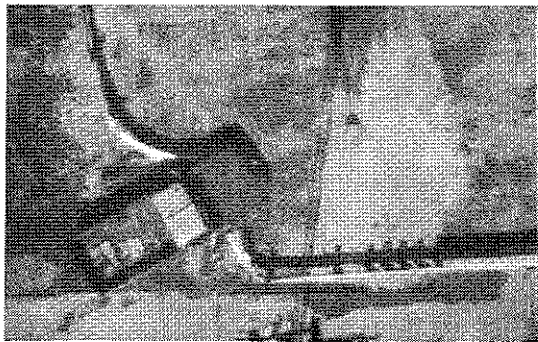
Figure A-2. Sequential photographs for test 414424-1 (continued).  
(perpendicular and behind the rail views)



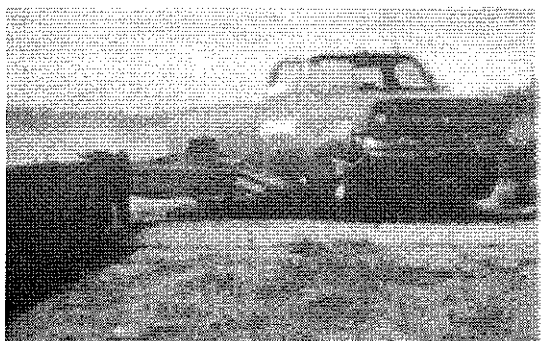
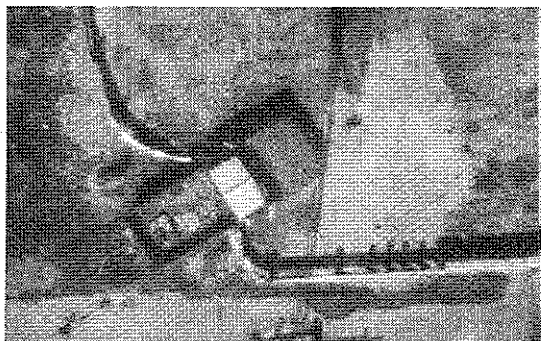
0.000 s



0.075 s

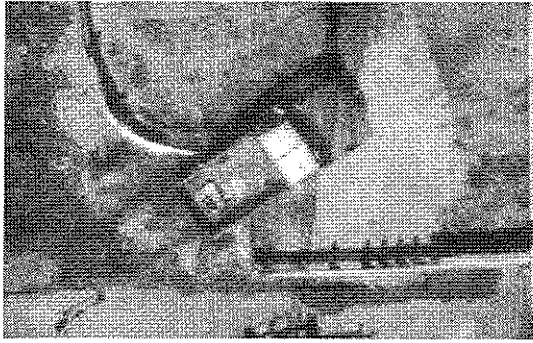


0.151 s

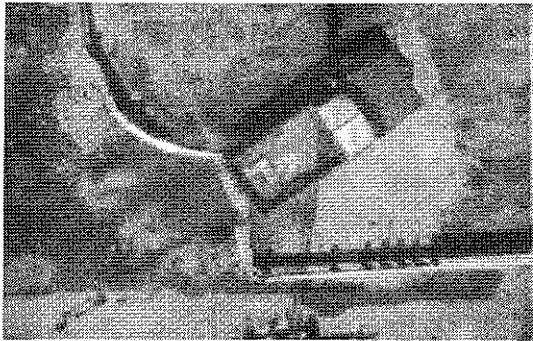
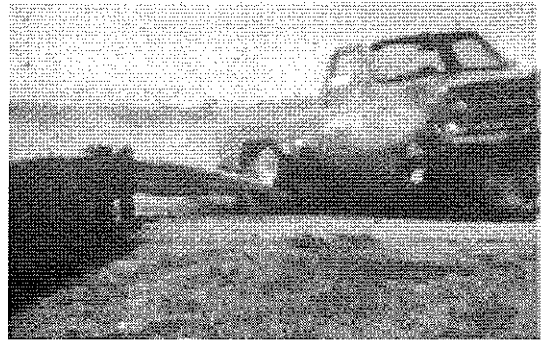


0.226 s

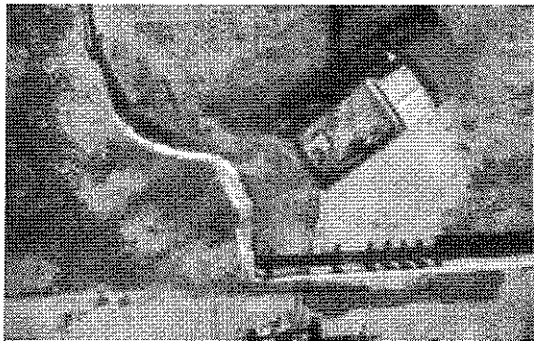
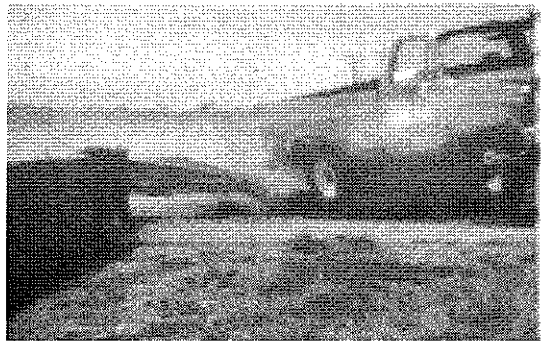
Figure A-3. Sequential photographs for test 414424-2.  
(overhead and frontal views)



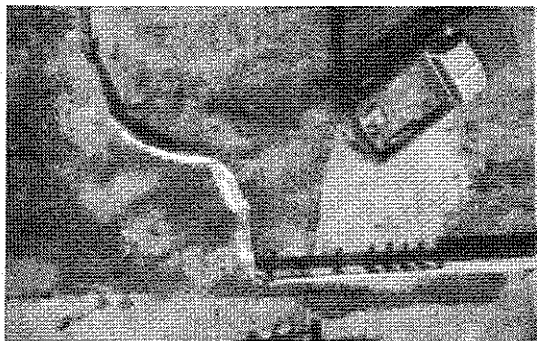
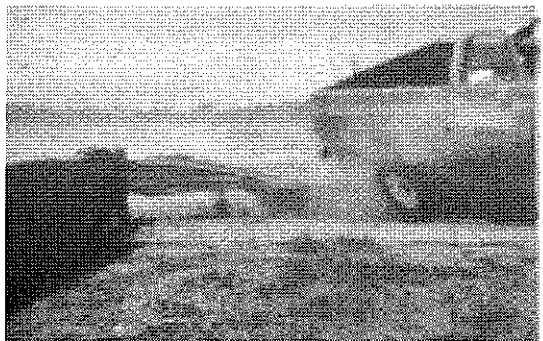
0.301 s



0.376 s



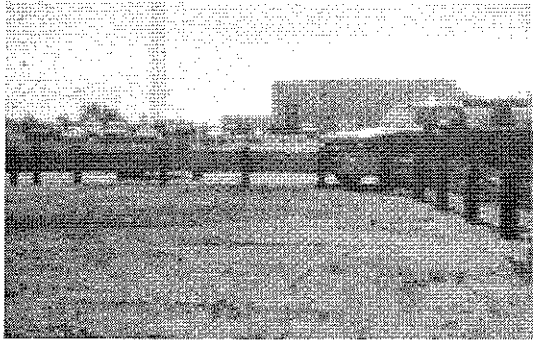
0.452 s



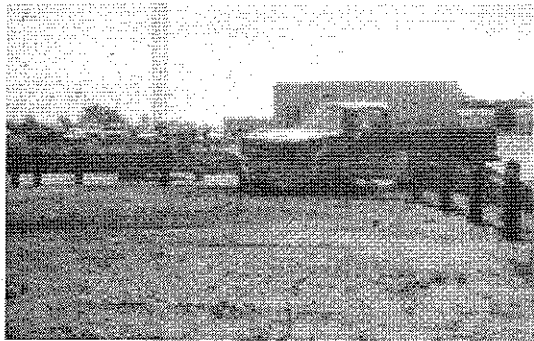
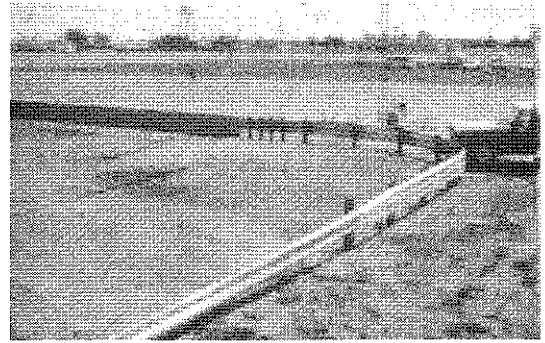
0.527 s



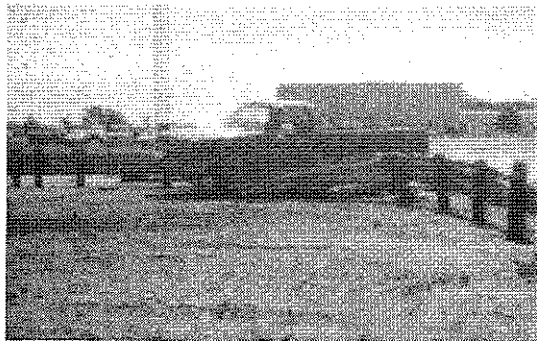
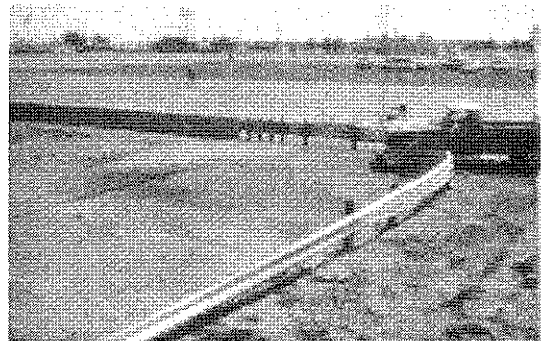
FigureA-3. Sequential photographs for test 414424-2 (continued).  
(overhead and frontal views)



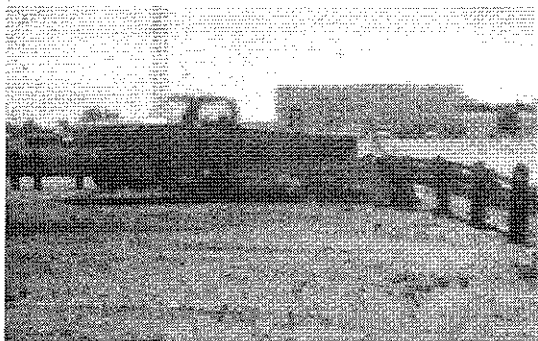
0.000 s



0.075 s



0.151 s



0.226 s

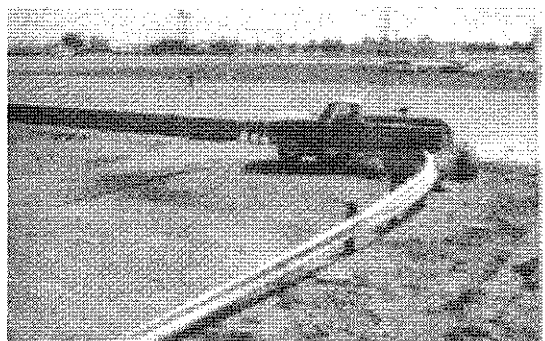
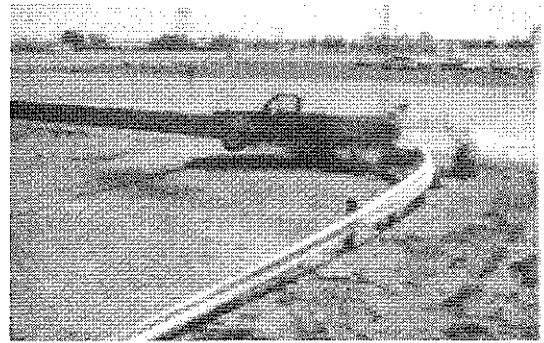
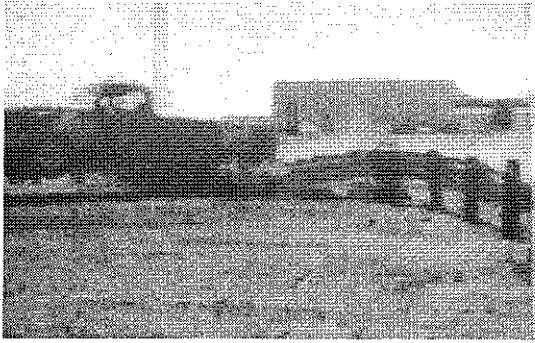
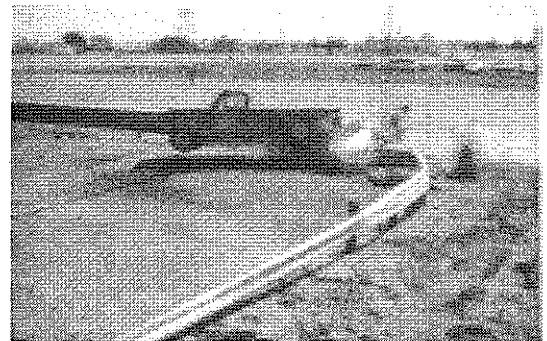
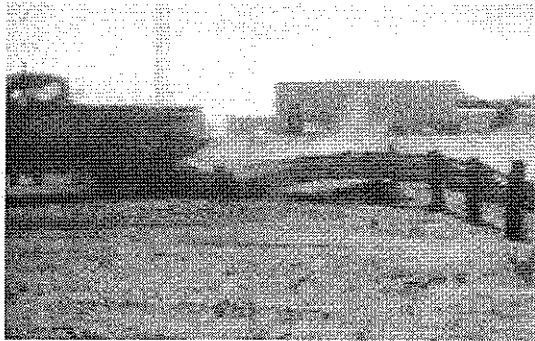


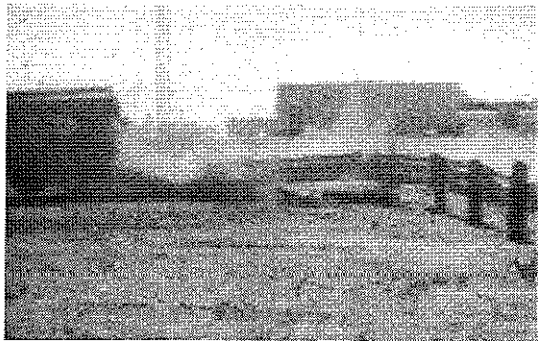
Figure A-4. Sequential photographs for test 414424-2.  
(behind the rail and oblique views)



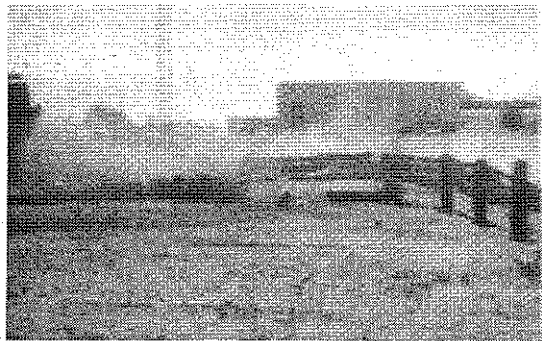
0.301 s



0.376 s

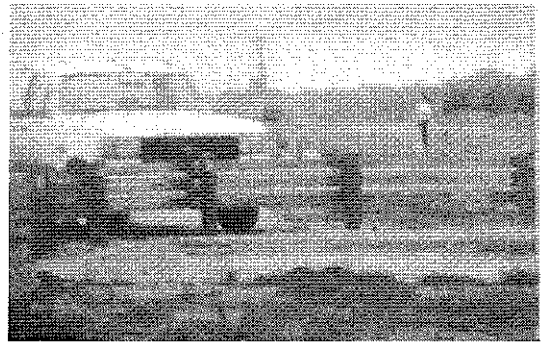
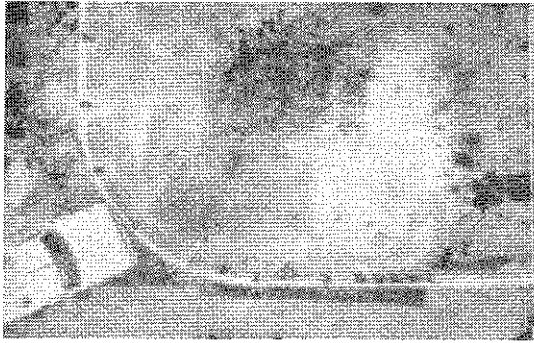


0.452 s

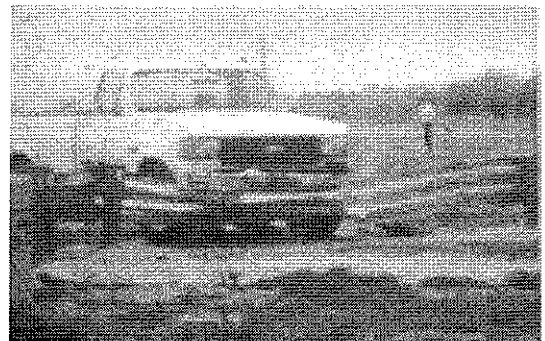


0.527 s

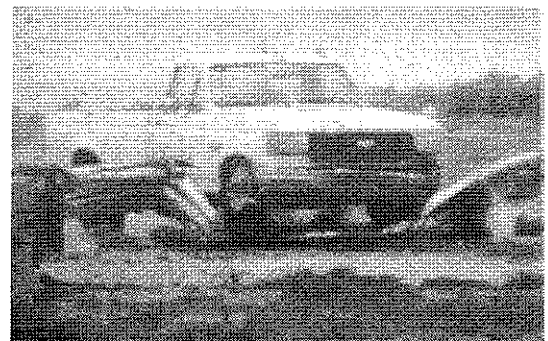
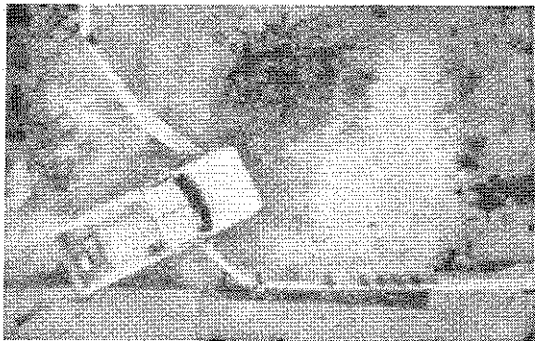
FigureA-4. Sequential photographs for test 414424-2 (continued).  
(behind the rail and oblique views)



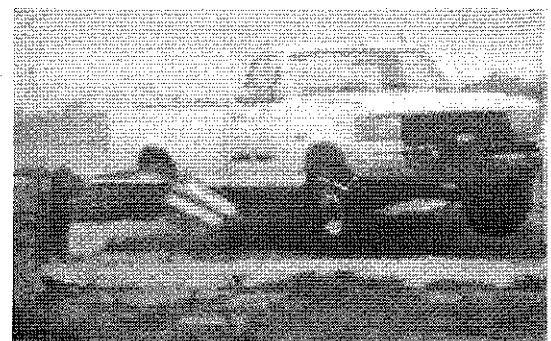
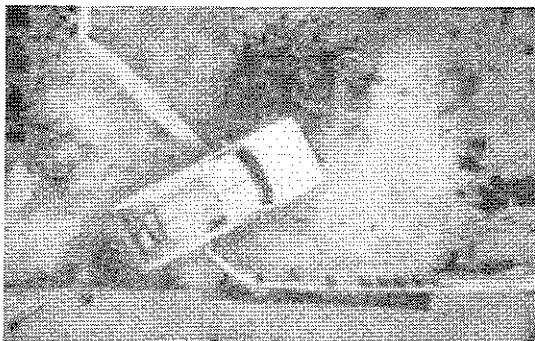
0.000 s



0.074 s



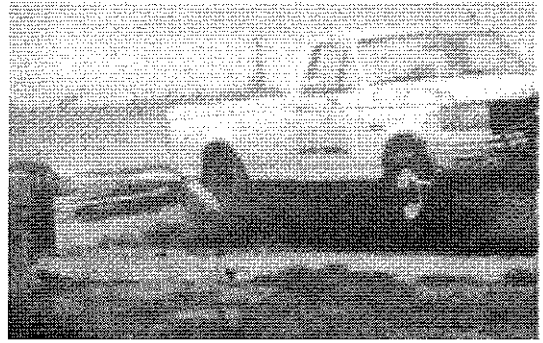
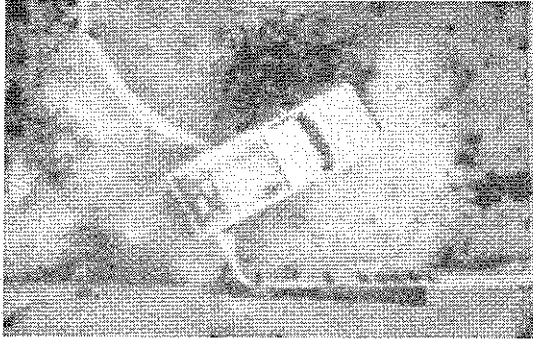
0.148 s



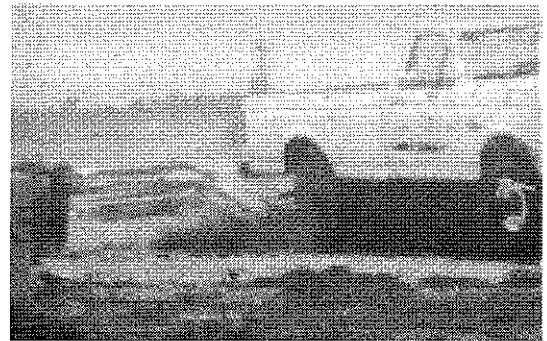
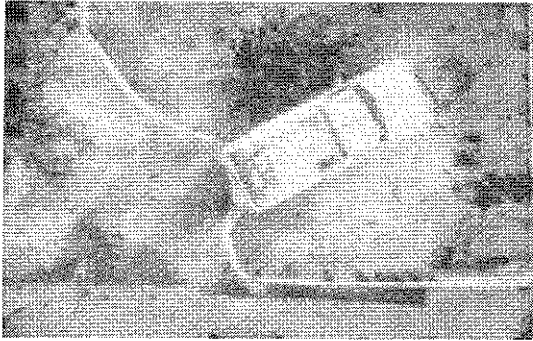
0.223 s

Figure A-5. Sequential photographs for test 414424-3.  
(overhead and frontal views)

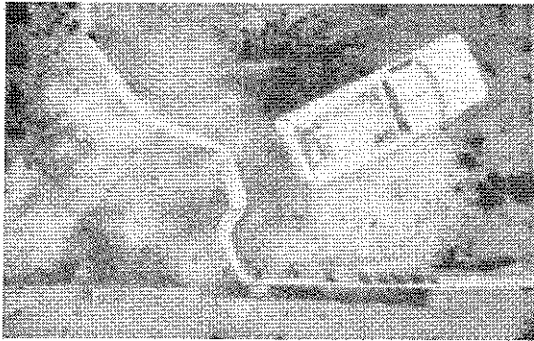




0.297 s



0.371 s

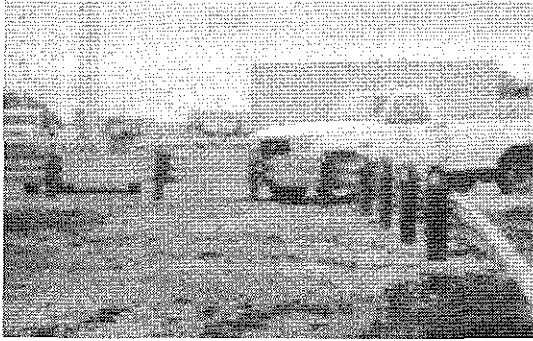


0.445 s



0.519 s

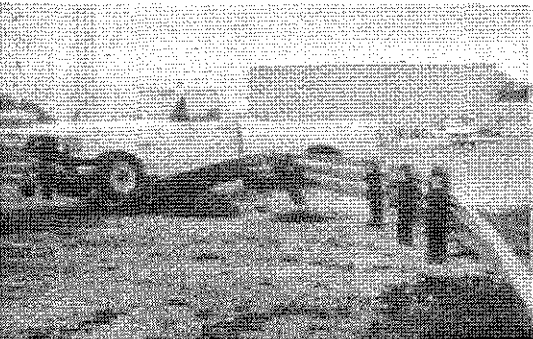
Figure A-5. Sequential photographs for test 414424-3 (continued).  
(overhead and frontal views)



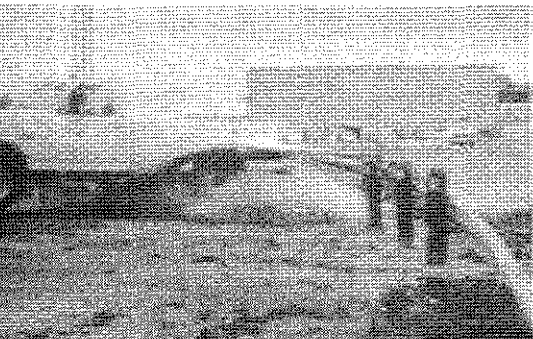
0.000 s



0.074 s

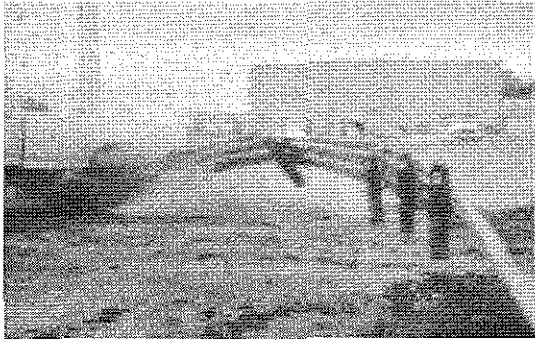


0.148 s

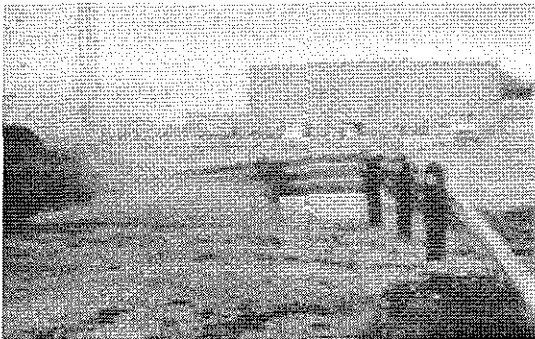
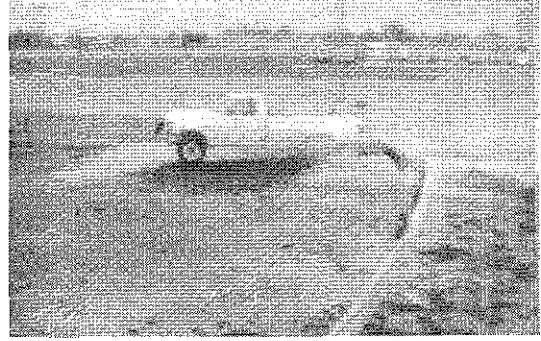


0.223 s

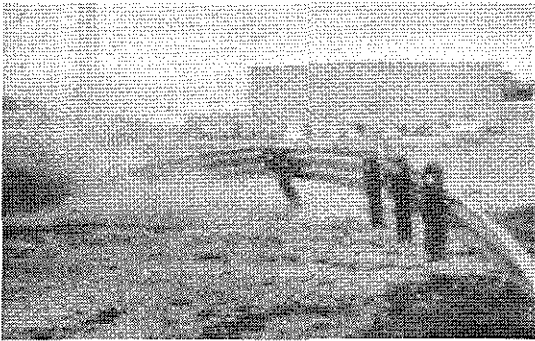
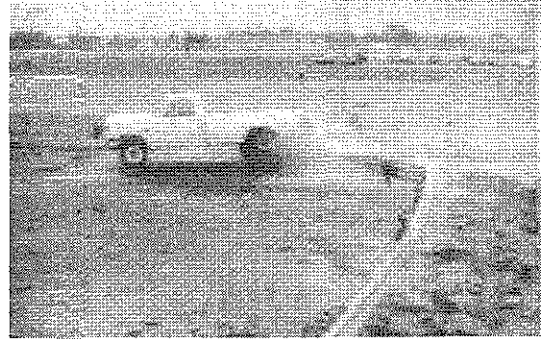
Figure A-6. Sequential photographs for test 414424-3.  
(behind the rail and oblique views)



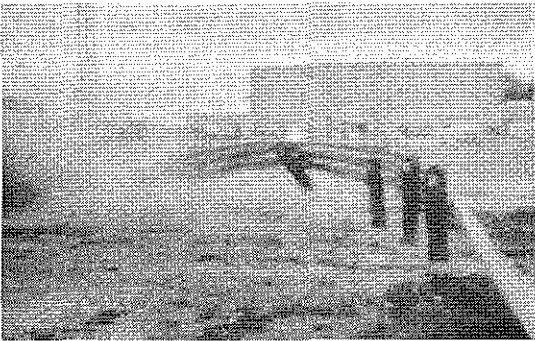
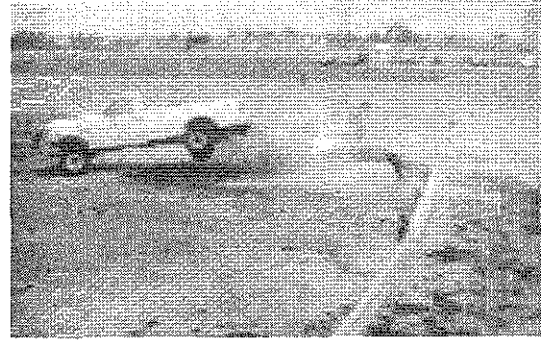
0.297 s



0.371 s



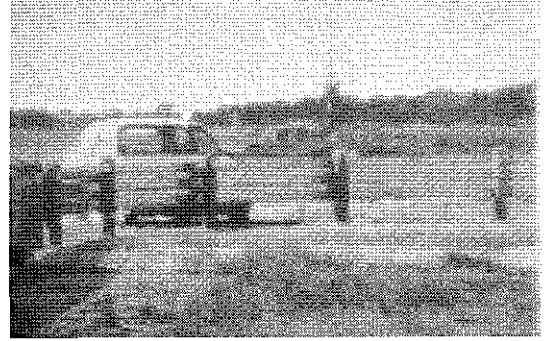
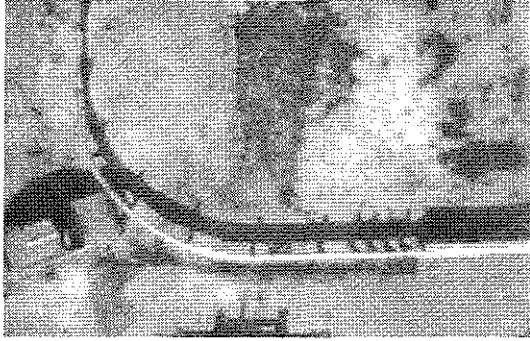
0.445 s



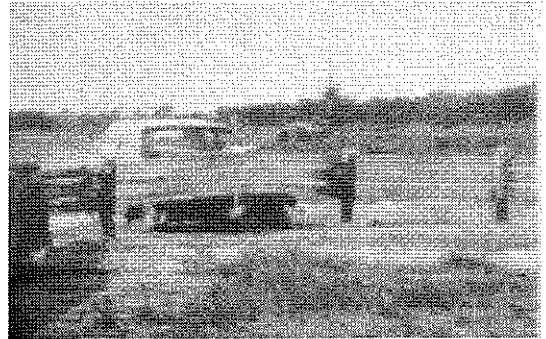
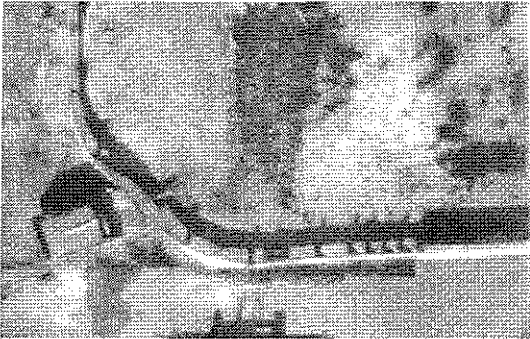
0.519 s



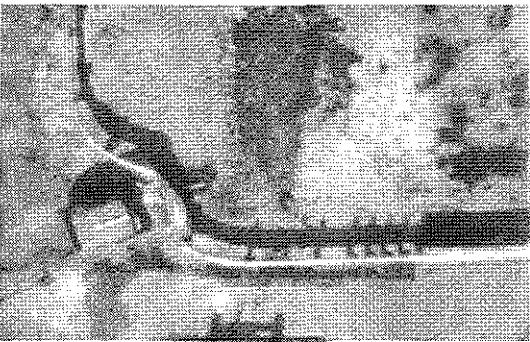
Figure A-6. Sequential photographs for test 414424-3 (continued).  
(behind the rail and oblique views)



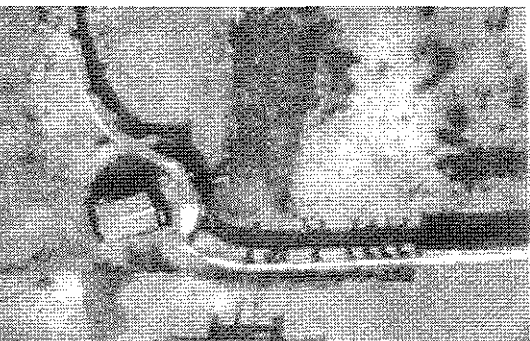
0.000 s



0.051 s

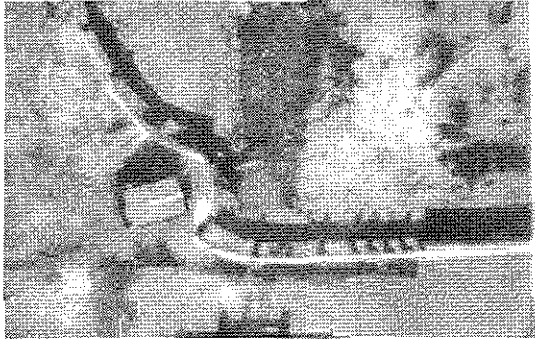


0.102 s

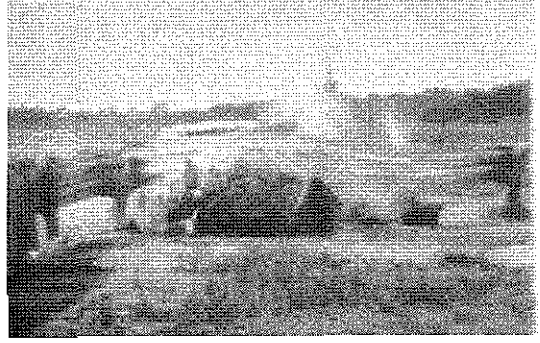


0.152 s

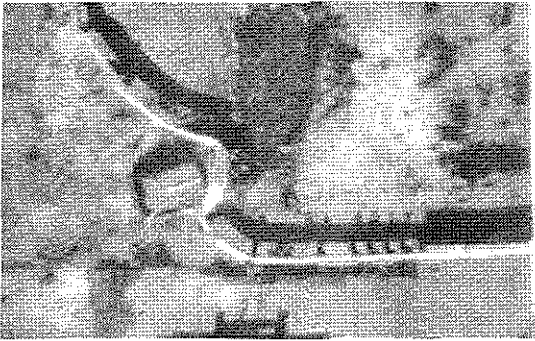
Figure A-7. Sequential photographs for test 414424-4.  
(overhead and frontal views)



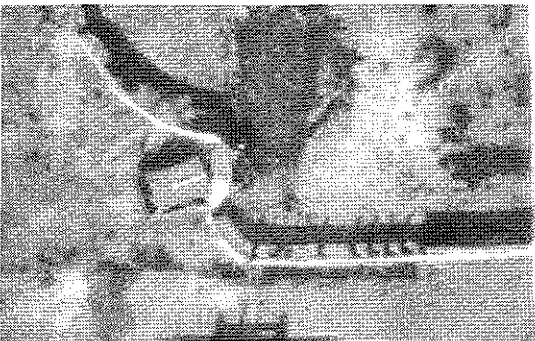
0.203 s



0.254 s



0.305 s



0.356 s

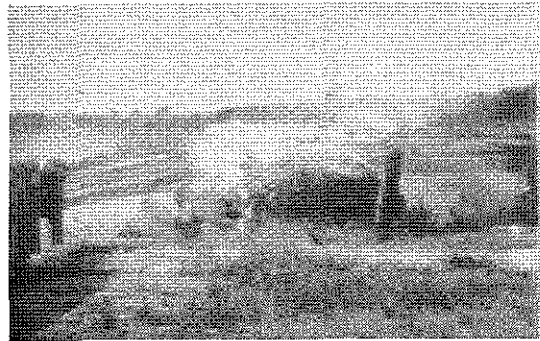
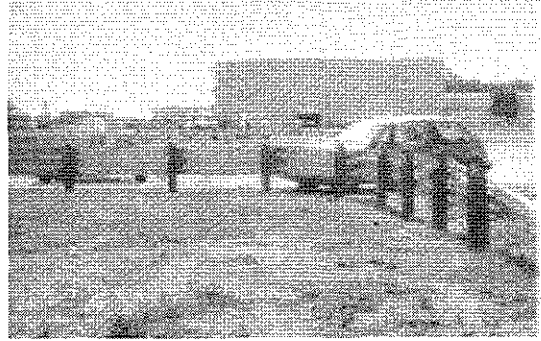
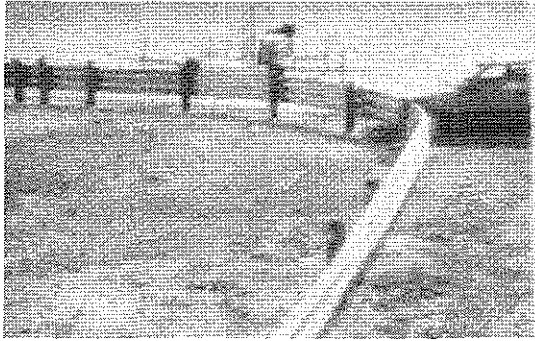
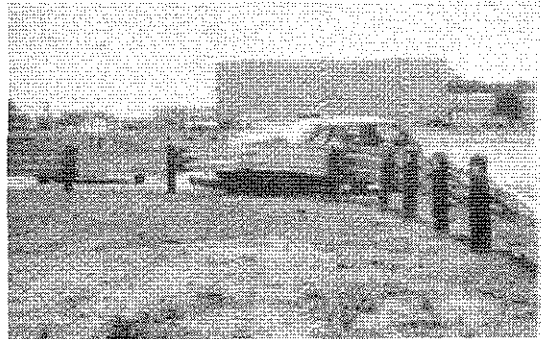
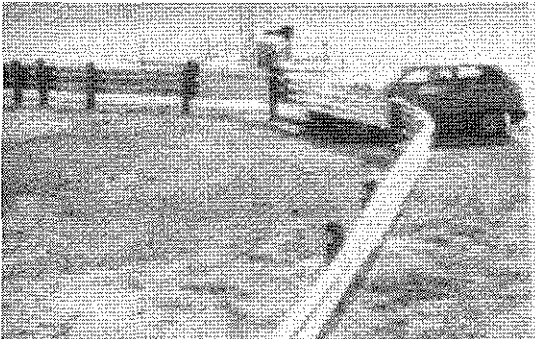


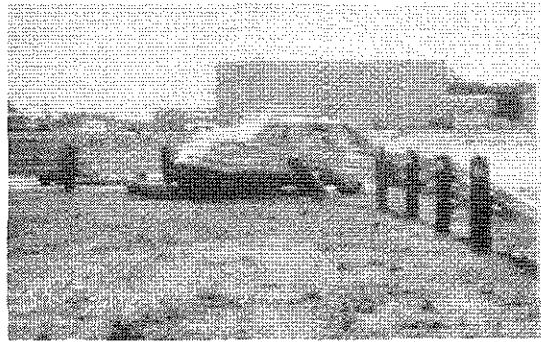
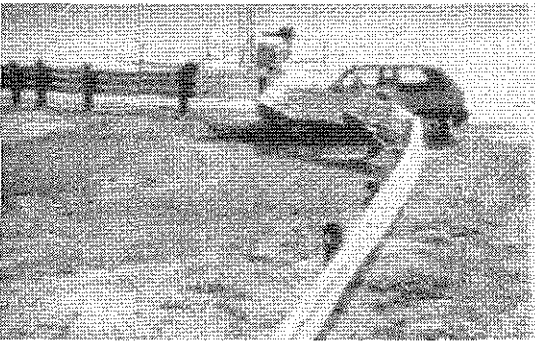
Figure A-7. Sequential photographs for test 414424-4 (continued).  
(overhead and frontal views)



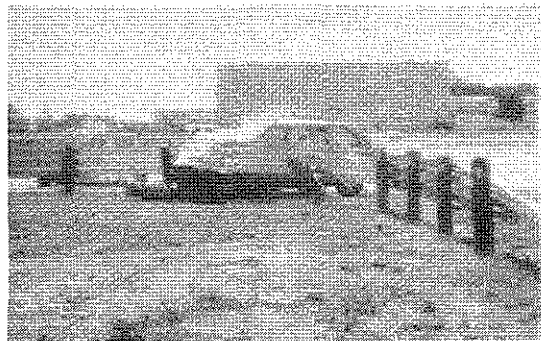
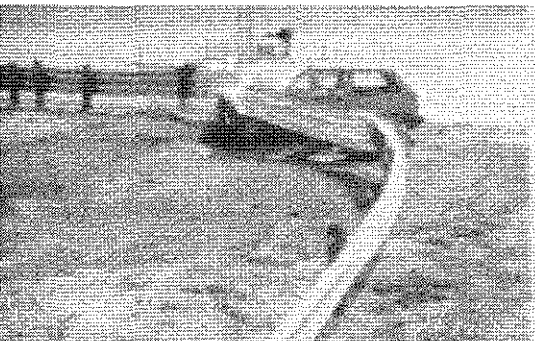
0.000 s



0.051 s

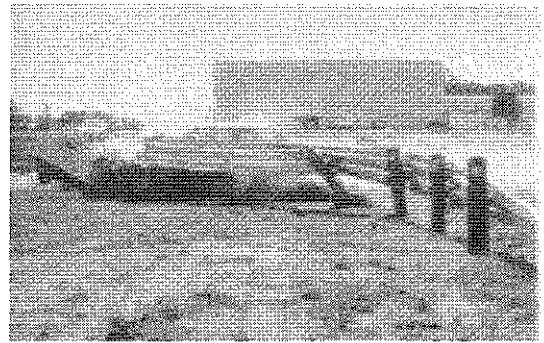
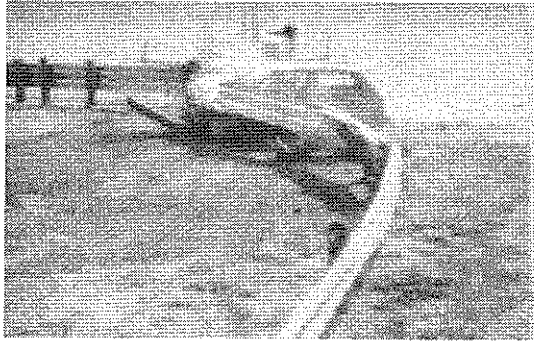


0.102 s

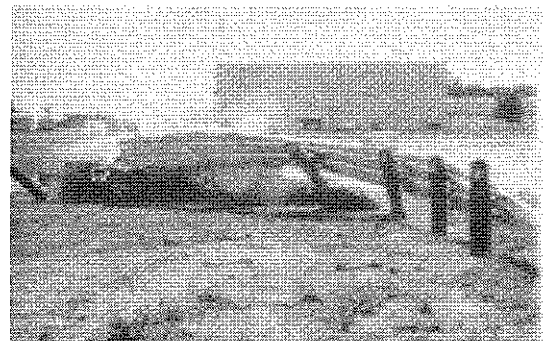


0.152 s

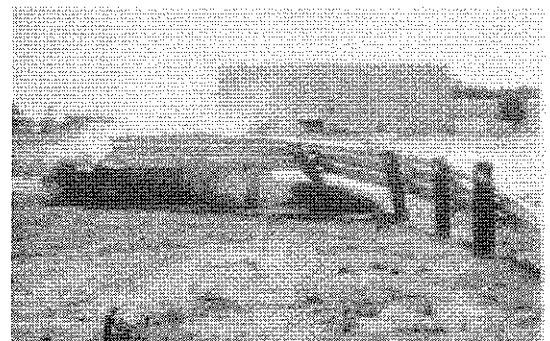
Figure A-8. Sequential photographs for test 414424-4.  
(perpendicular and behind the rail views)



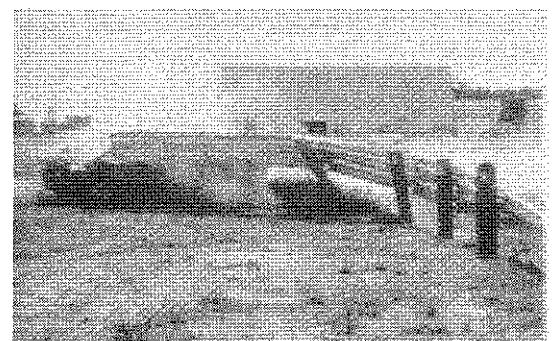
0.203 s



0.254 s

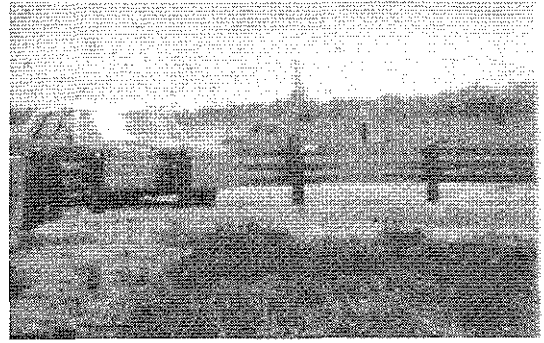
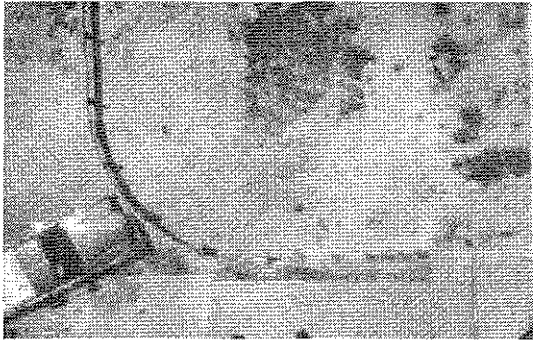


0.305 s

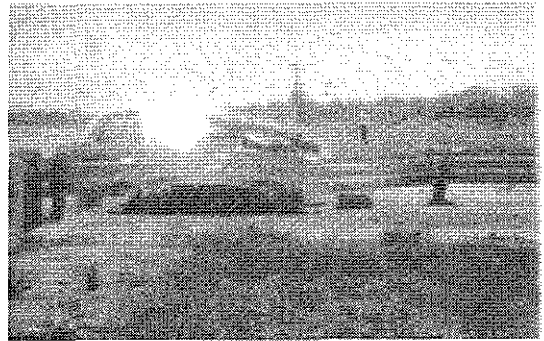
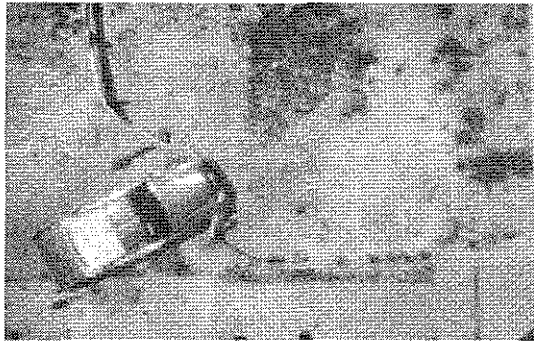


0.356 s

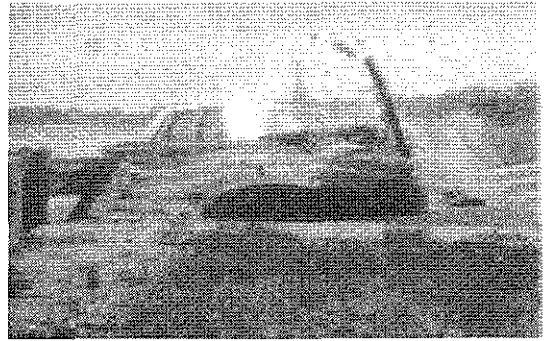
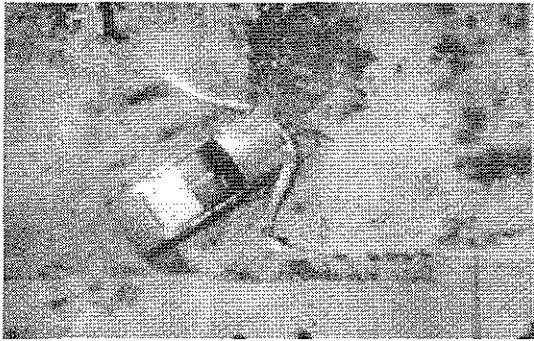
Figure A-8. Sequential photographs for test 414424-4 (continued).  
(perpendicular and behind the rail views)



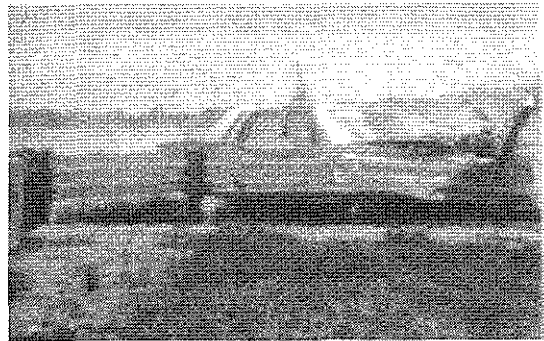
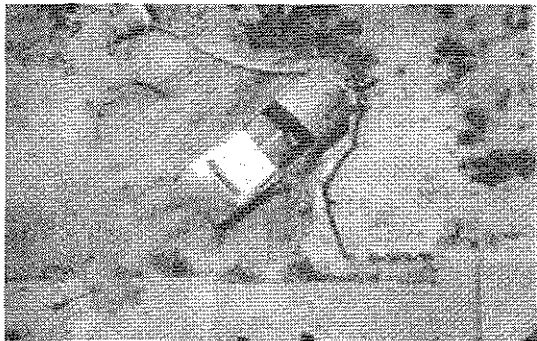
0.000 s



0.112 s



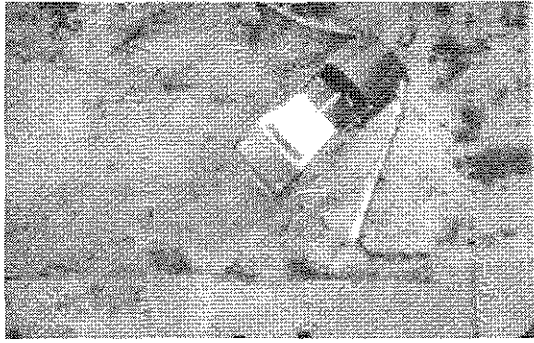
0.223 s



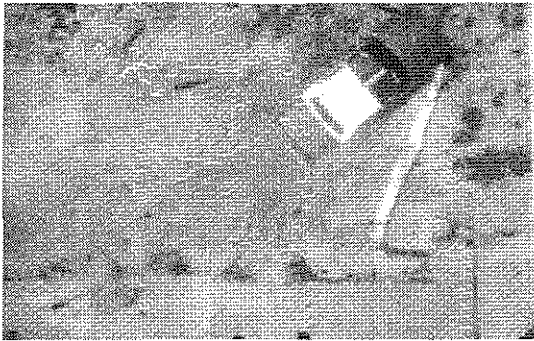
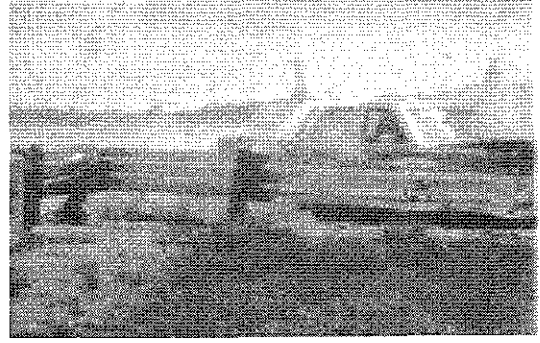
0.335 s

Figure A-9. Sequential photographs for test 414424-5.  
(overhead and frontal views)

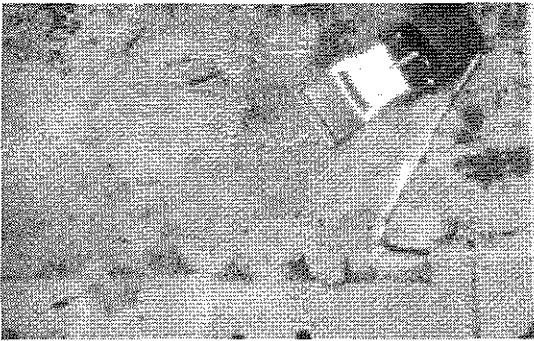




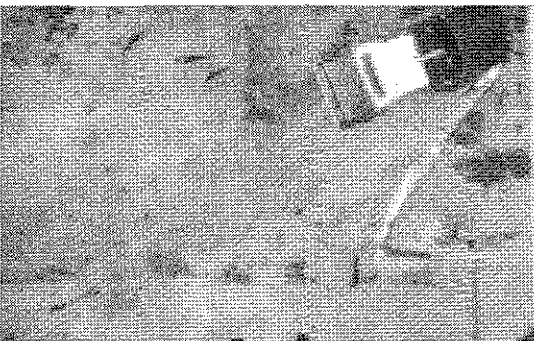
0.447 s



0.558 s



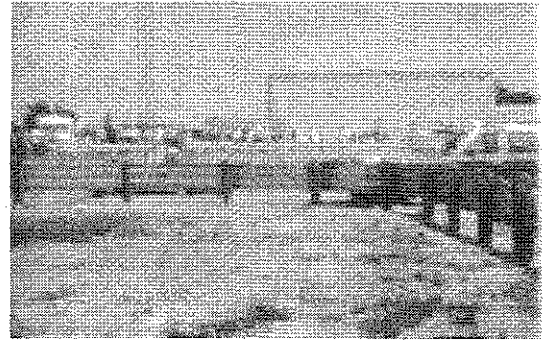
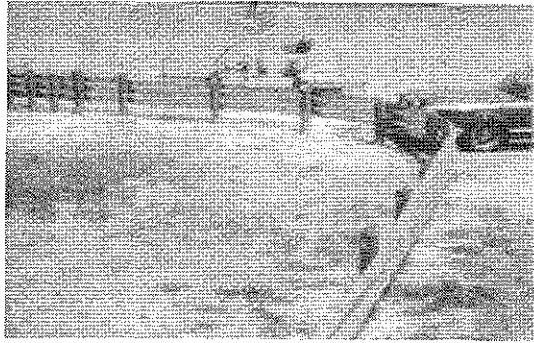
0.670 s



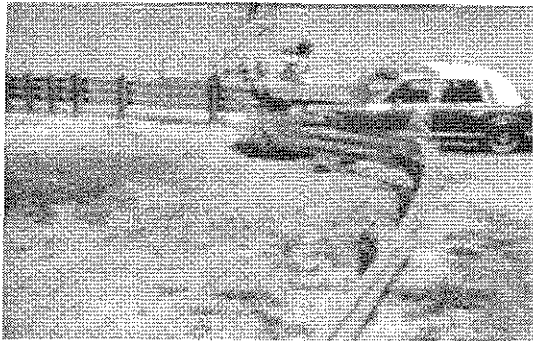
0.780 s



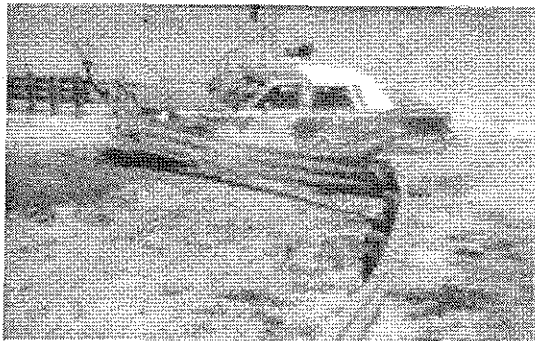
Figure A-9. Sequential photographs for test 414424-5 (continued).  
(overhead and frontal views)



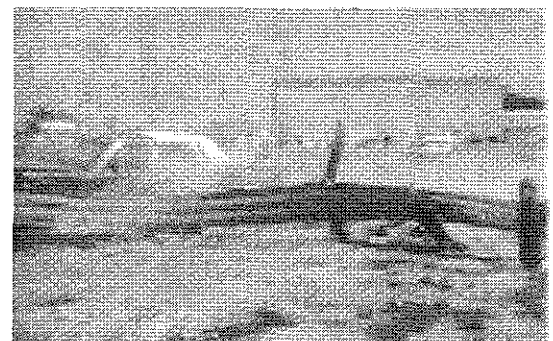
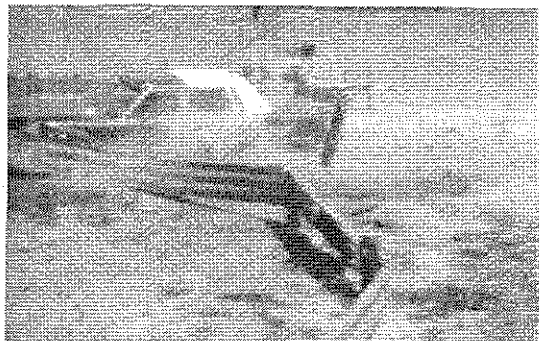
0.000 s



0.112 s

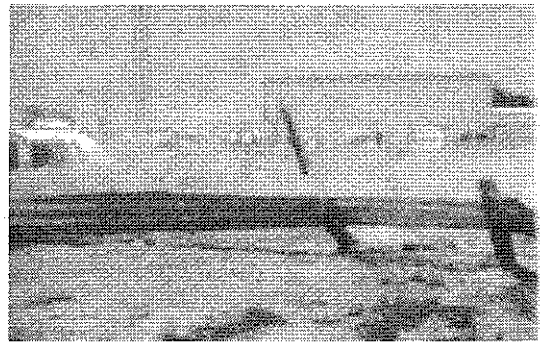


0.223 s



0.335 s

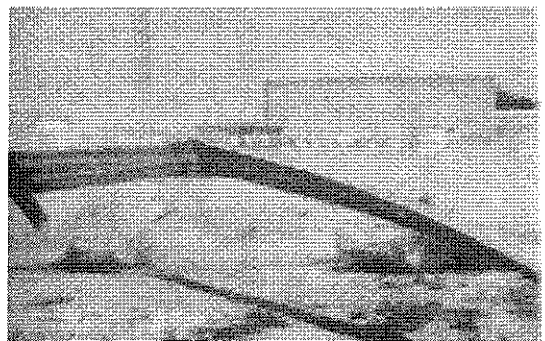
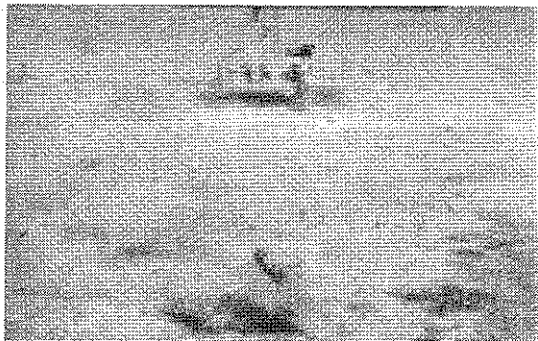
Figure A-10. Sequential photographs for test 414424-5.  
(perpendicular and behind the rail views)



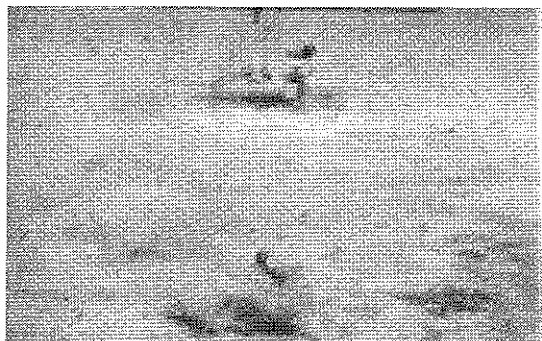
0.447 s



0.558 s



0.670 s



0.782 s

Figure A-10. Sequential photographs for test 414424-5 (continued).  
(perpendicular and behind the rail views)

**APPENDIX B**  
**VEHICULAR ACCELERATIONS**

CRASH TEST 414424-1  
Accelerometer at center-of-gravity

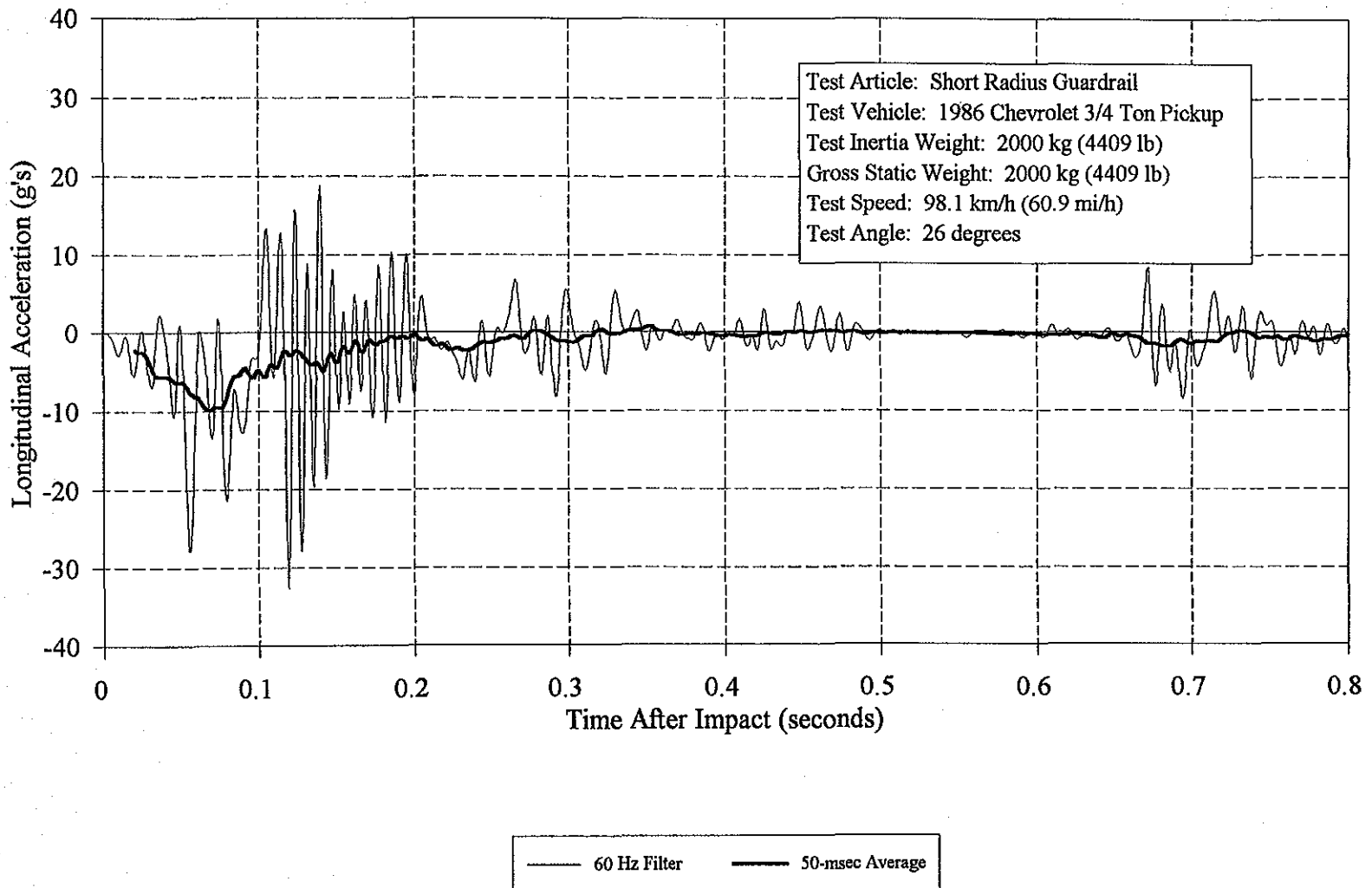


Figure B-1. Vehicle longitudinal accelerometer trace for test 414424-1.

CRASH TEST 414424-1  
Accelerometer at center-of-gravity

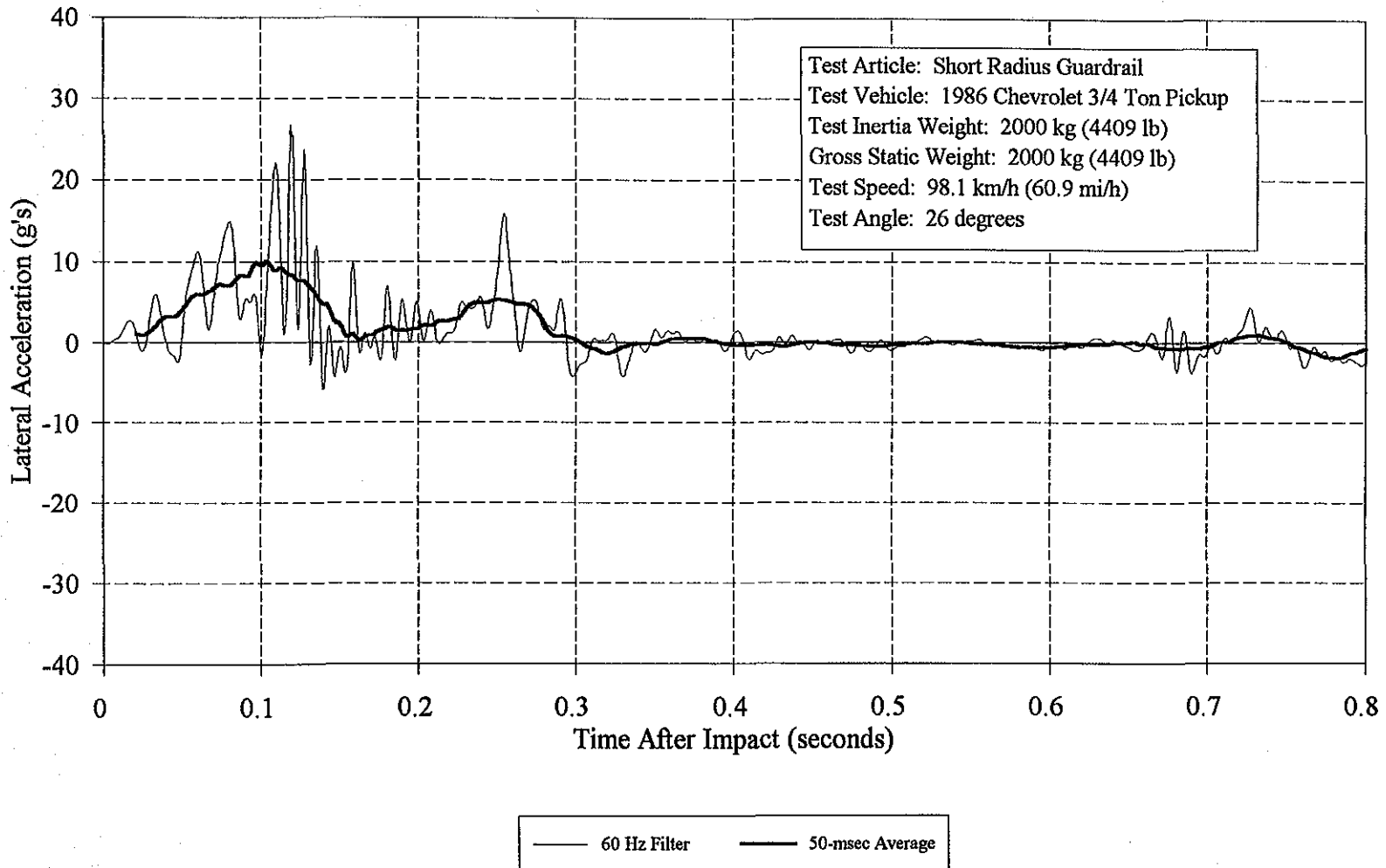


Figure B-2. Vehicle lateral accelerometer trace for test 414424-1.

**CRASH TEST 414424-1**  
Accelerometer at center-of-gravity

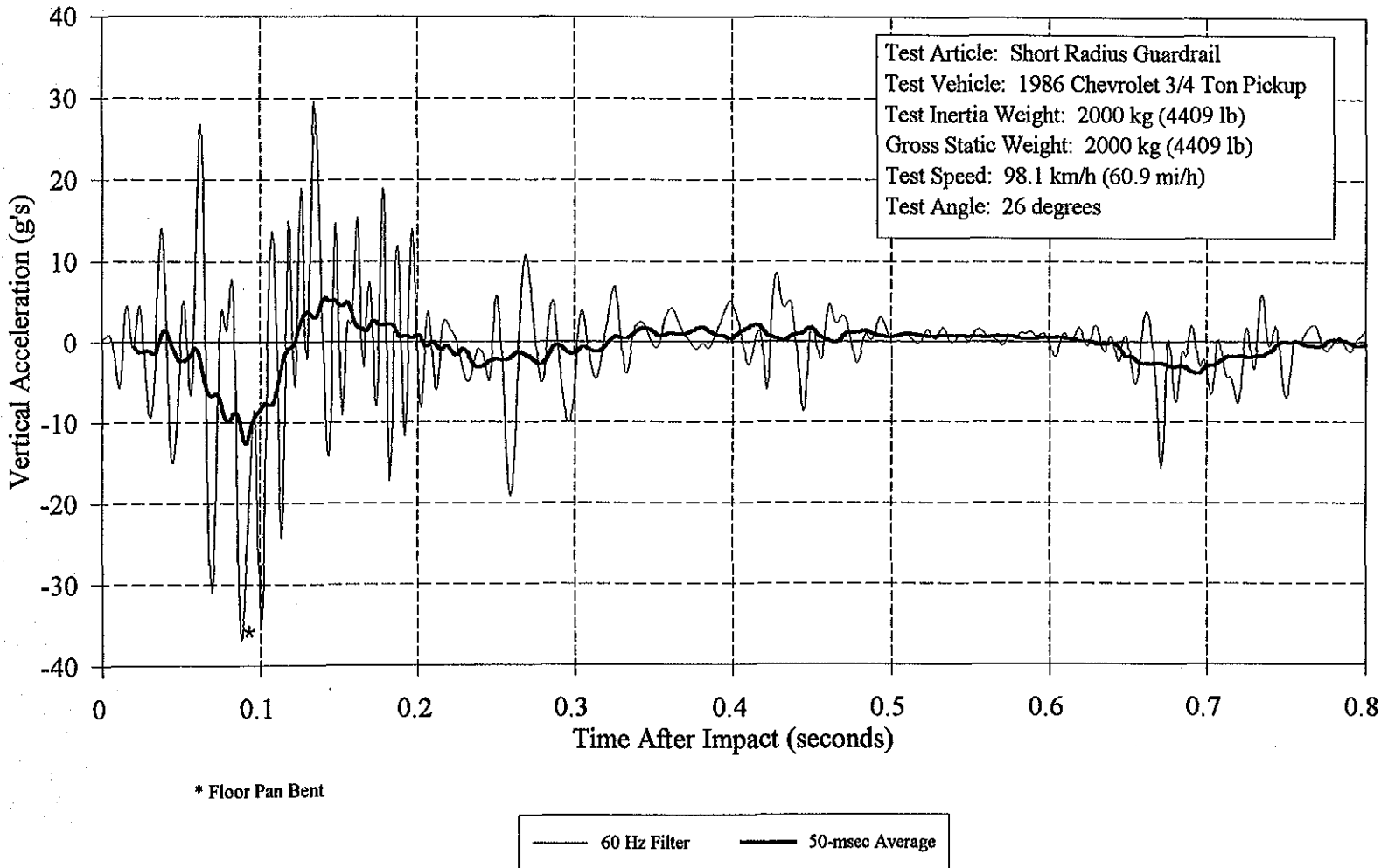
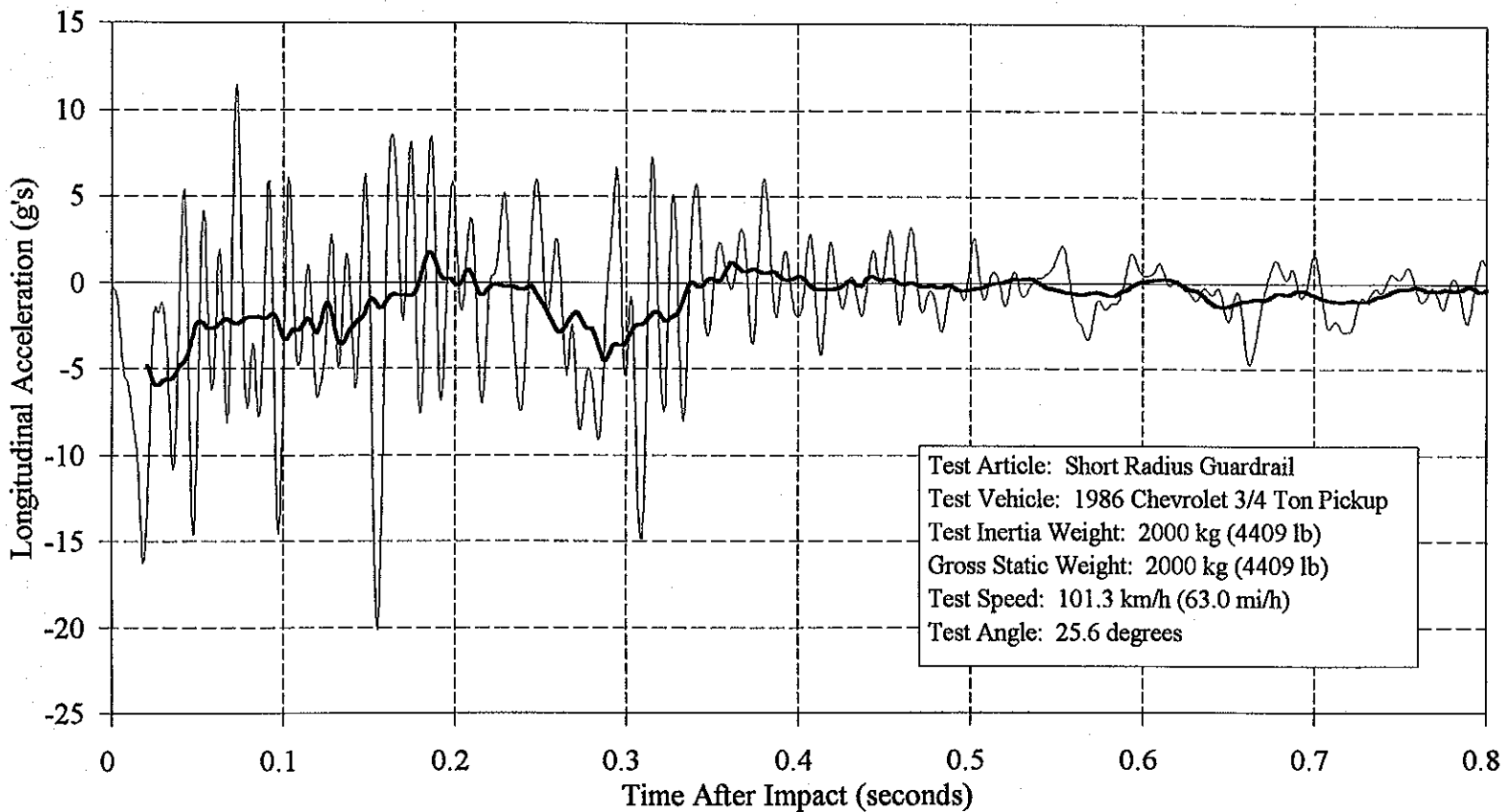


Figure B-3. Vehicle vertical accelerometer trace for test 414424-1.

CRASH TEST 414424-2  
Accelerometer at center-of-gravity



86

— 60 Hz Filter      — 50-msec Average

Figure B-4. Vehicle longitudinal accelerometer trace for test 414424-2.



**CRASH TEST 414424-2**  
Accelerometer at center-of-gravity

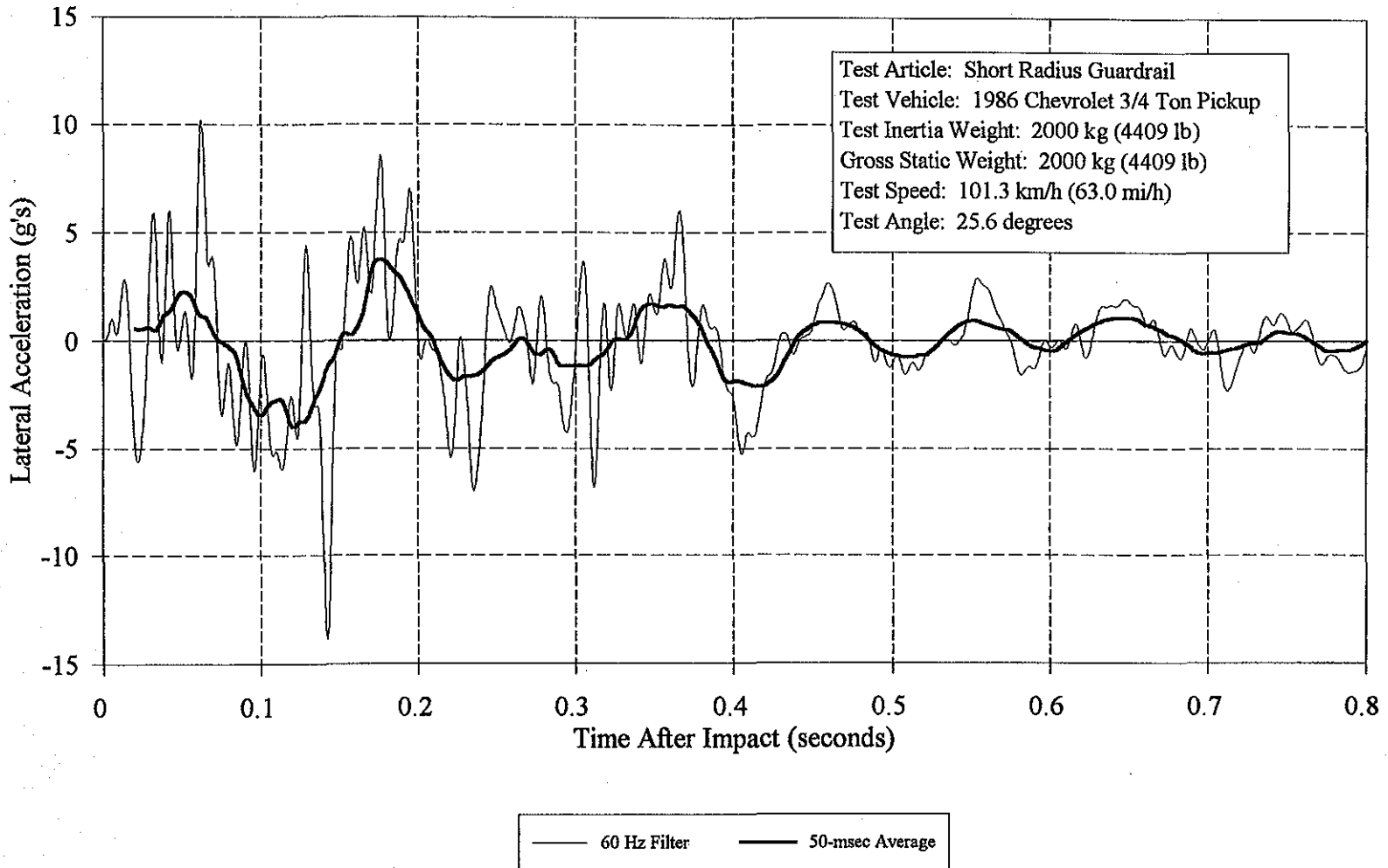


Figure B-5. Vehicle lateral accelerometer trace for test 414424-2.

**CRASH TEST 414424-2**  
Accelerometer at center-of-gravity

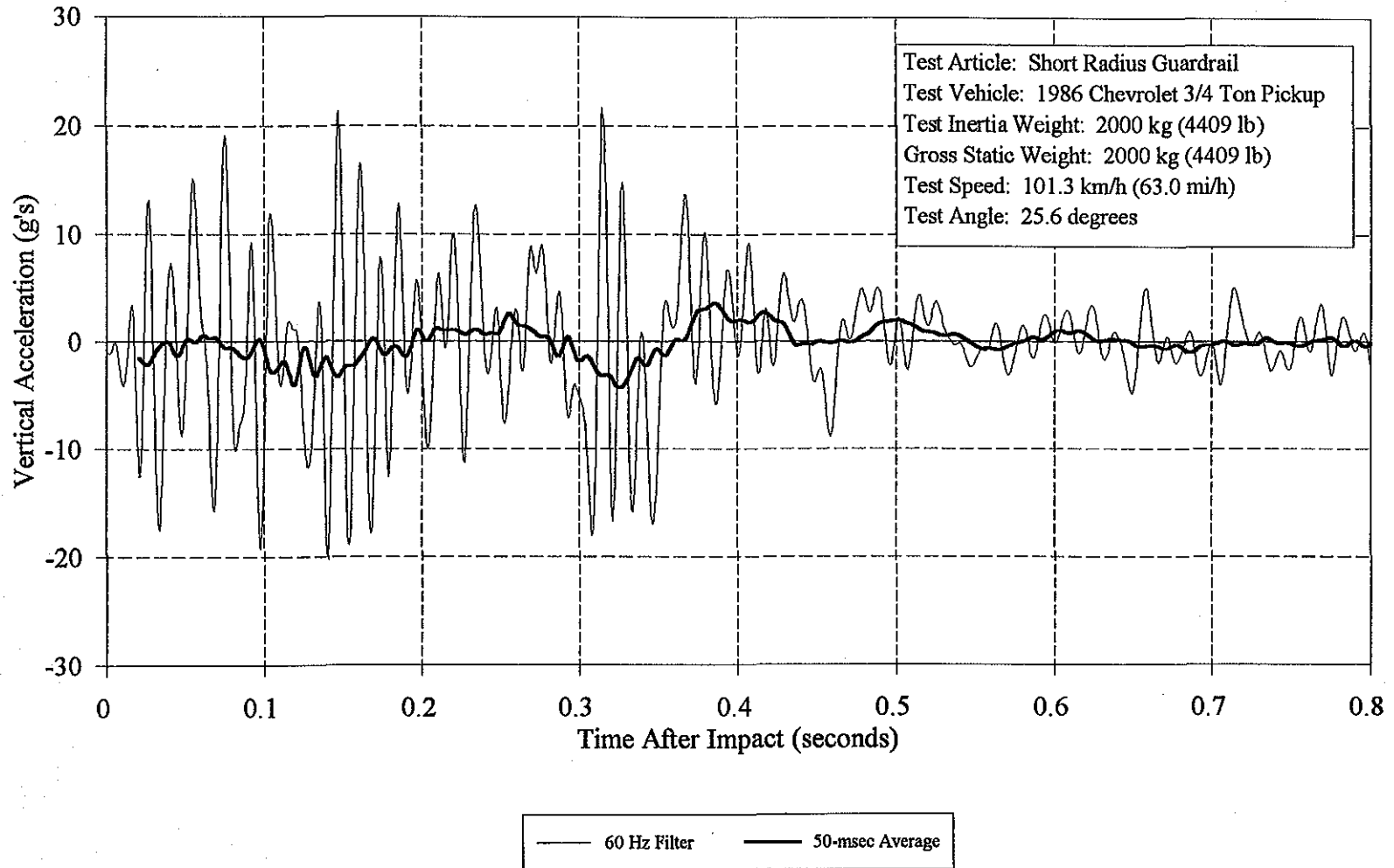


Figure B-6. Vehicle vertical accelerometer trace for test 414424-2.

CRASH TEST 414424-3  
Accelerometer at center-of-gravity

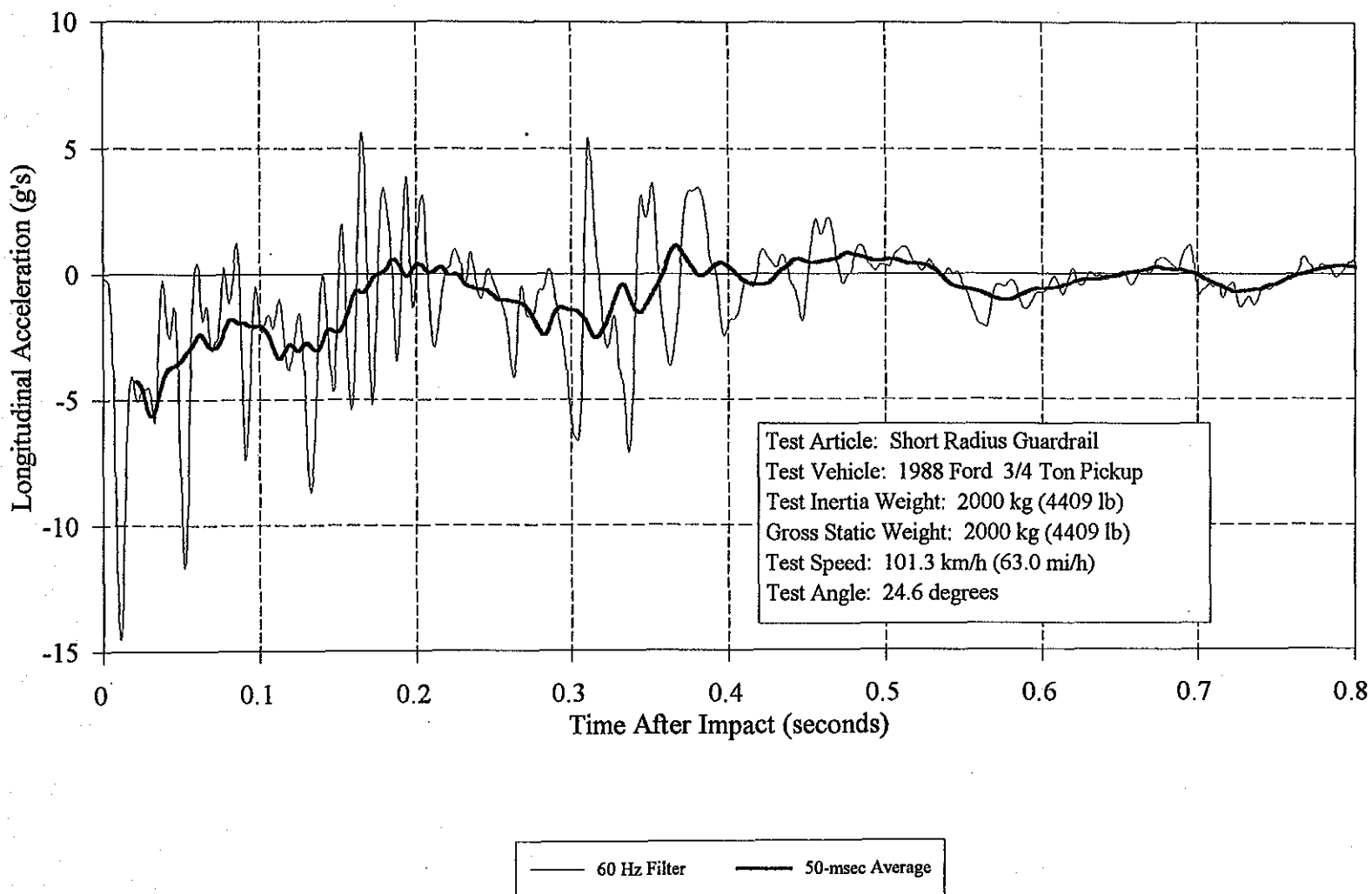


Figure B-7. Vehicle longitudinal accelerometer trace for test 414424-3.

**CRASH TEST 414424-3**  
Accelerometer at center-of-gravity

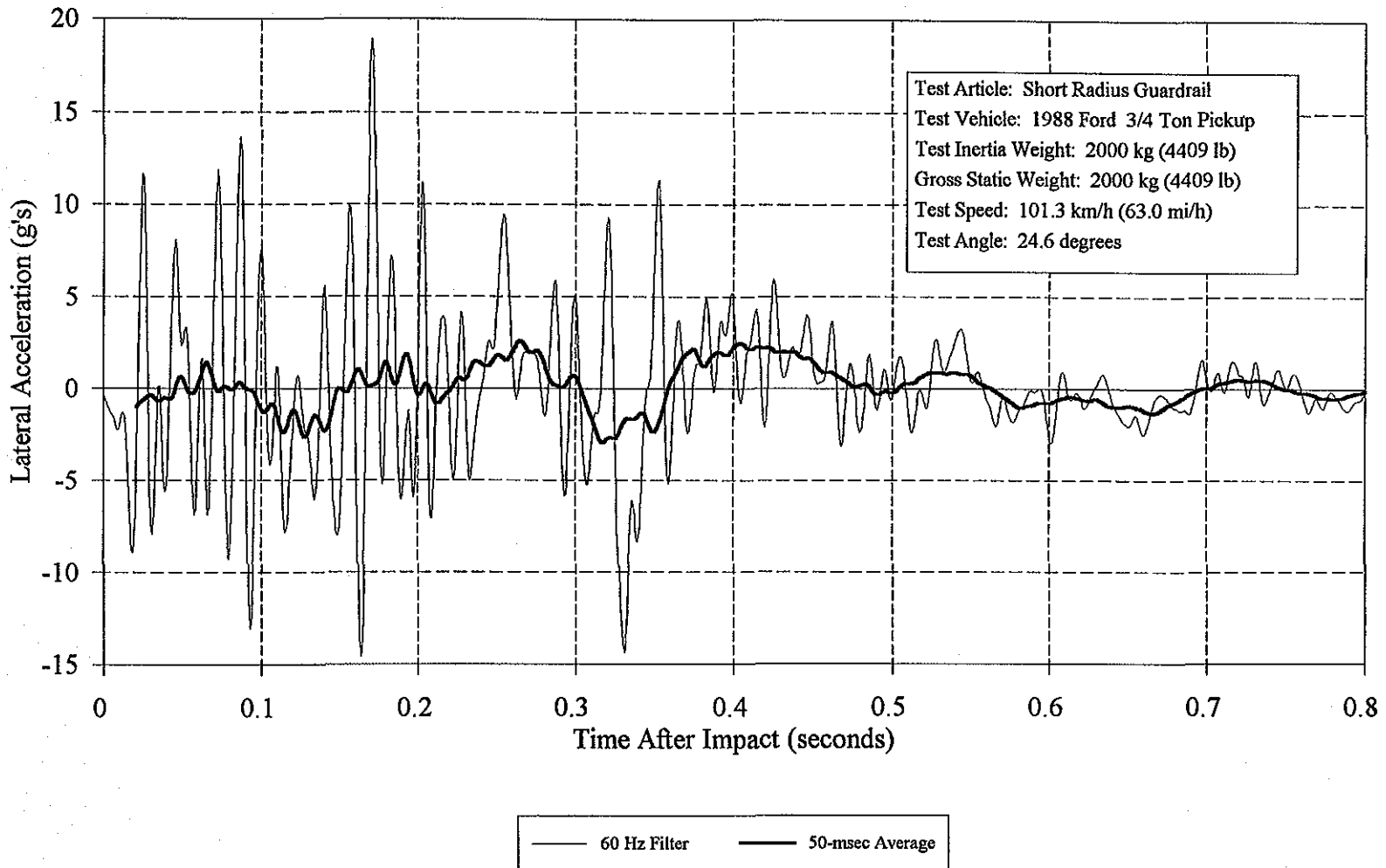


Figure B-8. Vehicle lateral accelerometer trace for test 414424-3.

**CRASH TEST 414424-3**  
Accelerometer at center-of-gravity

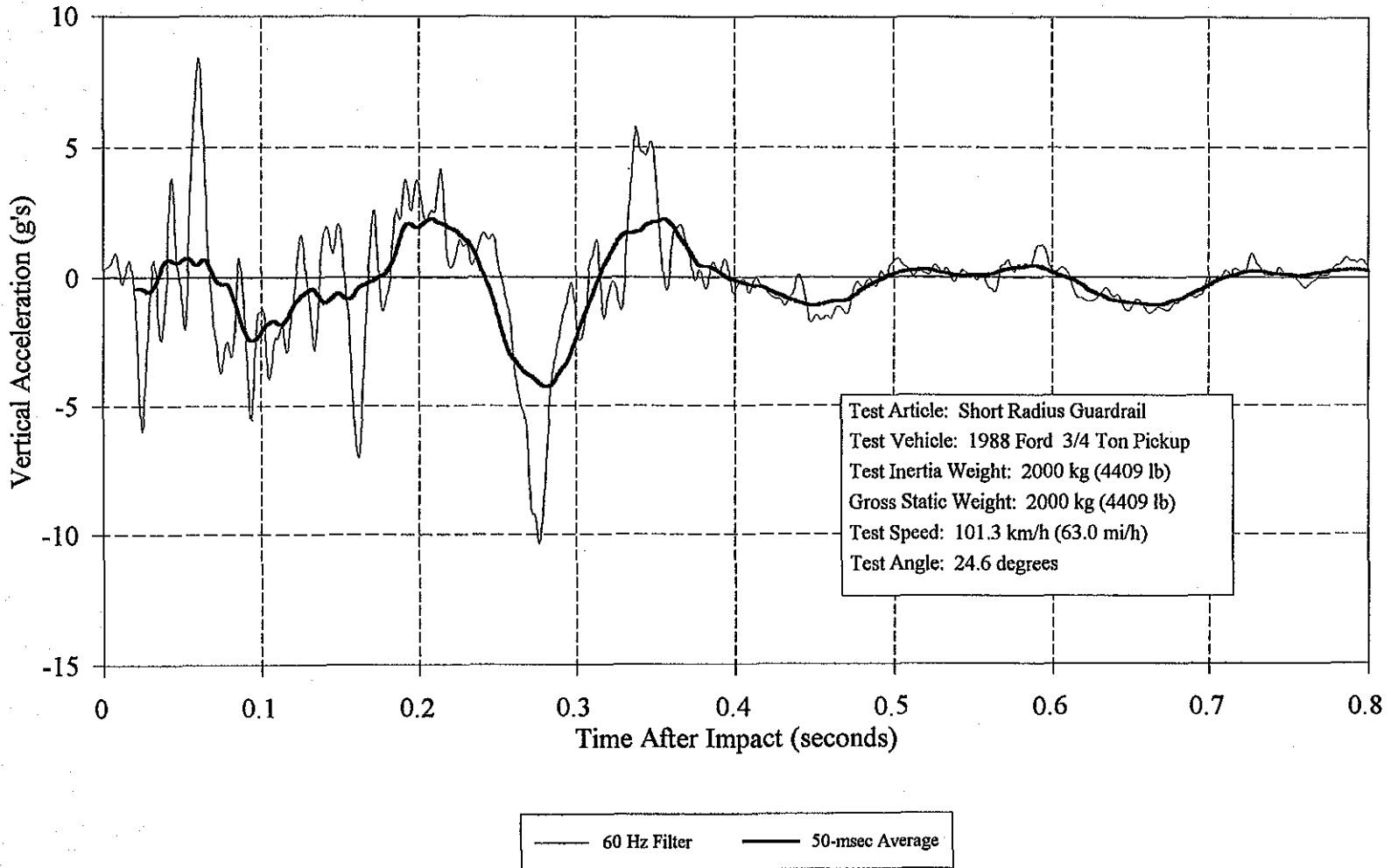


Figure B-9. Vehicle vertical accelerometer trace for test 414424-3.

**CRASH TEST 414424-4**  
Accelerometer at center-of-gravity

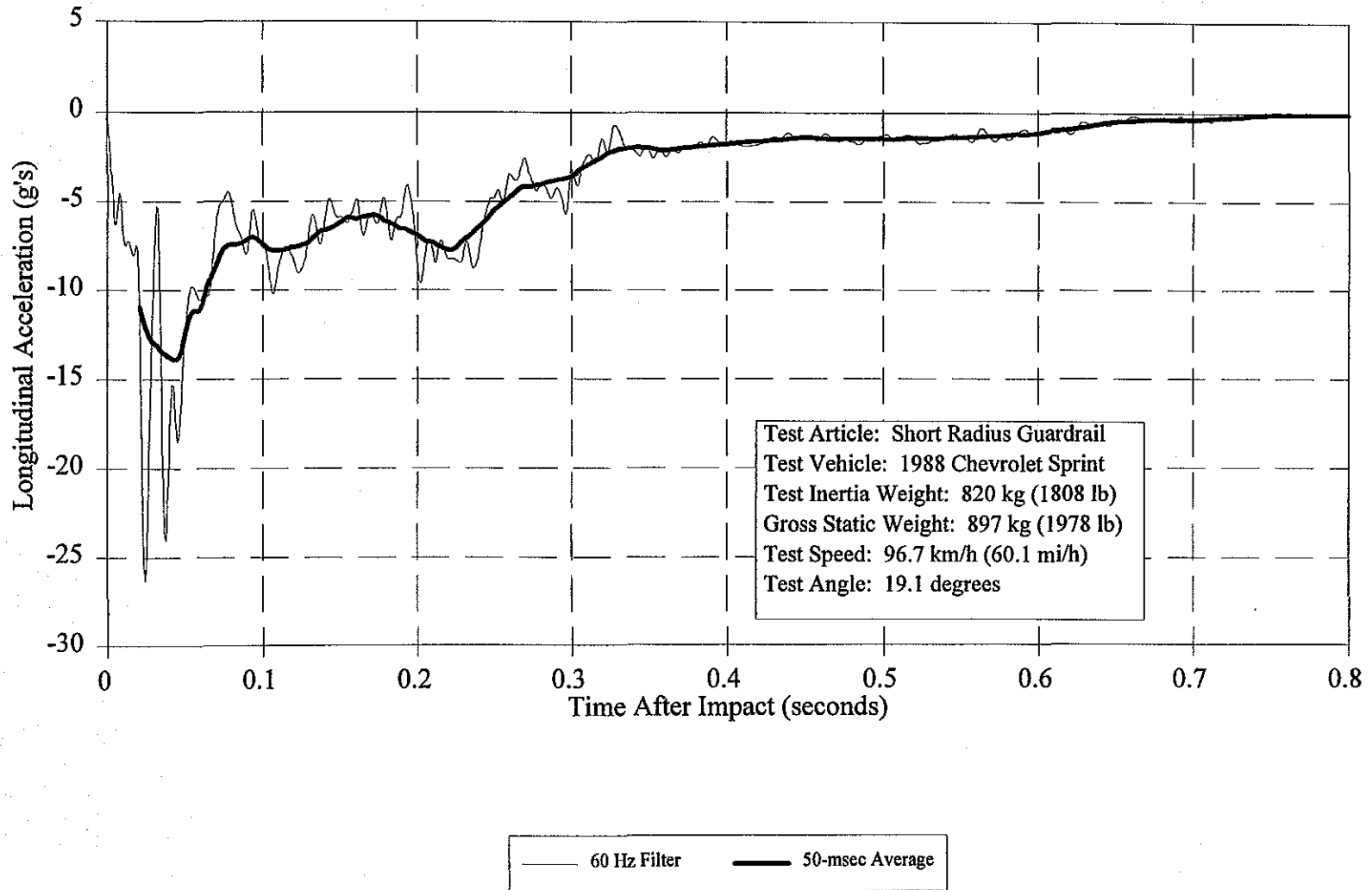


Figure B-10. Vehicle longitudinal accelerometer trace for test 414424-4.

**CRASH TEST 414424-4**  
Accelerometer at center-of-gravity

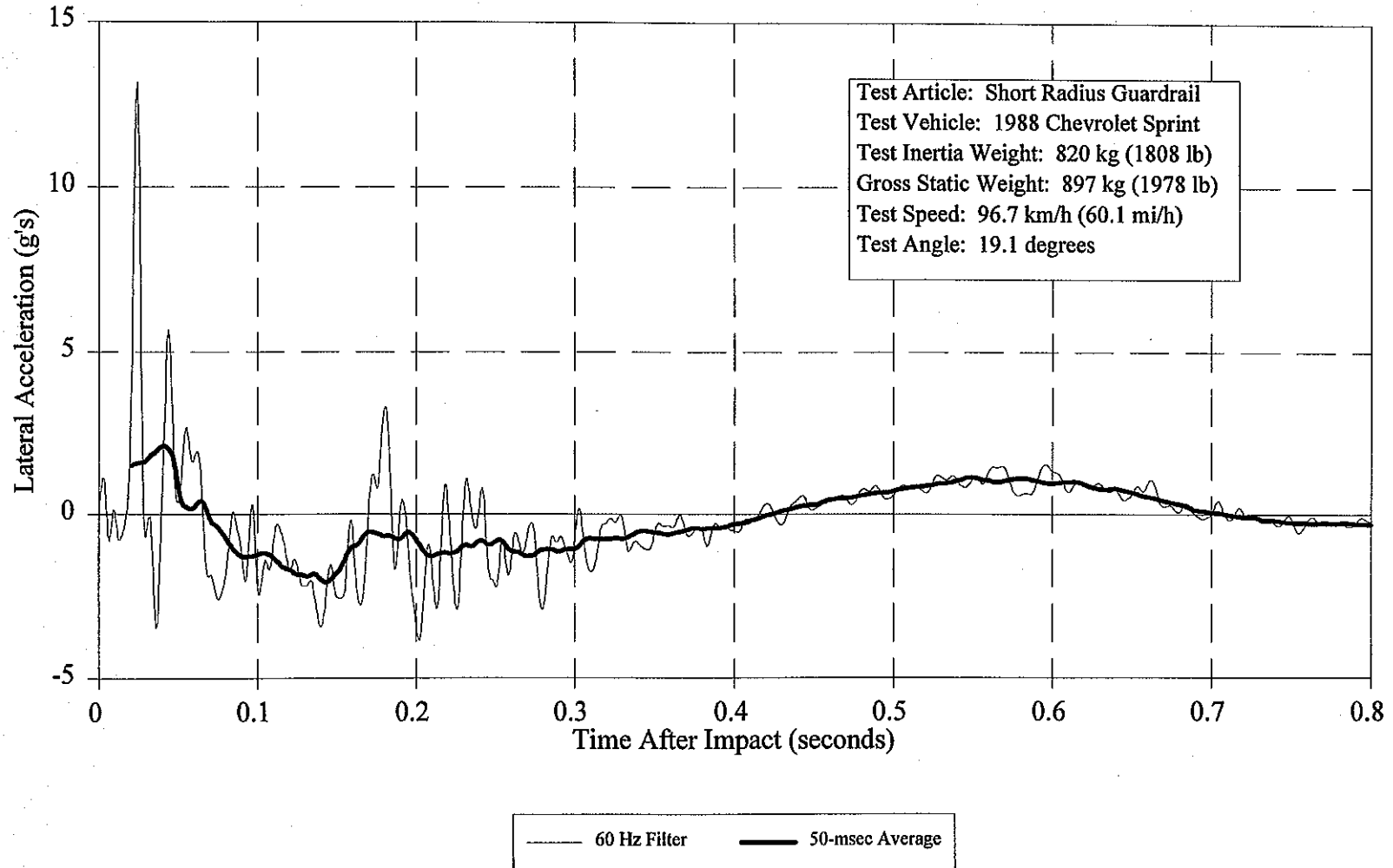


Figure B-11. Vehicle lateral accelerometer trace for test 414424-4.

**CRASH TEST 414424-4**  
Accelerometer at center-of-gravity

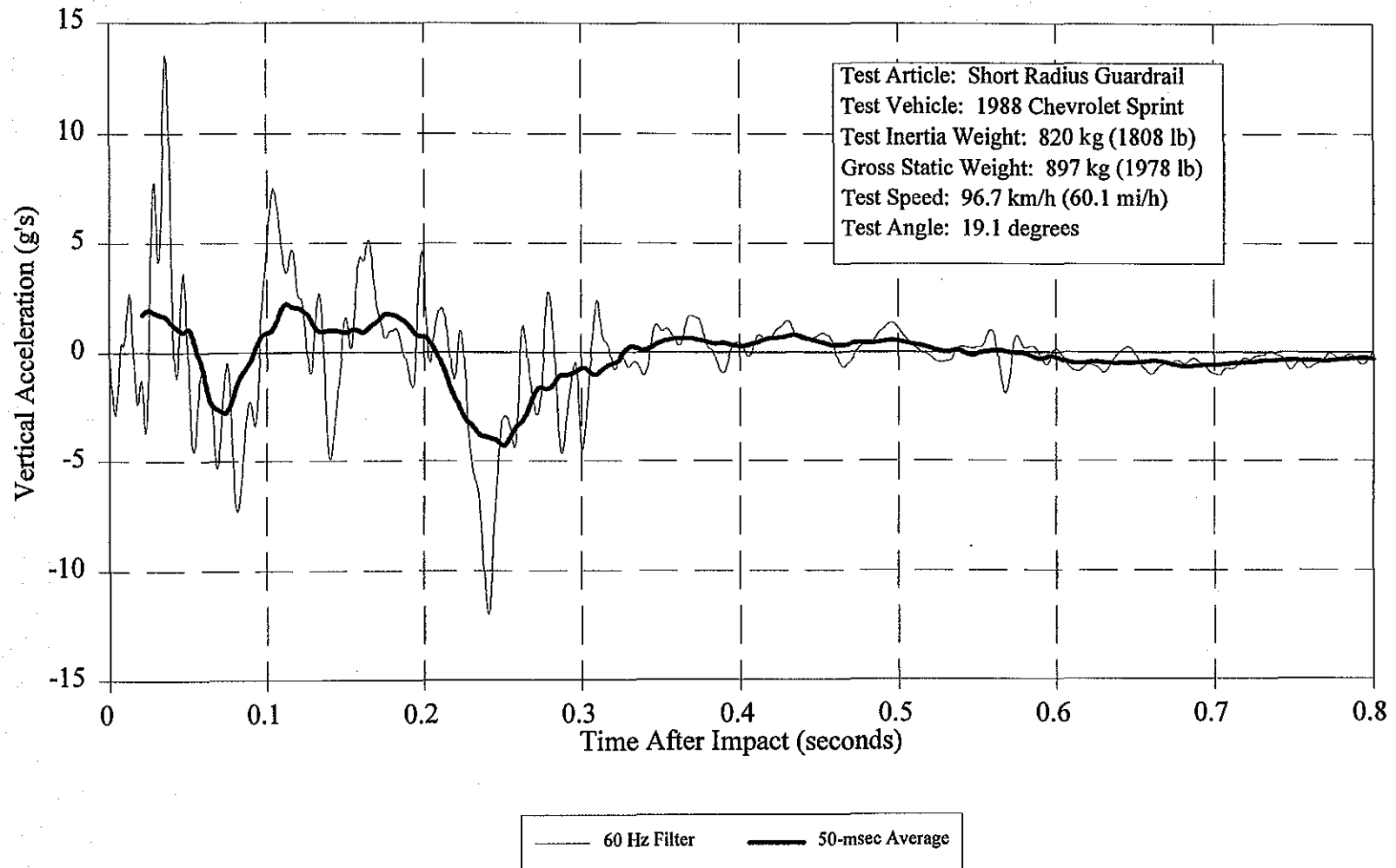


Figure B-12. Vehicle vertical accelerometer trace for test 414424-4.



**CRASH TEST 414424-5**  
Accelerometer at center-of-gravity

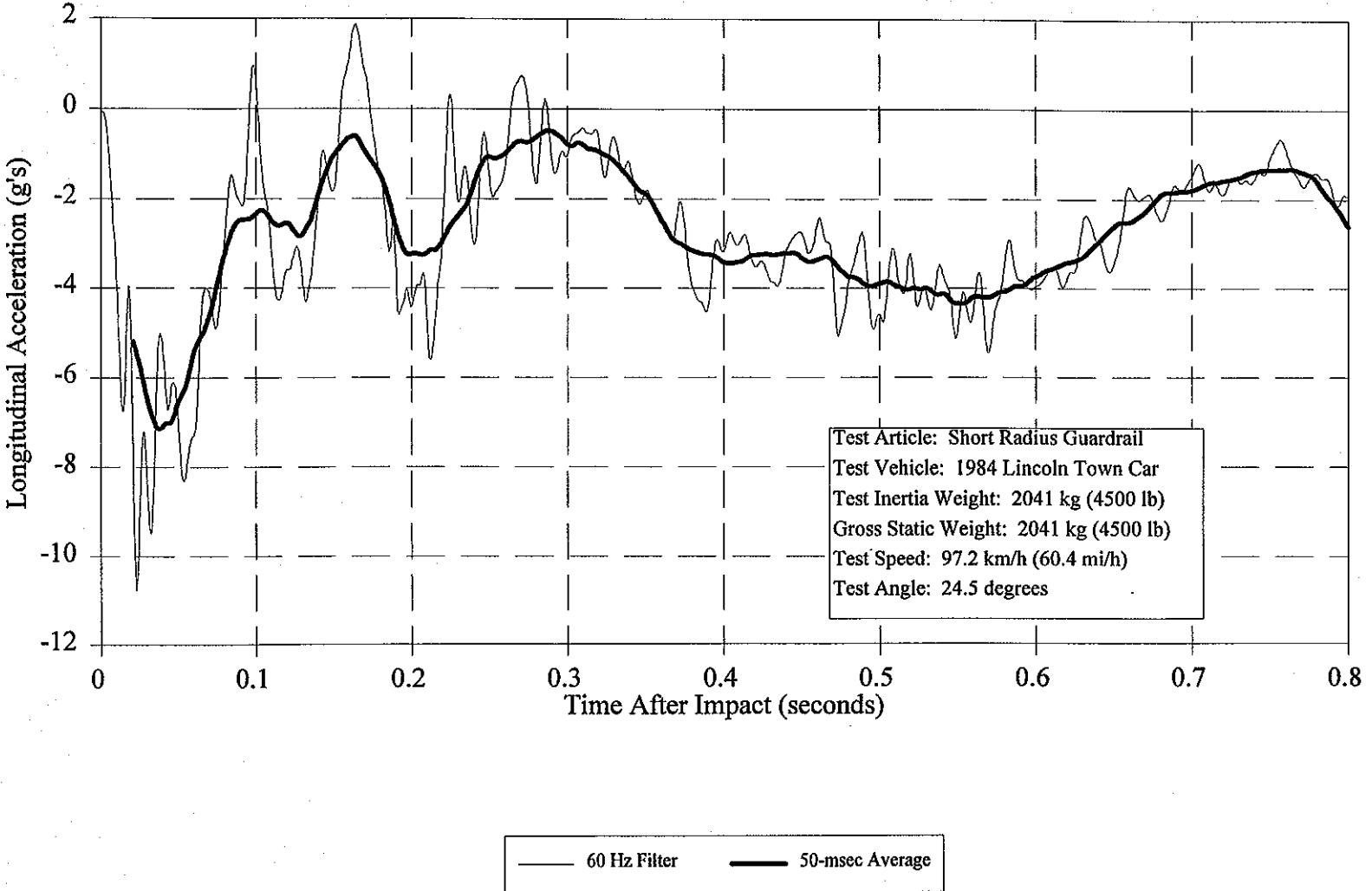


Figure B-13. Vehicle longitudinal accelerometer trace for test 414424-5.

CRASH TEST 414424-5  
Accelerometer at center-of-gravity

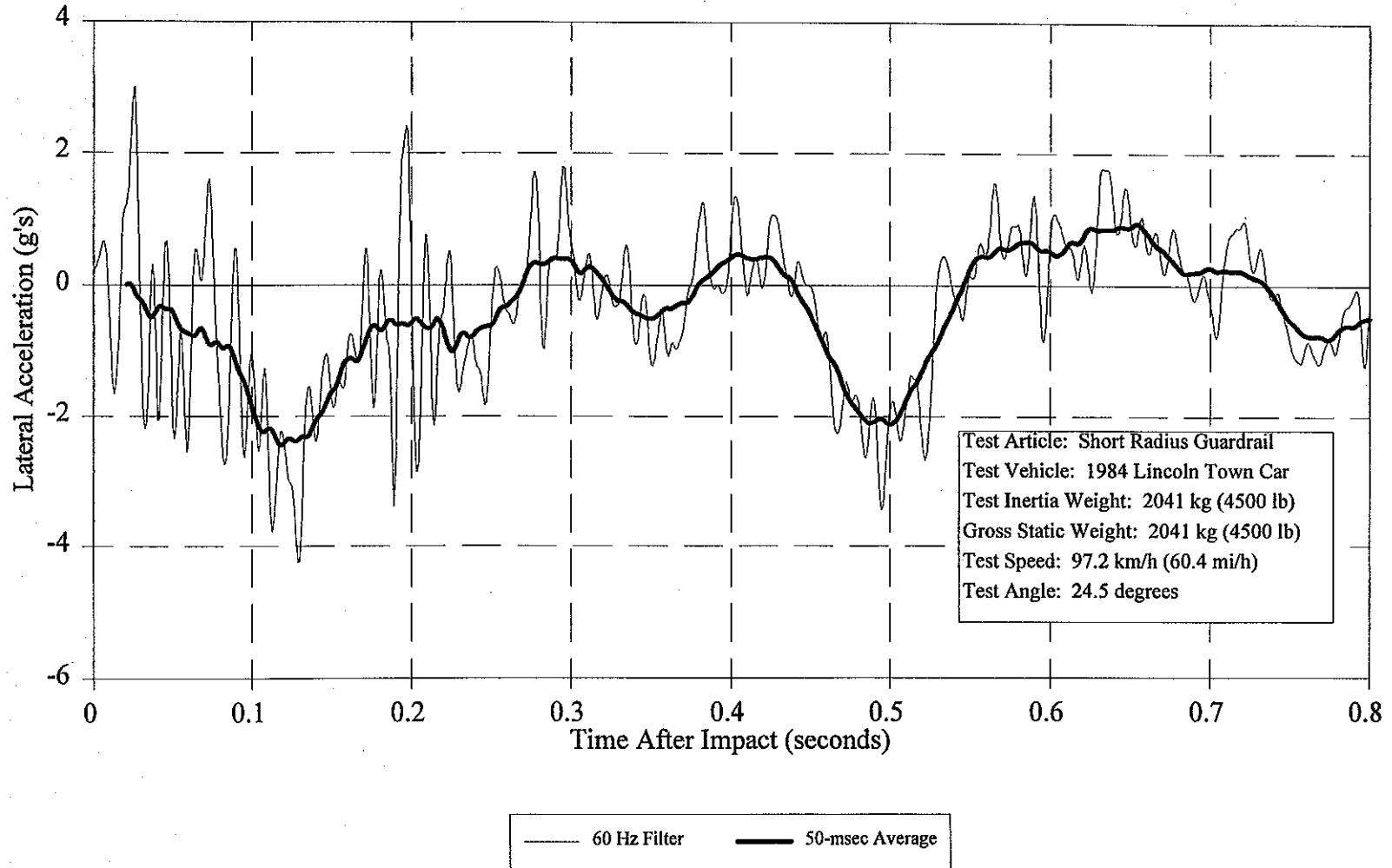


Figure B-14. Vehicle lateral accelerometer trace for test 414424-5.

CRASH TEST 414424-5  
Accelerometer at center-of-gravity

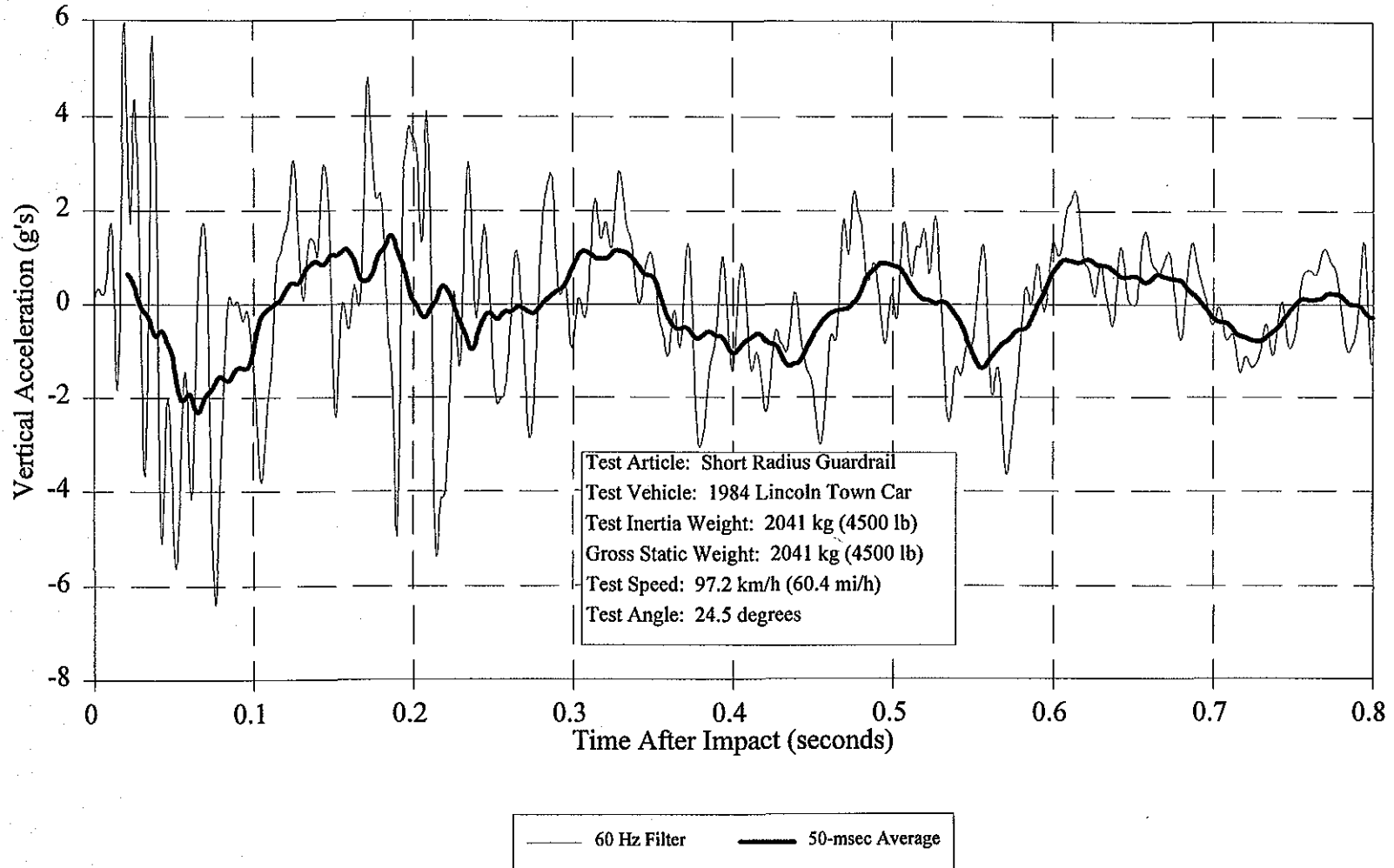
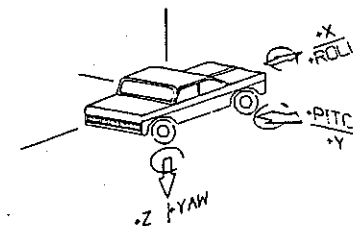
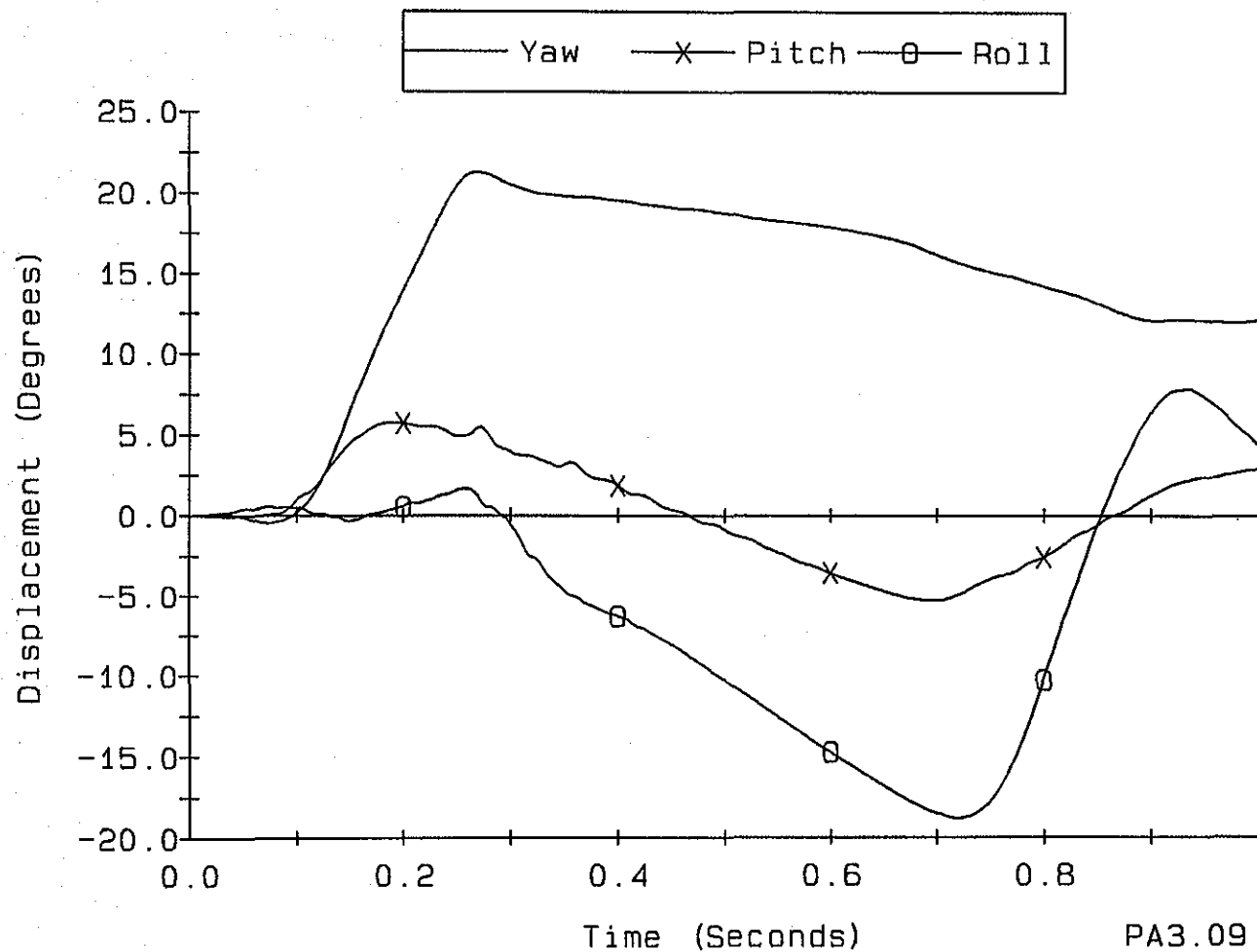


Figure B-15. Vehicle vertical accelerometer trace for test 414424-5.

## **APPENDIX C**

### **VEHICULAR ANGULAR DISPLACEMENTS**

414424-1

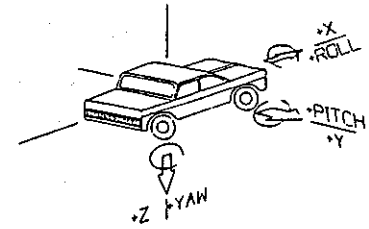
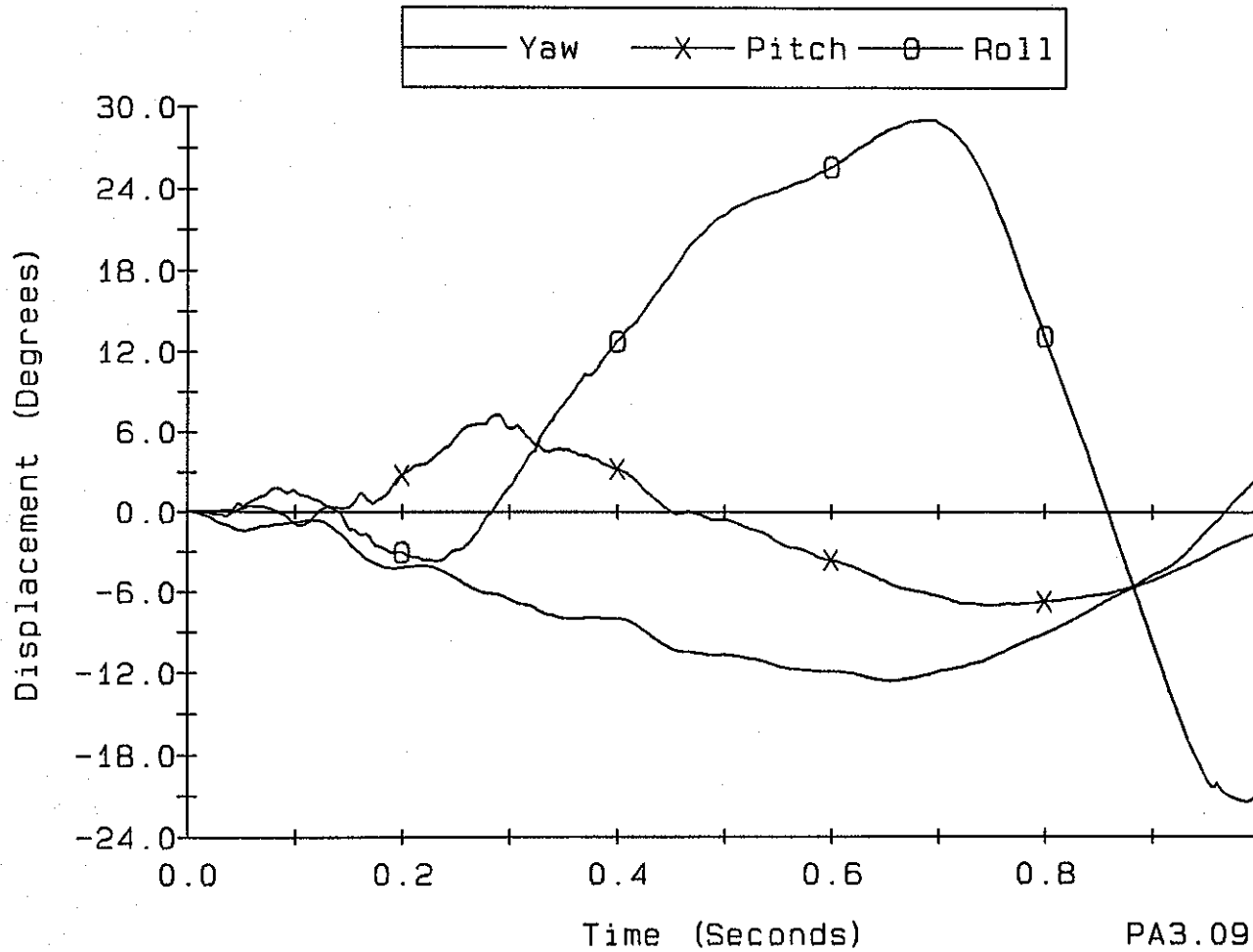


Axes are vehicle fixed.  
Sequence for determining orientation is:

1. Yaw
2. Pitch
3. Roll

Figure C-1. Vehicle angular displacements during test 414424-1.

414424-2

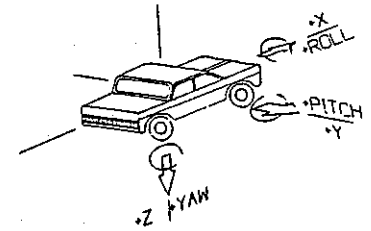
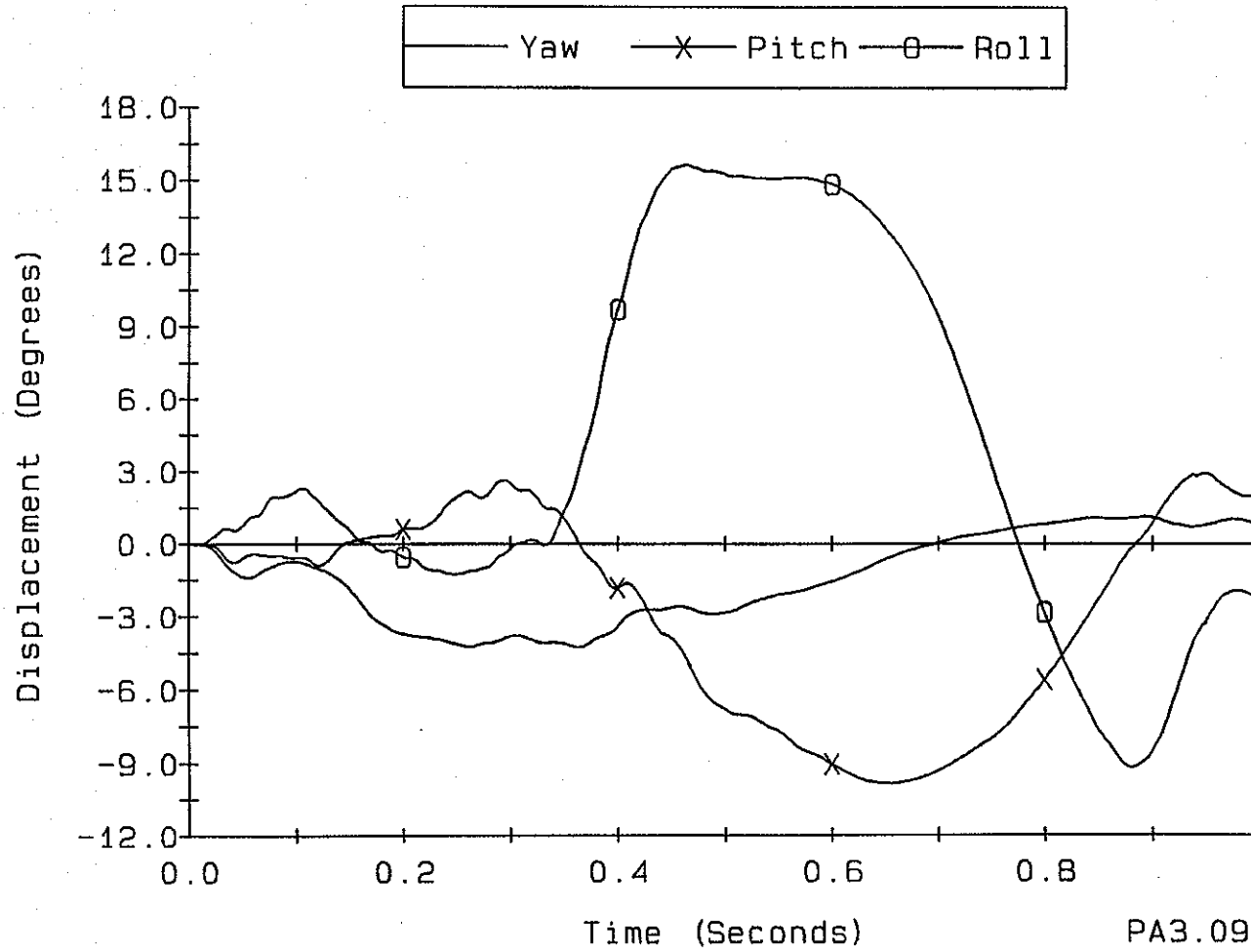


Axes are vehicle fixed.  
Sequence for determining  
orientation is:

1. Yaw
2. Pitch
3. Roll

Figure C-2. Vehicle angular displacements during test 414424-2.

414424-3



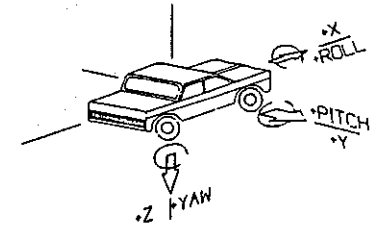
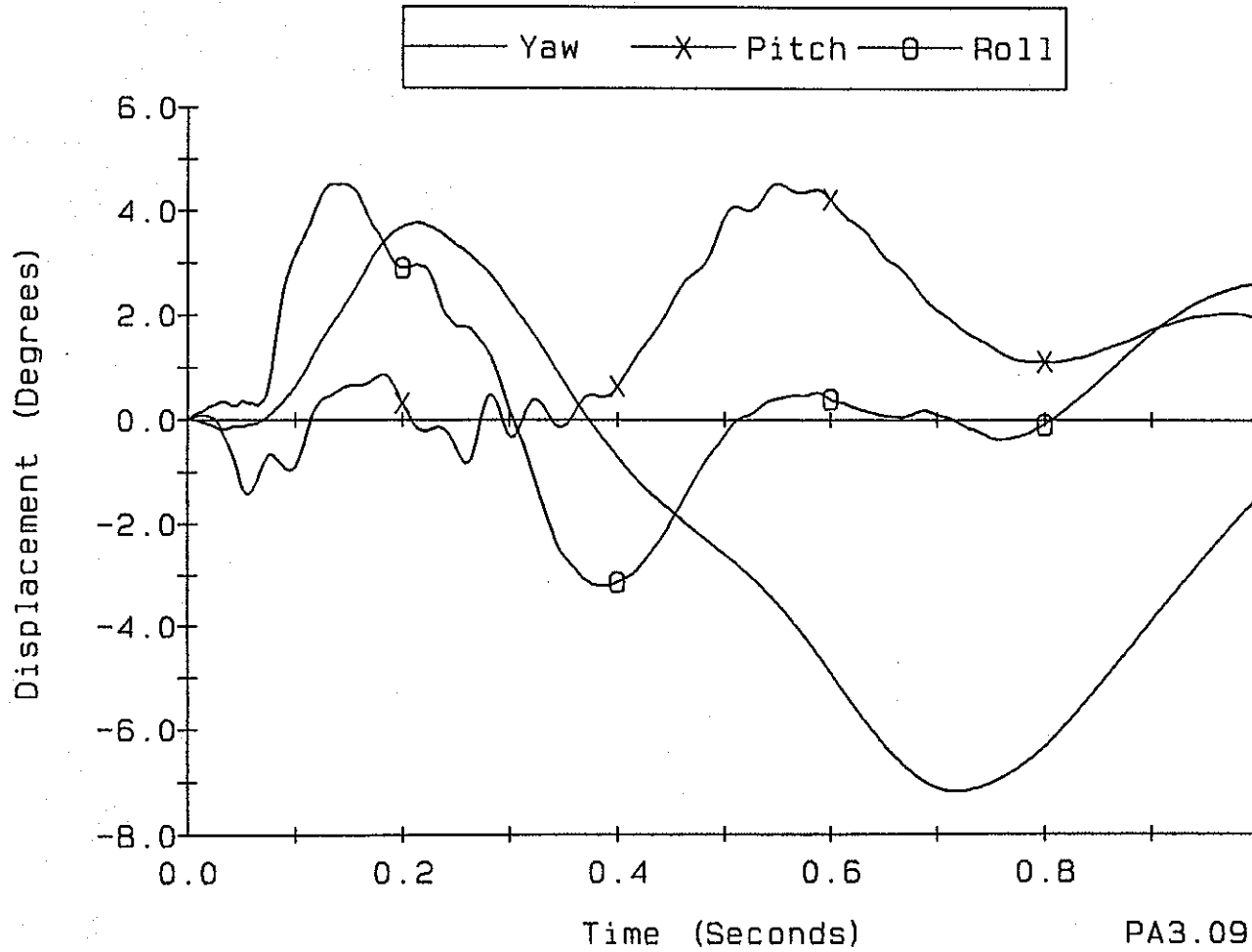
Axes are vehicle fixed,  
Sequence for determining  
orientation is:

1. Yaw
2. Pitch
3. Roll

PA3.09

Figure C-3. Vehicle angular displacements during test 414424-3.

414424-4



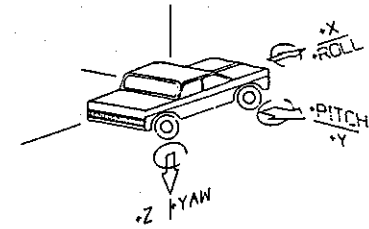
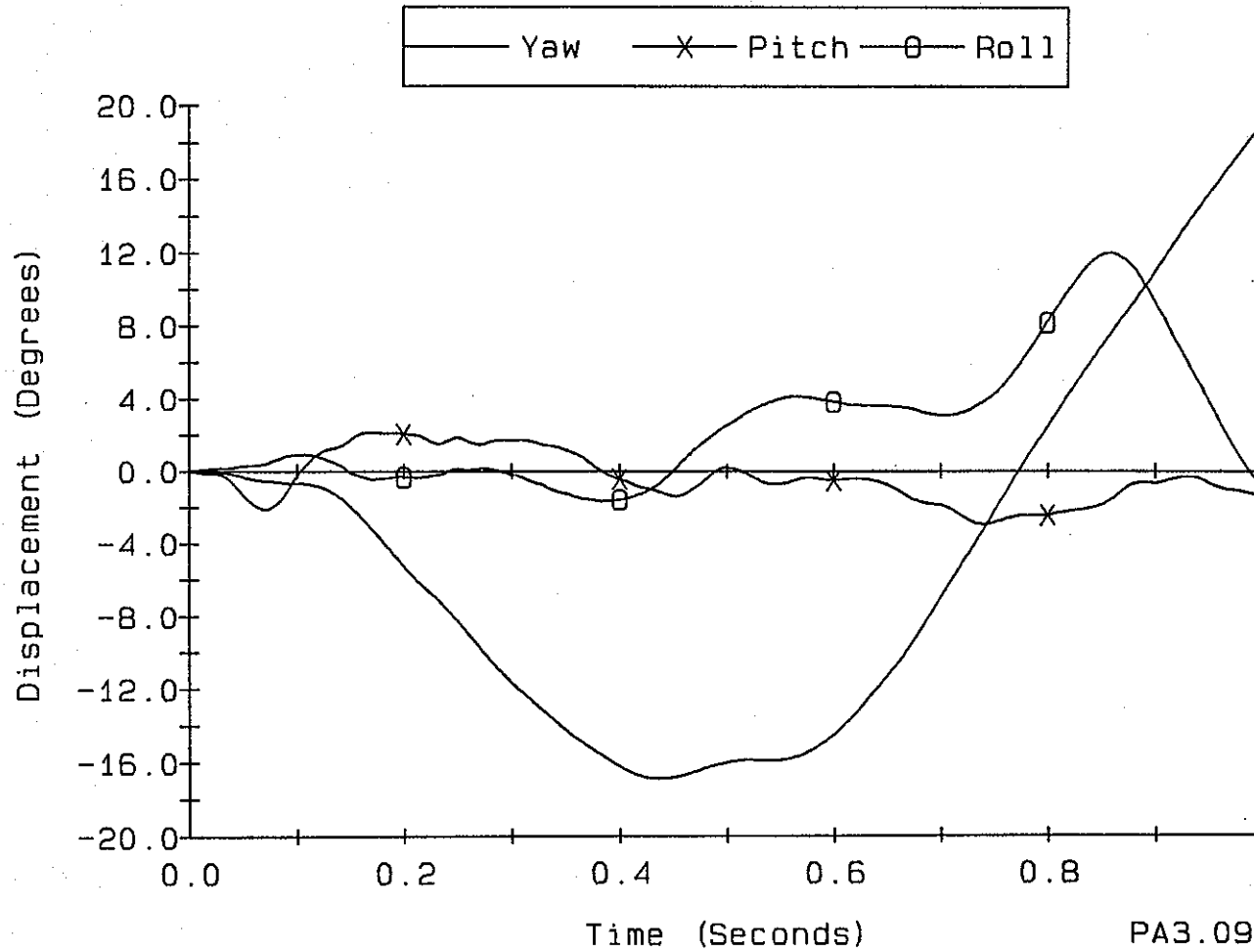
Axes are vehicle fixed.  
Sequence for determining orientation is:

1. Yaw
2. Pitch
3. Roll

Figure C-4. Vehicle angular displacements during test 414424-4.



414424-5



Axes are vehicle fixed.  
Sequence for determining orientation is:

1. Yaw
2. Pitch
3. Roll

Figure C-5. Vehicle angular displacements during test 414424-5.



**APPENDIX D**

**CONSTRUCTION DRAWINGS OF SHORT-RADIUS  
THREE-BEAM TREATMENT**



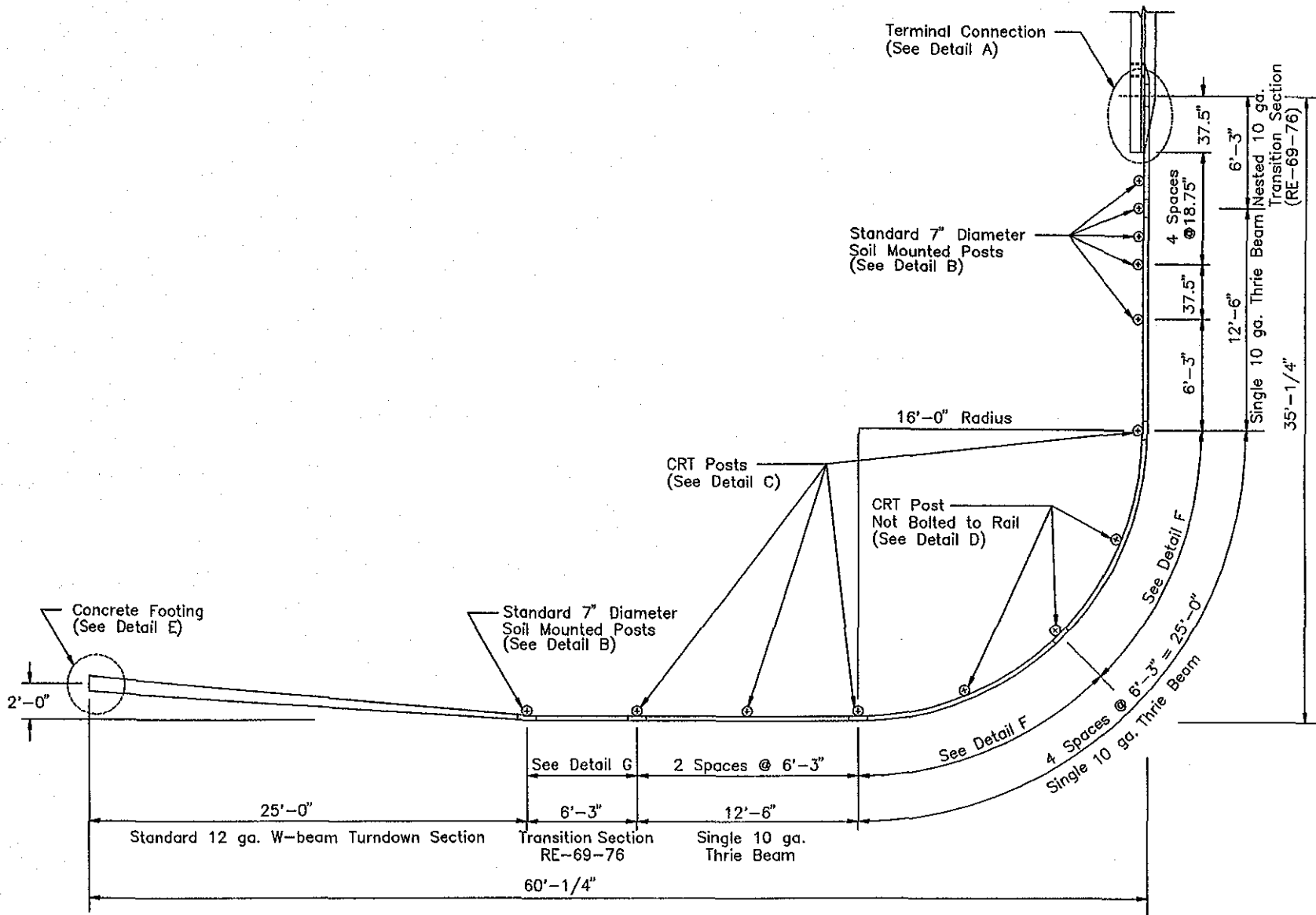
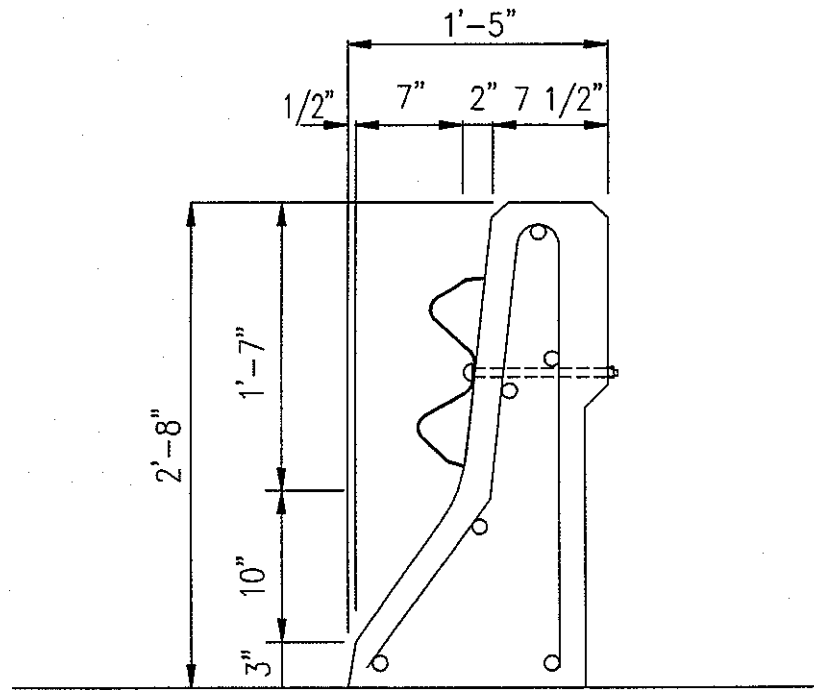
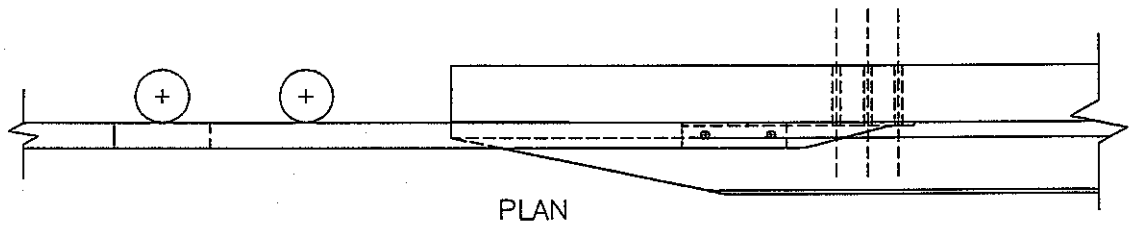
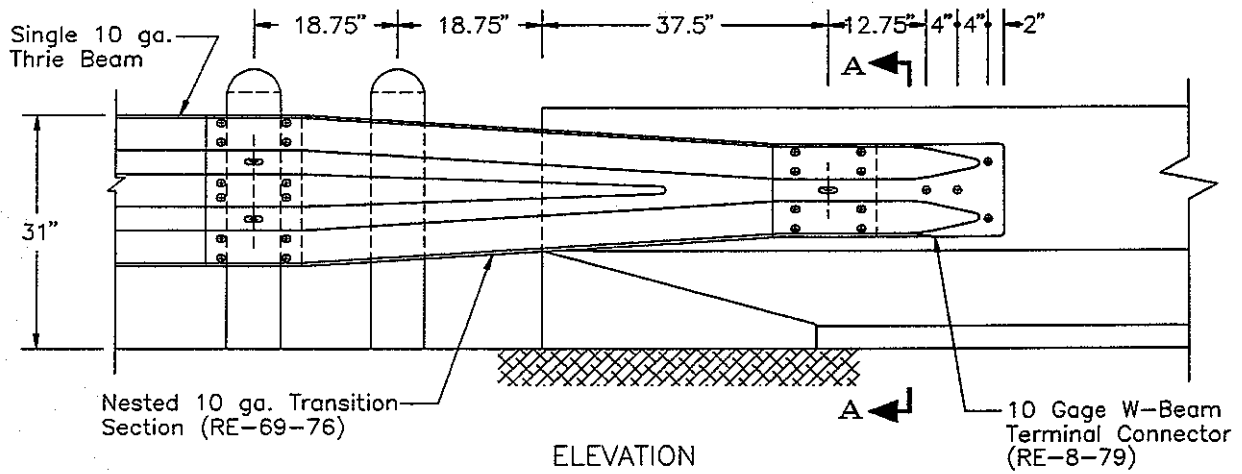
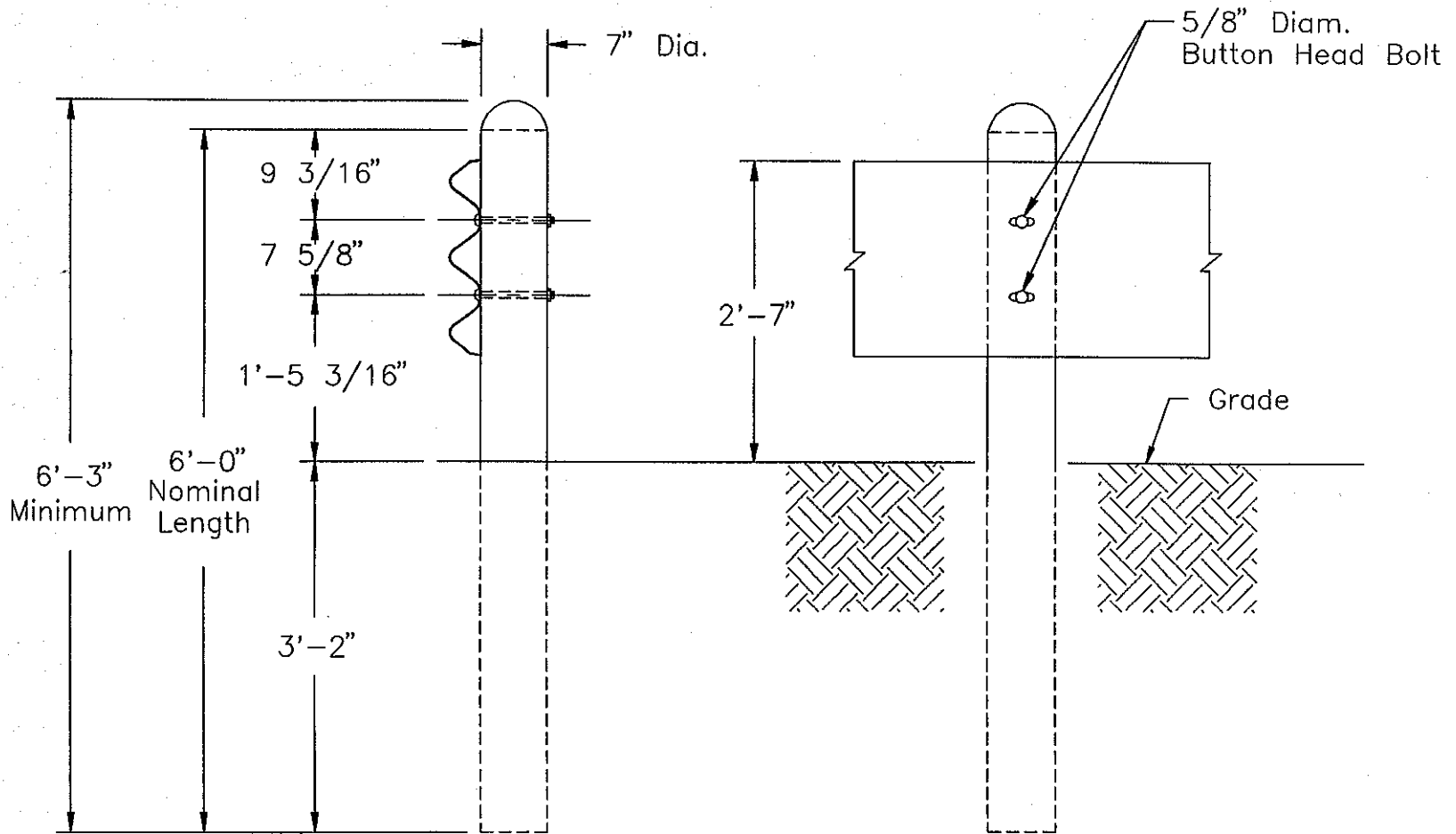


Figure D-1. Construction drawing for short-radius thrie-beam guardrail treatment.



DETAIL A  
TERMINAL CONNECTION

Figure D-1. Construction drawing for short-radius thrie-beam guardrail treatment (continued).



DETAIL B  
STANDARD POST

Figure D-1. Construction drawing for short-radius thrie-beam guardrail treatment (continued).

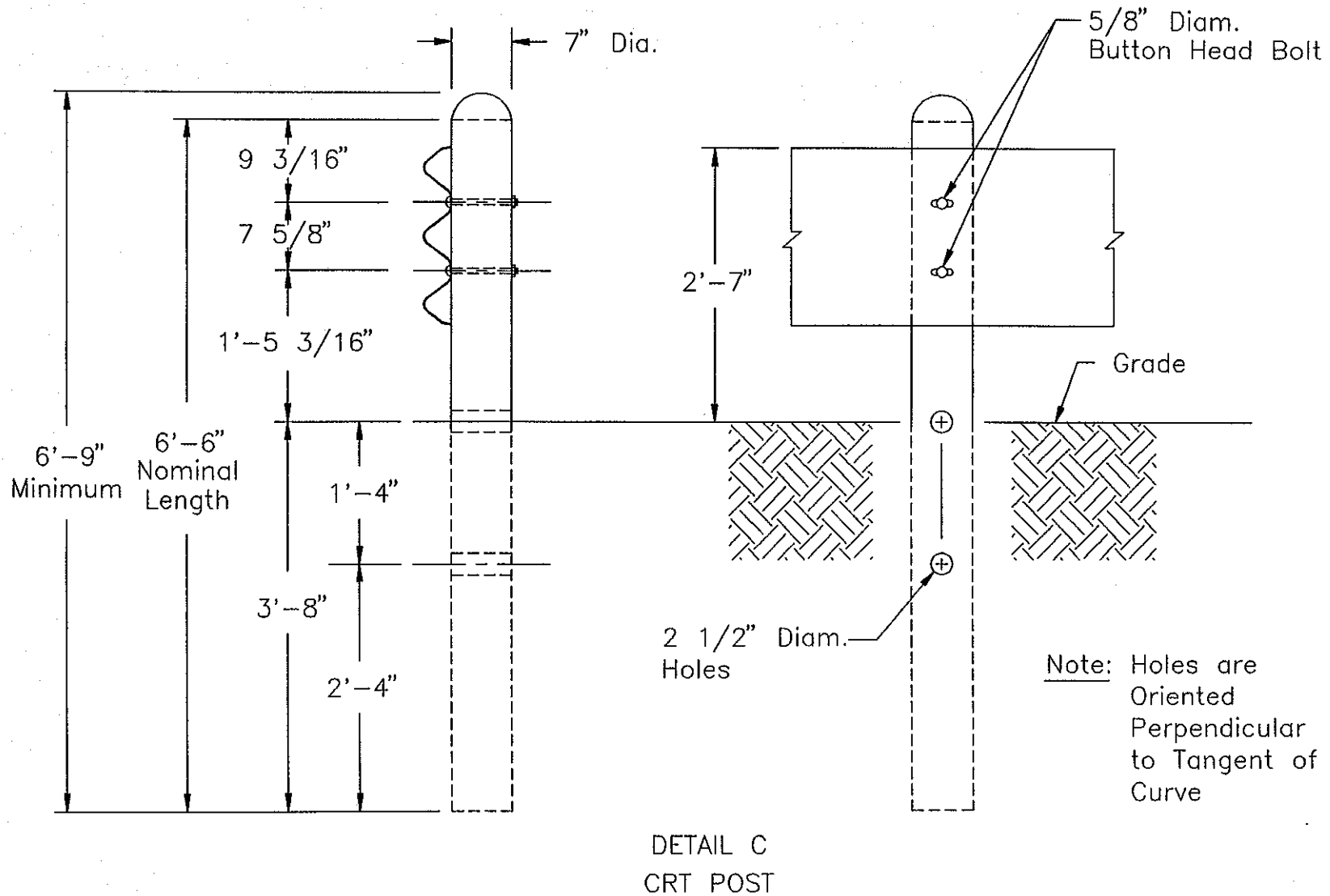
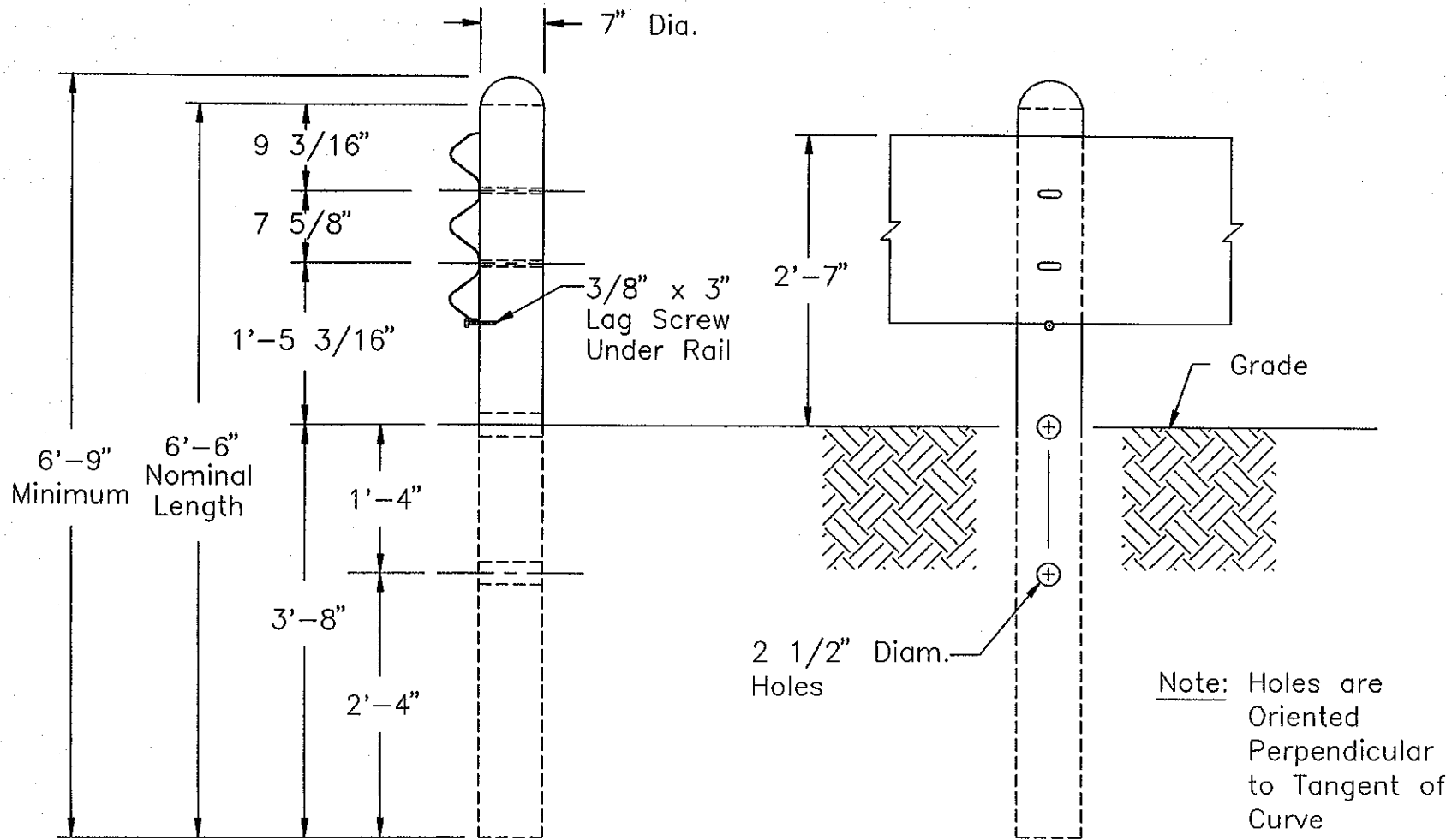


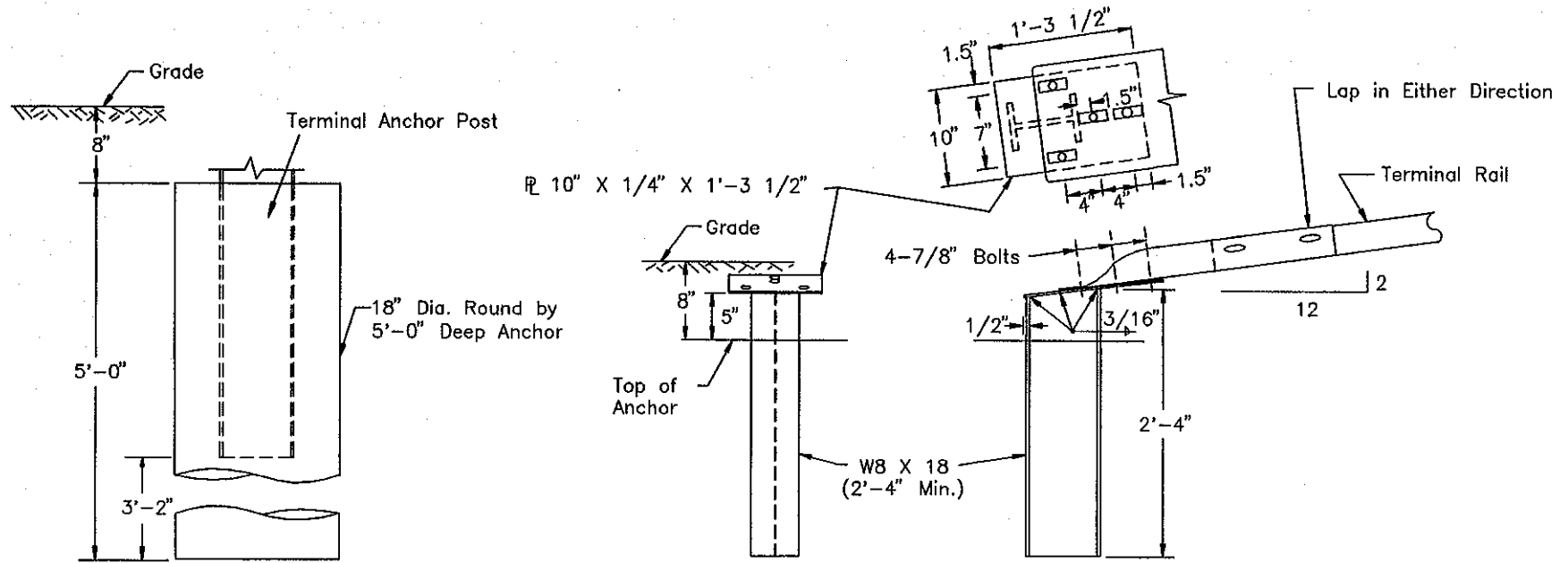
Figure D-1. Construction drawing for short-radius thrie-beam guardrail treatment (continued).





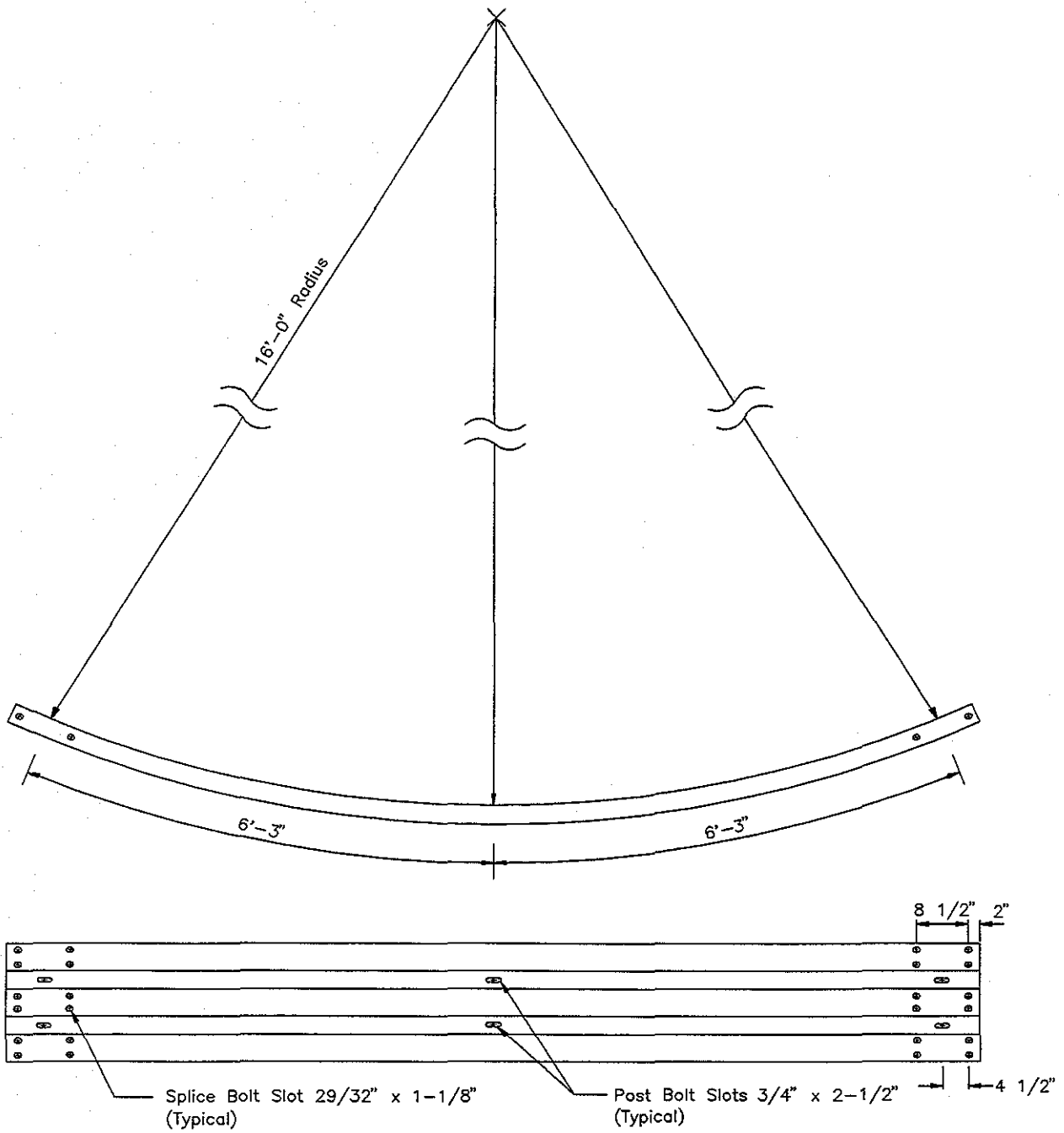
DETAIL D  
RAIL/POST CONNECTION IN CURVE

Figure D-1. Construction drawing for short-radius three-beam guardrail treatment (continued).



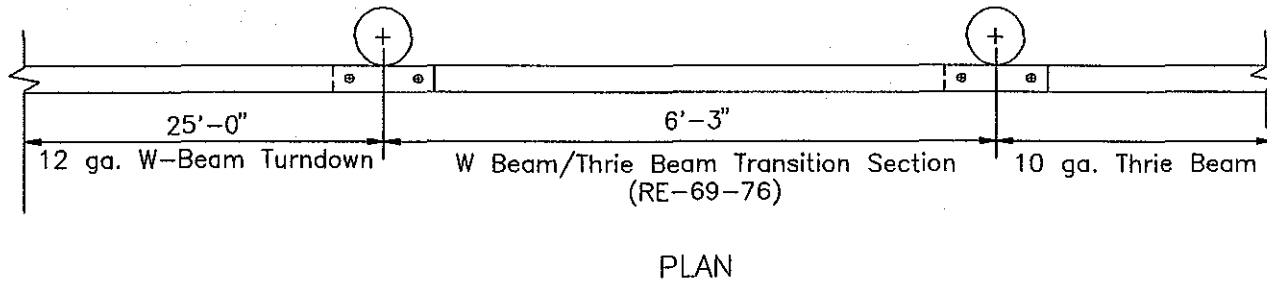
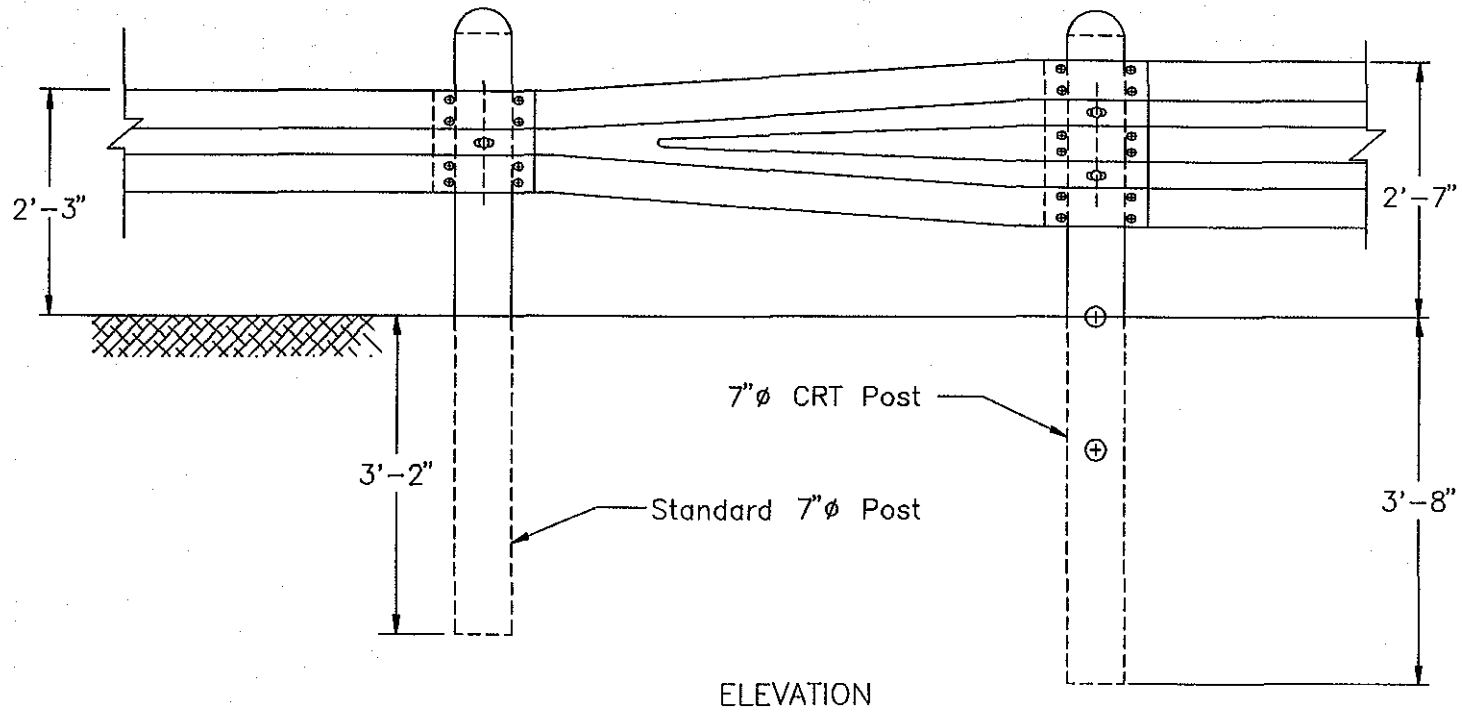
DETAIL E  
TURNDOWN ANCHOR

Figure D-1. Construction drawing for short-radius three-beam guardrail treatment (continued).



DETAIL F  
FULLY CURVED RAIL SECTION

Figure D-1. Construction drawing for short-radius three-beam guardrail treatment (continued).



DETAIL G  
THRIE BEAM/W-BEAM TRANSITION

Figure D-1. Construction drawing for short-radius thrie-beam guardrail treatment (continued).